AD NUMBER	
AD381197	
CLASSIFICATION CHANGES	
TO:	**UNCLASSIFIED**
FROM:	**CONFIDENTIAL**
LIMITATION CHANGES	
TO: **Approved for public release; distribution is unlimited.**	
FROM: **Distribution authorized to U.S. Gov't. agencies and their contractors; Administrative/Operational Use; 22 MAR 1967. Other requests shall be referred to U.S. Naval Ordnance Lab., White Oak, Silver Spring, MD 20910.**	
AUTHORITY	
31 Mar 1979, DoDD 5200.10, per document marking USNOL ltr dtd 29 Aug 1974	

GENERAL DECLASSIFICATION SCHEDULE

IN ACCORDANCE WITH

DOD 5200.1-R & EXECUTIVE ORDER 11652

THIS DOCUMENT IS:

CLASSIFIED BY________________________________

Subject to General Declassification Schedule of Executive Order 11652-Automatically Downgraded at 2 Years Intervals- DECLASSIFIED ON DECEMBER 31,

BY

Defense Documentation Center
Defense Supply Agency
Cameron Station
Alexandria, Virginia 22314

SECURITY
MARKING

The classified or limited status of this report applies to each page, unless otherwise marked.
Separate page printouts MUST be marked accordingly.

THIS DOCUMENT CONTAINS INFORMATION AFFECTING THE NATIONAL DEFENSE OF THE UNITED STATES WITHIN THE MEANING OF THE ESPIONAGE LAWS, TITLE 18, U.S.C., SECTIONS 793 AND 794. THE TRANSMISSION OR THE REVELATION OF ITS CONTENTS IN ANY MANNER TO AN UNAUTHORIZED PERSON IS PROHIBITED BY LAW.

NOTICE: When government or other drawings, specifications or other data are used for any purpose other than in connection with a definitely related government procurement operation, the U. S. Government thereby incurs no responsibility, nor any obligation whatsoever; and the fact that the Government may have formulated, furnished, or in any way supplied the said drawings, specifications, or other data is not to be regarded by implication or otherwise as in any manner licensing the holder or any other person or corporation, or conveying any rights or permission to manufacture, use or sell any patented invention that may in any way be related thereto.

CONFIDENTIAL

NOLTR 67-7

AD 381197

UNDERWATER EXPLOSION TESTS OF TWO STEAM PRODUCING EXPLOSIVES II. 50- and 300-lb CHARGE TESTS (U)

22 MARCH 1967

NOL

UNITED STATES NAVAL ORDNANCE LABORATORY, WHITE OAK, MARYLAND

NOLTR 67-7

NOTICE: This material contains information affecting the national defense of the United States within the meaning of the Espionage Laws, Title 18, U.S.C. Sections 793 and 794, the transmission or revelation of which in any manner to an unauthorized person is prohibited by law.

Downgraded at 3 Year Intervals
Declassified after 12 Years. DOD Dir 5200.10

CONFIDENTIAL

UNDERWATER EXPLOSION TESTS OF TWO STEAM PRODUCING EXPLOSIVES
II. 50- and 300-lb CHARGE TESTS (U)

by

D. E. Phillips
R. L. Willey

ABSTRACT: Charges of Lithanol and H_2O_2/Al weighing 50 and 300 pounds were fired under water to obtain shock wave and bubble measurements. Both compositions showed acceptable agreement in reproducing the condensation effects of a nuclear bubble. Simultaneous simulation of the shock wave effects was not obtained. An initiation problem with the H_2O_2/Al composition was apparent from the results; no initiation problem was indicated for Lithanol. An increase in bubble parameters with increasing charge weight was evident for both compositions.

UNDERWATER EXPLOSIONS DIVISION
EXPLOSIONS RESEARCH DEPARTMENT
U. S. NAVAL ORDNANCE LABORATORY
WHITE OAK, SILVER SPRING, MARYLAND

NOLTR 67-7 22 March 1967

UNDERWATER EXPLOSION TESTS OF TWO STEAM PRODUCING EXPLOSIVES
II. 50- and 300-lb CHARGE TESTS

This report discusses the results of underwater tests of two steam generating compositions being developed for use as nuclear bubble simulants. The development of these compositions is part of a continuing program to improve knowledge of bubble phenomena resulting from the underwater detonation of both nuclear and conventional explosives. This work was supported by the Defense Atomic Support Agency, under WEPTASK No. 51001/212-8/F008-21-03(003) (DASA NWER 14.086), Nuclear Underwater Explosion Bubble Phenomena, and under WEPTASK No. 51001/212-8/F008-21-03(005) (DASA NWER 14.108), Field Simulation Trials. Mention of commercially available products does not constitute an endorsement or criticism by the Laboratory.

E. F. SCHREITER
Captain, USN
Commander

C. J. Aronson

C. J. ARONSON
By direction

CONTENTS

		Page
1.	INTRODUCTION AND BACKGROUND	1
	1.1 Introduction	1
	1.2 Background	1
	1.3 Condensible Product (Steam) Charges	3
2.	EXPERIMENTAL PROGRAMS	6
	2.1 Instrumentation	6
	2.2 Charges	8
	2.2.1 Pentolite	8
	2.2.2 Lithanol	8
	2.2.3 H_2O_2/Al	9
	2.3 Charge and Instrument Rigging	10
3.	LITHANOL RESULTS	22
	3.1 Underwater Shock Wave	22
	3.1.1 50-lb Charges	23
	3.1.2 300-lb Charges	24
	3.2 Bubble	24
	3.2.1 50-lb Charges	24
	3.2.2 300-lb Charges	26
4.	H_2O_2/Al RESULTS	39
	4.1 Underwater Shock Wave	39
	4.1.1 50-lb Charges	39
	4.1.2 300-lb Charges	40
	4.2 Bubble	40
	4.2.1 50-lb Charges	40
	4.2.2 300-lb Charges	41
5.	PHOTOGRAPHIC RESULTS	49
	5.1 50-lb Charges	49
	5.2 300-lb Charges	50
	5.2.1 Pentolite	51
	5.2.2 Lithanol	52
	5.2.3 H_2O_2/Al	53
	5.2.4 Summary	53
	5.3 Other Surface Phenomena Results	53
6.	COMPARISON WITH PREVIOUS WORK	66
	6.1 Previous Lithanol and H_2O_2/Al Data	66
	6.1.1 Shock Wave	66
	6.1.2 Bubble	66
	6.2 Comparison with Nuclear Explosions	67
7.	SCALING OF STEAM CHARGE RESULTS	77

CONTENTS (continued)

		Page
8.	CONCLUSIONS AND RECOMMENDATIONS	81
	8.1 Conclusions	81
	8.2 Recommendations	82
ACKNOWLEDGEMENTS		83
BIBLIOGRAPHY		84
APPENDIX A		A-1
APPENDIX B		B-1

TABLES

Table	Title	Page
1.1	Shock Wave and Bubble Parameters	5
2.1	Experimental Conditions	12
2.2	Actual Composition of H_2O_2/Al Charges	14
3.1	Bubble Periods and Computed K for 50-lb Charges	29
3.2	Measured Maximum Bubble Radius for 50-lb Charges	30
3.3	Bubble Periods and Computed K for 300-lb Charge (1964)	31
3.4	Summary of Ranging Results for 300-lb Charge (1964)	32
3.5	Bubble Probe Results for 300-lb Charges (1964)	33
4.1	Bubble Periods and Computed K for 300-lb Charge (1965)	43
4.2	Summary of Ranging Results for 300-lb Charges (1965)	44
4.3	Measured Maximum Bubble Radius and Computed J for 300-lb Charges (1965)	45
5.1	Arrival Time of Bubble Contents at Surface for 50-lb Charges	55
5.2	Times of Discontinuities in Height-vs-Time Curves for 300-lb Charges	56
6.1	Summary of Shock Wave Parameters for All Weights of the Steam Compositions	70
6.2	Summary of Bubble Parameters for All Weights of the Steam Compositions	71
7.1	Umbrella and Baker Scaled Depths for Various Weights of Lithanol	80

CONTENTS (continued)

FIGURES

Figure	Title	Page
2.1	Probe Calibration Curves	15
2.2	300-lb Pentolite Charge	16
2.3	300-lb Lithanol Charge Case	17
2.4	300-lb H_2O_2/Al Charge Case	18
2.5	300-lb H_2O_2/Al Charges	19
2.6	Charge and Instrumentation Rigging	20
2.7	Probe Support Methods	21
3.1	Typical Shock Wave Records	34
3.2	Typical Bubble Pulse Records, 50-lb Pentolite	35
3.3	Typical Bubble Pulse Records, 50-lb Lithanol	36
3.4	Typical Bubble Pulse Records, 300-lb Pentolite	37
3.5	Typical Bubble Pulse Records, 300-lb Lithanol	38
4.1	Typical Shock Wave Records	46
4.2	Typical Bubble Pulse Records, 50-lb H_2O_2/Al	47
4.3	Typical Bubble Pulse Records, 265-lb H_2O_2/Al	48
5.1	Bubble Arrival for 50-lb Pentolite and Lithanol Charges Fired at a Depth of 100 Feet	57
5.2	Plume Phenomena from 300-lb Pentolite Charges	58
5.3	Comparison of Above Surface Effects with Bubble Migration, 300-lb Pentolite at 60 Feet	59
5.4	Comparison of Above Surface Effects with Bubble Migration, 300-lb Pentolite at 80 Feet	60
5.5	Comparison of Above Surface Effects with Bubble Migration, 300-lb Pentolite at 100 Feet	61
5.6	Plume Phenomena from 300-lb Lithanol Charges	62
5.7	Comparison of Above Surface Effects with Bubble Migration, 300-lb Lithanol at 60 Feet	63
5.8	Comparison of Above Surface Effects with Bubble Migration, 300-lb Lithanol at 80 Feet	64
5.9	Comparison of Above Surface Effects with Bubble Migration, 300-lb Lithanol at 100 Feet	65
6.1	Comparison of Peak Pressures Obtained with Various Weights of H_2O_2/Al	72
6.2	Increase of Bubble Coefficients J and K with Increasing Charge Weight	73
6.3	Comparison of Predicted and Measured Second Period Ratio	74
6.4	Comparison of Predicted and Measured Third Period Ratio	75
6.5	Bubble Migration to First Minimum	76
6.6	Bubble Migration Between First and Second Minimum	76
A.1	Geometry of Bubble Ranging	A-3

UNDERWATER EXPLOSION TESTS OF TWO STEAM PRODUCING EXPLOSIVES
II. 50- and 300-lb CHARGE TESTS (U)

1. INTRODUCTION AND BACKGROUND

1.1 INTRODUCTION

In the study of the effects of underwater nuclear explosions, considerable use is made of experimental tests using conventional explosives. While there are similarities between nuclear and conventional high explosive phenomena, there are considerable differences in scaling or studying effects which depend on the bubble contents, such as migration and blowout. The nuclear bubble consists primarily of steam resulting from the vaporization of the surrounding water; on the other hand, conventional explosives generate permanent gases as a result of their chemical reaction. Thus, condensation processes of the steam will affect the nuclear bubble behavior; no significant condensation will take place with conventional charges.

Two compositions have been developed which produce a condensible gas bubble and which can be fired in sizes up to several tons. Eight and sixteen-lb charges of these compositions have previously been fired (Heathcote and Phillips, 1966)*. As part of their evaluation, 50- and 300-lb charges of these compositions were also fired. This report presents the results of these tests.

1.2 BACKGROUND

When an explosion takes place under water, energy is radiated outward in the form of a shock wave. The gases from the detonation reaction are contained by the surrounding water. The high internal pressure of these gases pushes this water outward and, if the explosion takes place at a sufficient depth, a spherical bubble is formed. This bubble continues to expand and, because of inertia, reaches a maximum size with the internal gas pressure lower than the hydrostatic pressure of the surrounding water. The bubble then contracts, reaches a minimum size, and re-expands. At the time the bubble reaches its minimum size, a pressure pulse is emitted. The bubble also migrates upward during the time shortly before and after the minimum.

The maximum bubble radius, A_{max}, which the gas bubble attains is given by (Cole, 1948):

$$A_{max} = J \frac{W^{1/3}}{Z^{1/3}} \qquad (1.1)$$

where: A_{max} = maximum bubble radius, ft
J = bubble radius coefficient characteristic of the particular explosive

* Bibliography is on page 84.

W = charge weight, lb
Z = hydrostatic pressure at charge depth, ft H_2O

The period, or time at which the minimum radius occurs, is given by:

$$T_1 = K \frac{W^{1/3}}{Z^{5/6}} \tag{1.2}$$

where: T_1 = first bubble period, sec
K = bubble period coefficient characteristic of the particular explosive

For conventional field explosives such as pentolite, TNT, and HBX-1, it has been found that the ratio of J to K is essentially constant, (Snay, 1964), thus:

$$\frac{J}{K} \cong 2.90 \tag{1.3}$$

For field size explosions, J has generally been calculated from the above equation, using the measured period to calculate K. However, it is well known that T_1, and thus K, are affected by the proximity of surface and bottom. These effects must be fully accounted for to obtain an accurate value of J. In addition, Snay (1960) has predicted that for highly aluminized explosives this ratio will decrease by about four percent. Since both the steam producing charges contain a relatively high percentage of aluminum, the relationship given in Equation 1.3 may not be valid. In order to obtain an independent measurement of A_{max}, and to check on the possible reduction in the J/K ratio, a probe has been developed to measure this phenomenon (Phillips and Scott, 1965).

The bubble continues to pulsate and migrate upward until its energy is dissipated or until it reaches the water surface. In the case of a nuclear bubble, the gaseous contents are primarily steam. As the nuclear bubble pulsates and migrates toward the surface, energy is rapidly dissipated through condensation of this steam. Snay (1960) has predicted that the nuclear bubble will show no more than three significant bubble pulses because of this condensation. Conventional high explosive charges have been known to pulsate as many as seven times (Arons et al, 1947).

Very little information is currently available on the pulsation, migration, and dissipation of energy of a nuclear bubble. Bubble period measurements have been obtained on only one underwater nuclear test, Operation Wigwam, a 32-kt device fired at a depth of 2,000 feet (Aronson et al, 1956). No pulse was observed on Shots Wahoo of Operation Hardtack and Sword Fish of Operation Dominic; Shots Baker of Operation Crossroads and Umbrella of Operation Hardtack were too shallow to produce pulses.

In addition to the nuclear data, some information on non-migrating steam bubbles was obtained with small bubbles produced in a tank with sparks (Hudson, 1955). A chemical explosive detonator which produces a condensible product bubble is currently being developed at NOL for use in small scale tank studies. Exploding wire techniques have been used by the Naval Radiological Defense Laboratory (NRDL) in their test tank for studies of migration and the resulting distribution of radioactive debris from an underwater nuclear explosion (Buntzen, 1964).

Results obtained in tanks utilizing these various steam generating techniques are used to develop scaling methods for extrapolating the results to full scale nuclear explosions. It is necessary, however, to check the validity of these scaled results with some full-scale test results. Because of the limited amount of actual nuclear test data currently available and the uncertainty that more will be obtained, it is necessary to obtain such information of field scale experiments using charges producing condensible bubbles.

In the case where the explosion takes place at a shallow depth, (generally defined as a depth shallower than the maximum bubble radius) the bubble does not migrate but pushes the water outward above the original water surface. The bubble is contained by a seal of continuous water which eventually ruptures and, if the internal pressure of the gas is higher than atmospheric, an outflow of these gases will occur. This outflow is referred to as blowout and, in the case of a nuclear explosion, expels radioactive contaminants into the atmosphere. It is believed that blowout is affected by the steam in the bubble which, upon meeting the ambient atmosphere, condenses and thus tends to seal up these holes. Because of this condensation effect, it is not possible to study realistically the phenomena of blowout (especially the transition region from blowout to blow-in*) using conventional explosives.

At shallow burst depths, the column is moving at or near supersonic speed and an air shock wave is formed which may affect the safe delivery range in the case of an air-delivered nuclear weapon. It is believed the peak pressures in this shock wave are enhanced in the presence of blowout. Thus, it is desirable to use a steam charge to study blowout and airblast resulting from shallow underwater explosions, in order to obtain more realistic safe delivery ranges for a nuclear burst.

1.3 CONDENSIBLE PRODUCT (STEAM) CHARGES

Two compositions have been developed by the Chemical Engineering Division at NOL, after extensive laboratory tests, as possible explosives for field scale experiments that require a condensible product (steam) bubble (Murphy, 1963). The first of these explosives is a lithium perchlorate trihydrate/aluminum composition ($LiClO_4 \cdot 3H_2O/Al$) mixed in a 69/31 percent ratio by weight. This composition is referred to as Lithanol. The second is a hydrogen peroxide/aluminum composition (H_2O_2/Al)

* Under certain conditions, the seal of water ruptures when the internal pressure is less than atmospheric so that air rushes into the bubble. This is called blow-in.

mixed in a 65/35 percent ratio by weight. Both compositions are stoichiometrically balanced, the aluminum combining with the excess oxygen to form aluminum oxide (Al_2O_3), a solid residue. Other products formed are water soluble solids and water in the form of steam. The chemical reactions taking place for these compositions are:

$$3\ LiClO_4 \cdot 3H_2O + 8\ Al \rightarrow 3\ LiCl + 4\ Al_2O_3 + 9\ H_2O \qquad (1.3)$$

$$3\ H_2O_2 + 2\ Al \rightarrow Al_2O_3 + 3\ H_2O \qquad (1.4)$$

Underwater tests have been made with both compositions using 8- and 16-lb charges (Phillips and Heathcote, 1966), and information was obtained on both shock wave and bubble parameters. These results are summarized in Table 1.1.

The data obtained are sufficient for computing the conditions where these compositions would scale nuclear explosions. However, it was felt necessary to fire larger charges of both compositions. First, both explosives are relatively insensitive and may not be detonating properly in small sizes; thus the data in Table 1.1 may not be correct for large charges. Also, information on later bubble periods was not obtained; such information is needed for the study of the condensation processes. This information can be obtained only from fairly large charges fired deep enough to permit the bubble to oscillate several times. Finally, since very large (multi-ton) charges will eventually be required, fabrication and handling procedures must be developed using relatively large charges.

TABLE 1.1 SHOCK WAVE AND BUBBLE PARAMETERS

Variable	Lithanol 1/		H_2O_2/Al 1/		Pentolite 2/	
	C	α	C	α	C	α
Shock Wave:						
P_m	1.17×10^4	1.03	0.87×10^4	1.09	2.35×10^4	1.14
$E/W^{1/3}$	1.54×10^3	1.86	1.61×10^3	2.15	2.66×10^3	2.04
$I/W^{1/3}$	1.98	0.89	2.16	1.05	1.48	0.91
Bubble:						
J	15.2		16.1		12.6 3/	
K	5.36		5.84		4.36 3/	

1/ From Phillips and Heathcote (1966). Applicable to 8- and 16-lb charges only.

2/ From Thiel (1961).

3/ From NAVORD 2986.

$$\text{S/W Variable} = C \cdot \left(\frac{W^{1/3}}{R}\right)^{\alpha}$$

2. EXPERIMENTAL PROGRAMS

Two separate experimental programs were fired to obtain the information presented in this report. In the first program, five Lithanol and six pentolite charges were fired in the fall of 1964. All weighed approximately 300 lb. The second experimental program was carried out in the summer of 1965. This program consisted of four 50-lb and three 300-lb pentolite charges; four 50-lb Lithanol charges; and three 50-lb and six 300-lb H_2O_2/Al charges. Both programs were fired in Chesapeake Bay out of the Naval Ordnance Laboratory Test Facility, Solomons, Maryland. Charge depths for the 300-lb charges ranged from 60 feet to 100 feet in 150 feet of water. The 50-lb charges were all fired at a depth of 100 feet in 150 feet of water. Tabulated shot information is given in Table 2.1.

The first experimental program utilized the YSD-72, a seaplane-salvage ship. The initial portion of the 1965 experimental program was also fired from this ship, but the last portion employed a YCK stationed at NOLTF, Solomons. The YCK was a wooden hulled barge and had a 6-ton crane which was used in handling the charge and instrumentation.

2.1 INSTRUMENTATION

Both programs were instrumented in essentially the same manner to obtain measurements of several phenomena. These included shock wave pressure-time histories, bubble pulses and migration, maximum bubble radius, and above surface effects.

Shock wave and bubble pulse pressures were detected by a vertical array of piezoelectric (PE) gages. For the first program, up to 13 gages were located on two strings with depths ranging from 20 feet below the water surface to 20 feet below the charge. The gages were equally spaced vertically at 20-foot intervals for ranging purposes. For the second program, as many as 10 PE gages were used. Only one vertical string was used. Vertical gage spacing was the same as the previous program; however, some doubling up of gages was done at crucial stations to provide backup capability.

The signals generated by the PE gages were fed through approximately 1200 feet of signal-free cable to termination units and into a tape recorder located on the firing ship. The tape recorder used was an Ampex FR-600 14-channel magnetic tape recorder having a frequency response of about 20 Kcps. Recording speed of the FR-600 was 60 ips. 10 Kcps timing was applied to one channel; calibration steps for converting deflections to pressure were applied to the other channels immediately prior to each shot. The amplifier gain for each channel was set for the pressure level expected at that position. A gain changer was employed to increase the gain of the recording equipment by a factor of 15 after passage of the shock wave, so that the bubble pulses would produce about the same vertical deflection as did the shock wave.

Measurements of the maximum bubble radius were made with the NOL bubble probe, a continuous resistance type probe which detects the position of the bubble interface by measuring the resistance change caused by the non-conductivity of the bubble gases as compared to the conductivity of the saline water (Phillips and Scott, 1965). The change in resistance produces a change in current of an electrical circuit which is detected by an AC current probe. Recording was done on Polaroid film on a Tektronix 565 oscilloscope. The measuring length of the probe was about 4 feet.

Problems were experienced with the bubble probe on the initial program. In order to obtain adequate sensitivity, it is necessary that the fixed resistance of the transmission cable be small compared to the change in resistance producedby the displacement of water by the bubble. The high resistance of the long cable used, combined with greater conductivity of the water due to higher salinity than expected, rendered the probe relatively insensitive to changes produced by the bubble. The calibration curve obtained is shown in Figure 2.1; it will be noted that only a 12 percent change in current was obtained over the first half of the probe, rather than the 50 percent change that had been obtained in previous uses of the probe.

For the 1965 program, No. 0 cable was used which has a resistance of only 0.1 ohm/1000 feet. The calibration curve obtained on this program is also shown in Figure 2.1. For this series, a 40 percent change was obtained over the first half of the probe, which represents adequate sensitivity for obtaining the proper bubble measurements.

Photographic coverage was obtained by two 35mm cameras. The cameras were located aboard the firing ship, about 700 feet from the charge and were located on deck, about 15 feet above the water. These cameras generally were equipped with 50 and 100mm lenses and were operated at a speed of 64 fr/sec. Plus-X film was used and 100 cps timing dots were applied along the edge of the film for determining the actual frame rate. The photographic coverage was obtained primarily to correlate discontinuities in the observed surface effects with the times of the bubble pulses and to detect pulses near the surface which would not appear on the PE records.

Scales on the photographic records were determined by photographing a stadia pole located on the charge support barrel. The pole was approximately 12 feet long and painted alternating black and white stripes at one-foot intervals. A one-foot square white board, with a black line located horizontally through the center, was located at the top of the pole. Generally, the scale was determined by measuring the distance between the top of the charge barrel and the horizontal line. Since the stadia pole was constantly in motion due to wave action on the barrel, several frames were measured and the maximum value used to calculate the scale, as it was assumed that this measurement represented the pole in the vertical position.

During the course of the first experimental program, an accelerometer and velocity meter were added to the probe to detect any motion of the probe due to shock wave or water flow from the expanding bubble. The accelerometer used was a Statham strain gage linear accelerometer having a range of ± 25 g. The velocity meter was a Consolidated Electronic Company (CEC) inductance type meter. The output of both instruments was displayed on Tektronix oscilloscopes and recorded on Polaroid film. For the second experimental program, two accelerometers were used. Both were Statham strain gage accelerometers, one having a range of ± 10 g, the second a range of ± 25 g. Output of these strain gages were amplified and recorded on the FR-600.

On the 1965 series, a fiducial mark was provided on the timing channel of the FR-600 and to the timing lights of the motion picture cameras to indicate the actual time of detonation. This was done by monitoring the current flow through the bridge wire of the detonator, a decrease in current indicating when the bridge wire broke. The travel time to the PE gage located nearest the probe relative to this fiducial was converted into distance using the velocity of the detonation wave through the explosive and the shock wave through the water. As the position of the gage relative to the tip of the probe was accurately known, a value of the initial standoff of the probe was obtained. This method of determining initial standoff was included in this program because of the importance of this value and the possibility that the nominal standoff distance determined from surface suspension points would be subject to the unknown action of tides and currents. In most cases the nominal and measured distances agreed quite well; however, on some shots the probe was almost three feet closer than planned.

2.2 CHARGES

2.2.1 Pentolite. Both charge weights of pentolite were spherical in shape and were cast. Two of the 50-lb charges were cased, two were bare. Almost all of the 300-lb charges had the bottom half covered with a case, as this portion was used to suspend the charge. On a few charges, the upper portion of the case was left on. The cases were constructed of 1/8-inch thick aluminum. The charges were cast at the Naval Weapons Station (NWS), Yorktown, Virginia, except for the two bare 50-lb charges, which were cast at NOL. These two charges were centrally detonated by a single Engineers' Special detonators wired in parallel. No booster was necessary for these charges. A drawing of the 300-lb pentolite charge is shown in Figure 2.2.

2.2.2 Lithanol. The Lithanol charges were also spherical in shape. Because this explosive is a loose mixture, it was fully cased. These cases were also constructed of 1/8-inch thick aluminum. The explosive composition was mixed at NWS, sealed in plastic bags, and shipped to NOLTF, Solomons, where the charges were actually loaded. This procedure was followed because the lithium perchlorate is hygroscopic. While the trihydrate is the most stable of the lithium perchlorates, previous batches of this material were found to contain considerable excess water. The Lithanol charges were centrally boostered with pentolite spheres and detonated with Engineers' Special detonators. Two of the 50-lb charges contained 1-lb boosters and two contained 2-lb boosters. All of the 300-lb Lithanol charges contained 10-lb pentolite boosters. A drawing of a 300-lb Lithanol charge case is shown in Figure 2.3.

2.2.3 H_2O_2/Al. Unlike the other charges, the H_2O_2/Al charges were cylindrical ~~in shape~~. A drawing of the 300-lb case is shown in Figure 2.4. As with the 8- and 16-lb charges, this shape was necessary since the aluminum wool had to be compressed before it was loaded into the case; and pressing the wool into shapes that would fit a cylinder could be readily done. The cylindrical walls were constructed of 3/16-inch aluminum; the top and bottom were constructed of 3/4-inch aluminum.

Concentrated hydrogen peroxide is extremely reactive with certain metals and organic compounds (FMC Bulletin 104). Therefore, extreme caution was necessary in manufacturing the wool and cases. The aluminum wool used in the charges was made by machining solid bar stock at a controlled rate. No lubricating oil, which would contaminate the wool, was required for this process. Individual strands were about 0.005 inches thick and 0.012 inches wide and were quite similar to strands in steel wool. Type 11 - medium grade - hard temper 1060; Mil-A-4864(ASG) aluminum was used. Special handling was used at all times to insure that the wool would not become contaminated.

The wool was pressed into discs and toroidal shaped sections, 1-1/4 to 1-3/4 inches thick, so as to stack in the case and around the booster and detonator tube. Attempts were made to obtain uniform volumes for each section by pressing to machine stops rather than to a predetermined ram pressure. Rams and dies were made of aluminum and stainless steel in order to prevent contamination.

The hydrogen peroxide is a liquid, and a 98 percent concentrated solution was used. The booster and aluminum wool were loaded in the cases at NOL; however, the peroxide was not added until just before the charges were placed in the water for firing. While elaborate precautions had been taken in manufacturing the cases, in pressing and loading the aluminum wool, and in handling the cases to prevent contamination, it was possible that small amounts of contaminants remained in the case and wool. Contact of peroxide with these contaminants over a long period of time could produce sufficient gas to rupture the case or force some of the peroxide out of the case. Even if precautions were taken to prevent rupture or catch spillage, the amount of peroxide would be reduced and the required explosive output would not be obtained.

The loading procedure for the 50-lb H_2O_2/Al charges was similar to that used for the 8- and 16-lb charges. Because of the large cases and consequently greater amount of peroxide required for each charge, the procedure was modified somewhat for the 300-lb charges. This loading procedure is illustrated in Figure 2.5. The case was evacuated through the hose located on top of the case, and peroxide drawn from the shipping drum through the hose located in the bottom of the case. When peroxide appeared in traps located in the vacuum line, the case was considered loaded. The shipping drum was weighed before and after loading to determine the amount of peroxide loaded into each charge, with allowance made for spillage. Valves were located in both the vacuum and filling lines to control filling of the case. The filling line contained two valves; after completion of filling, the hose was cut between the two, the second valve being used to keep the peroxide in the case.

As with the 8- and 16-lb charges, difficulty was experienced in obtaining the proper percentage mixture of the constituents. The actual percentage composition of these charges is given in Table 2.2. As can be seen, the average percentage composition for the 50-lb charges was only about 0.6 percent different from the required composition; for the 300-lb charges, the average was about 2.2 percent different from that required. Fortunately, this percentage difference for the 300-lb charges was in terms of excess aluminum; excess hydrogen peroxide would have introduced permanent gases into the explosion bubble.

2.3 CHARGE AND INSTRUMENT RIGGING

The method of supporting the charge and instrumentation was essentially the same for both programs. The method used on the second series is illustrated in Figure 2.6. The charge and probe were supported by vertical cables attached to surface floats. Three 55-gallon drums were used in each of the two float assemblies for supporting the probe; the horizontal distance between the floats was 10 feet for the first series and 15 feet for the second series. The change in horizontal distance for the two programs was due to a change in the type of probe holder used. One 55-gallon drum was used to support the charge. The horizontal distance between the charge float and the front probe float varied from shot to shot as the suspension system was designed to position one half of the probe's measuring length (2 feet) within the bubble; thus, expected changes in bubble radii required changes in the charge-to-probe distance.

The vertical cables used to support the probe and charge were made up of sections of 3/8-inch wire rope. One end of each section was fitted with an end link and the other end was made up into an eye. The length of the sections was determined by the height capability of the crane used and the depth of the charge. When using the YSD, cable sections up to 40 feet in length could be handled. The maximum length which could be handled aboard the YCK was 20 feet. Shorter lengths were then used to adjust the overall length to the required charge depth.

A horizontal spacer cable was located just beneath the surface floats. Spacer cables were also located 20 feet above and below the charge. These spacer cables were used to insure proper stand-off distances between the probe and charge in case of unusually strong tidal currents at the charge depth. Weights were attached beneath the charge and probe to provide additional stability.

The two-point suspension for the probe was handled by using a strongback attached to the crane hook. When raising or lowering the probe, the end links were used to stop off the cable while the following sections were attached to the strongback for lifting. This procedure was repeated until the probe was supported on the floats. The lowering of the charge was also done in sections, using lines equipped with release hooks attached to successive end link sections.

In placing the rigging for a test, both the probe and the charge had to be lowered simultaneously, since the horizontal spacer cables near the charge were attached prior to lowering. Also, the horizontal spacer cables near the charge had to be under tension at all times to prevent fouling with the probe.

The method of holding the probe was somewhat different for the two programs and is illustrated in Figure 2.7. On the initial program, there was concern that cables between the probe and charge would wrap around the probe during the shot, thus shorting it out. Therefore, the probe was located at an angle of 45 degrees above the horizontal. After difficulty was experienced in obtaining data with the probes, the probe was moved to a horizontal position as it was considered possible that the probe was experiencing some unusual motion in the 45 degree position. As indicated previously, the problem was subsequently found to lie in the sensitivity of the probe.

Because no problems were experienced with shorting of the probe, a simpler suspension method was used for the 1965 program. The probe was located on the end of a solid circular steel bar 3-1/2 inches in diameter and 20 feet long. This bar, which weighed about 650 pounds, was used to provide mass and thus minimize any motion of the probe due to water flow from the expanding bubble.

The two vertical cables were also used to support the PE gage strings. Gages were located on both strings on the first program; only the front cable was utilized on the second.

After the entire rig was at the proper depth, it was then towed away from the ship to a distance of about 700 feet, where the charge was detonated. A series of floats (5-gallon cans) along the tow cable supported the PE gage, probe, and firing cables. The tow cable was attached to the spacer cable beneath the floats, and this line was kept under tension to maintain the proper spacing of probe and charge. The rig was also towed with the tide so that the current assisted in maintaining proper orientation.

TABLE 2.1 EXPERIMENTAL CONDITIONS

Shot No.	Date	Explosive	Total Weight of Explosive (lb)	Booster Weight (lb)	Depth of Burst[1] (ft)
PW-22	9/25/64	Pentolite	316	--	100
PW-23	10/1/64	Pentolite	310	--	80
PW-24	10/21/64	Pentolite	315	--	80
PW-25	10/26/64	Pentolite	314	--	100
PW-26	11/4/64	Lithanol	284	10	100
PW-27	11/9/64	Lithanol	285	10	100
PW-28	11/9/64	Pentolite	316	--	100
PW-29	11/10/64	Pentolite	312	--	60
PW-30	11/10/64	Lithanol	286	10	60
PW-31	11/16/64	Lithanol	300	10	60
PW-32	11/16/64	Lithanol	286	10	80
PW-34	8/5/65	Pentolite	50[2]	--	99.0
PW-35	8/12/65	Pentolite	50[2]	--	100
PW-36	8/13/65	H_2O_2/Al	41.1	1	100
PW-37	8/16/65	H_2O_2/Al	41.9	1	99.0
PW-38	8/17/65	H_2O_2/Al	44.7	1	99.3
PW-39	8/24/65	Pentolite	304	--	80
PW-40	8/25/65	H_2O_2/Al	257	9	80
PW-41	8/27/65	H_2O_2/Al	261	9	80
PW-42	8/30/65	Pentolite	306	--	100
PW-43	9/2/65	H_2O_2/Al	263	9	100

TABLE 2.1 EXPERIMENTAL CONDITIONS
(continued)

Shot No.	Date	Explosive	Total Weight of Explosive (lb)	Booster Weight (lb)	Depth of Burst 1/ (ft)
PW-44	9/3/65	H_2O_2/Al	265	9	100
PW-45	9/7/65	Pentolite	53.8	--	98.1
PW-46	9/7/65	Lithanol	52.0	1	98.0
PW-47	9/7/65	Lithanol	53.3	2	99.0
PW-48	9/9/65	Lithanol	52.2	1	97.5
PW-49	9/9/65	Lithanol	52.2	2	97.3
PW-50	9/9/65	Pentolite	53.8	--	97.0
PW-52	10/13/65	Pentolite	303	--	60
PW-53	10/13/65	H_2O_2/Al	267	9	60
PW-54	10/14/65	H_2O_2/Al	265	9	60

1/ Water depth for all shots was 150 ft.

2/ Nominal weight.

TABLE 2.2 ACTUAL COMPOSITION OF H_2O_2/Al CHARGES

Shot No.	Wt. of H_2O_2 (lb)	Wt. of Al (lb)	Total Weight (lb)		Percentage[1/] H_2O_2	Percentage[1/] Al	Booster Weight (lb)	Total Explosive Weight (lb)
PW-36	25.8	14.3	40.1		64.3	35.7	1.0	41.1
PW-37	26.6	14.2	40.8		65.2	34.8	1.0	41.8
PW-38	29.4	14.3	43.7		67.3	32.7	1.0	44.7
				MEAN	65.6	34.4		
PW-40	156.5	91.7	248.2		63.1	36.9	9.2	257.4
PW-41	161.5	90.7	252.2		64.0	36.0	9.2	261.4
PW-43	160.0	93.9	253.9		63.0	37.0	9.0	262.9
PW-44	160.0	96.3	256.2		62.5	37.5	9.1	265.4
PW-53	160.0	97.5	257.5		62.1	37.9	9.1	266.6
PW-54	158.0	97.2	255.2		61.9	38.1	9.4	264.6
				MEAN	62.8	37.2		

1/ Desired percentage composition was 65/35.

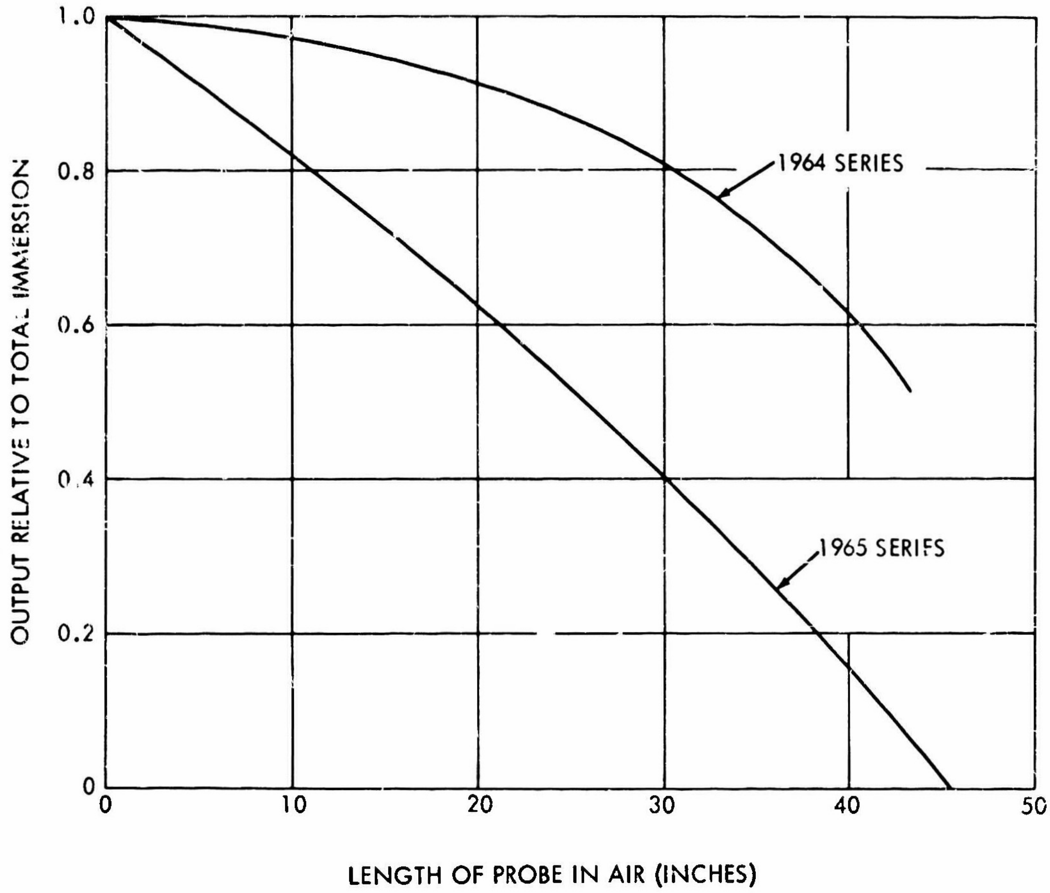

FIG.2.1 PROBE CALIBRATION CURVES

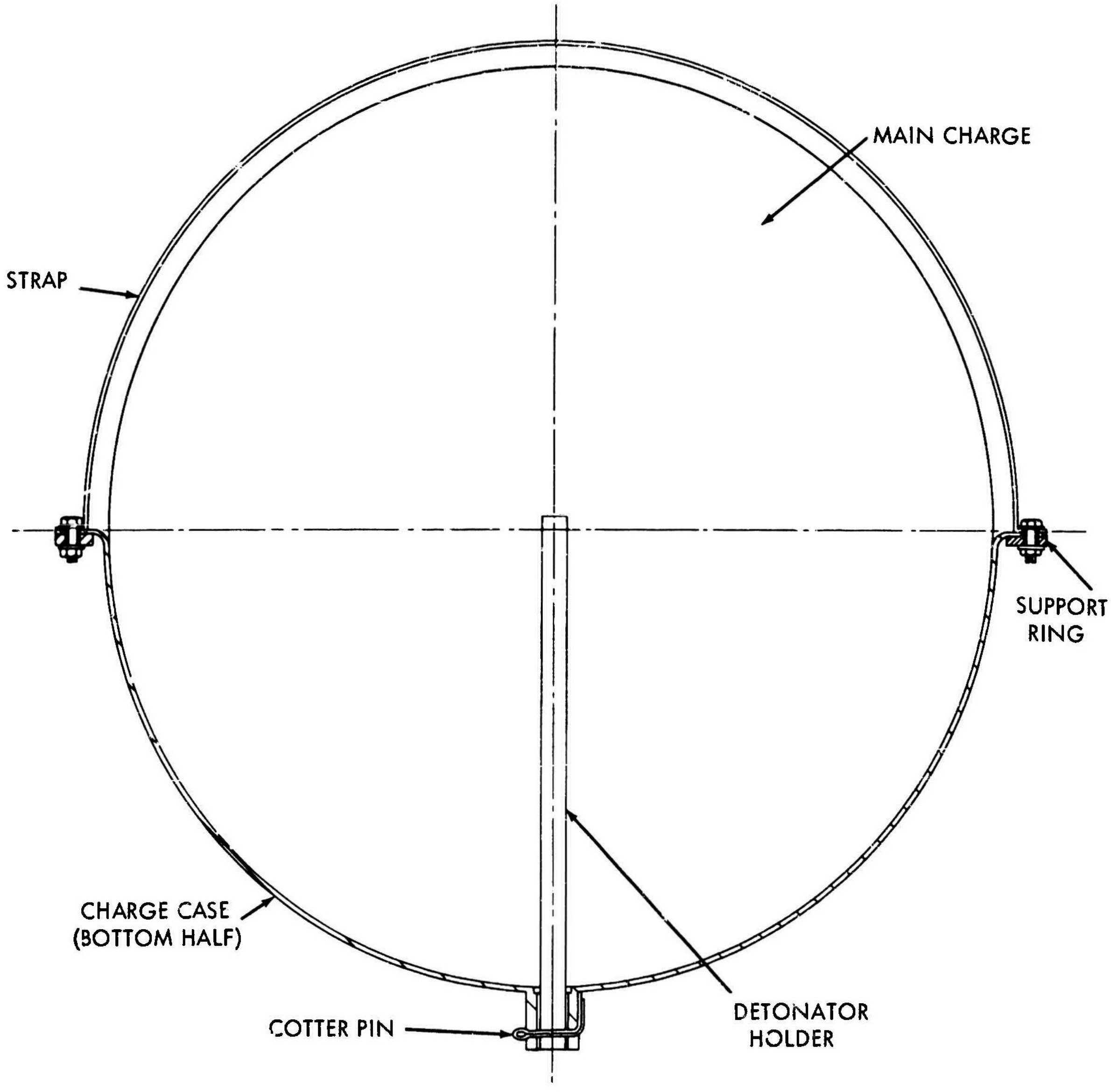

FIG. 2.2 300 - LB PENTOLITE CHARGE

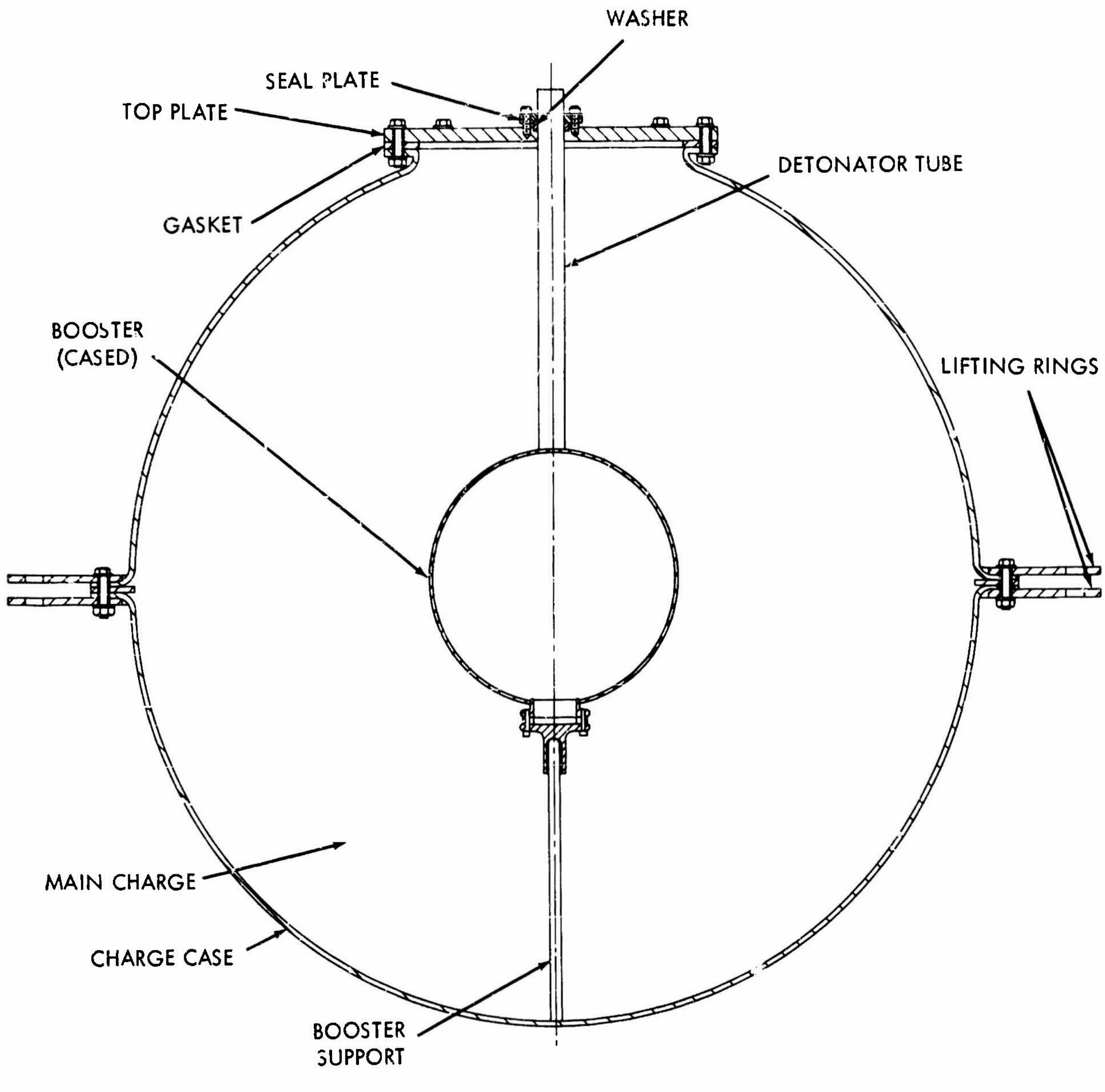

FIG. 2.3 300 - LB LITHANOL CHARGE CASE

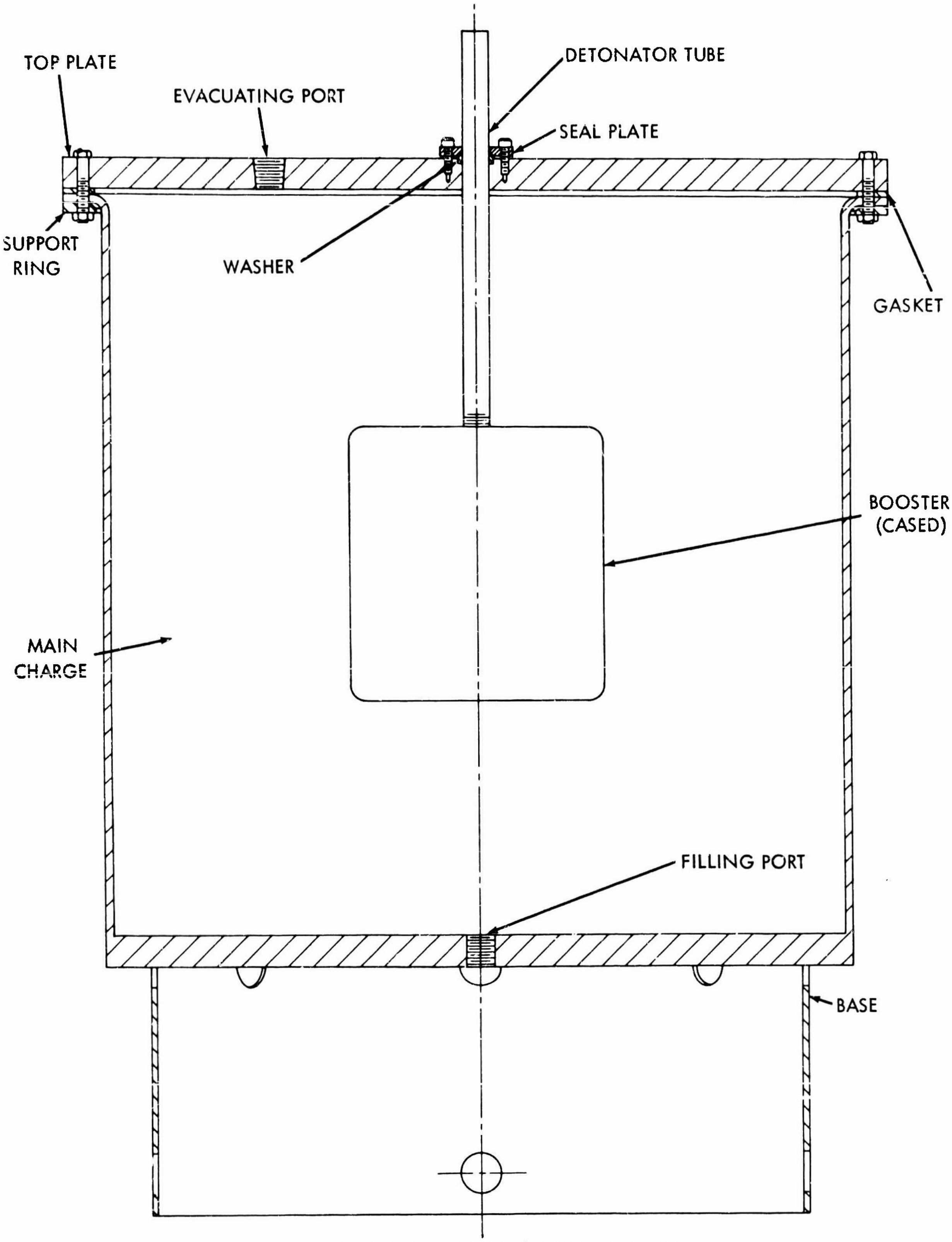

FIG. 2.4 300 - LB H_2O_2/Al CHARGE CASE

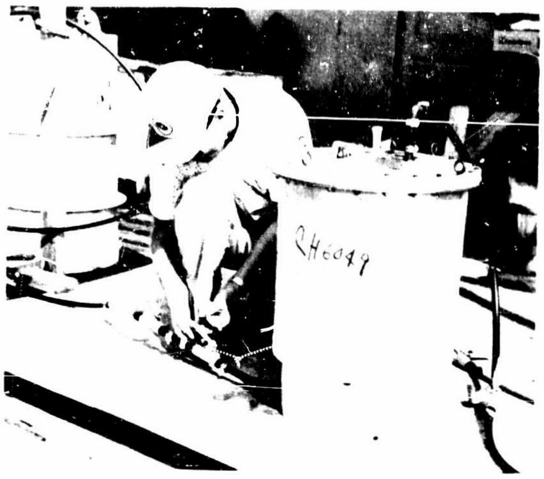

PREPARING 300-LB H_2O_2 Al CHARGE CASE FOR LOADING

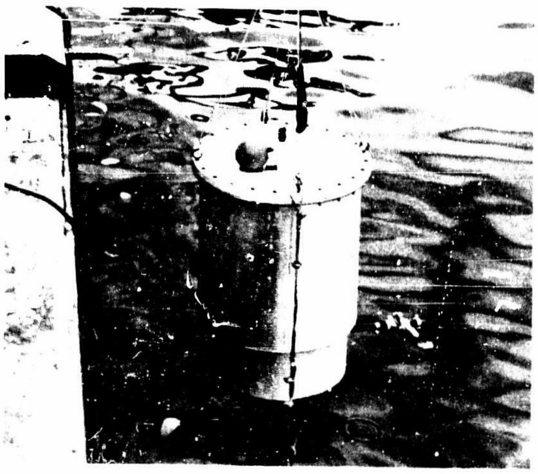

PLACING LOADED CHARGE IN WATER

FIG. 2.5 300-LB H_2O_2 Al CHARGES

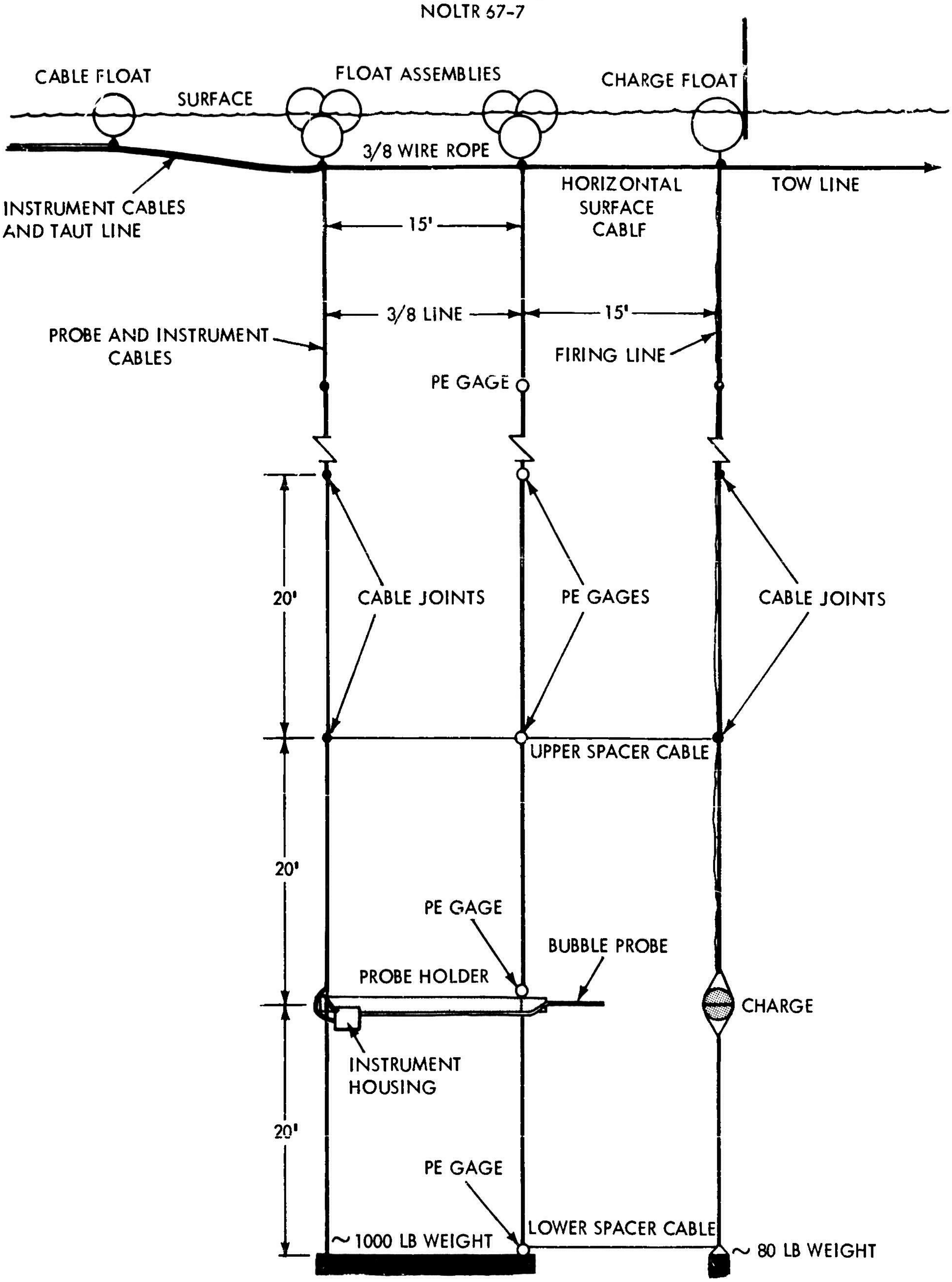

FIG. 2.6 CHARGE AND INSTRUMENTATION RIGGING

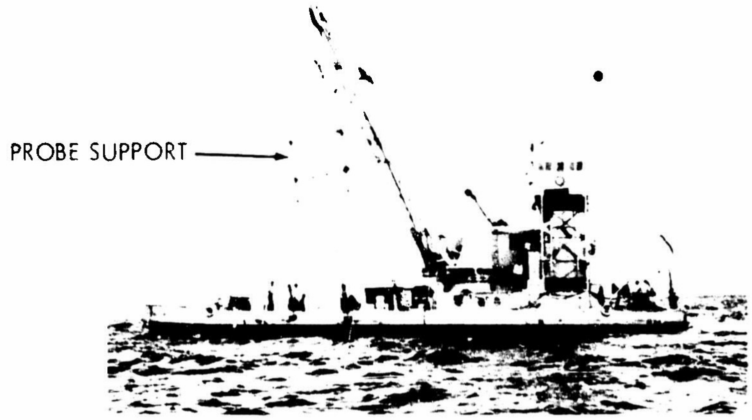

PROBE SUPPORT - 1964 PROGRAM

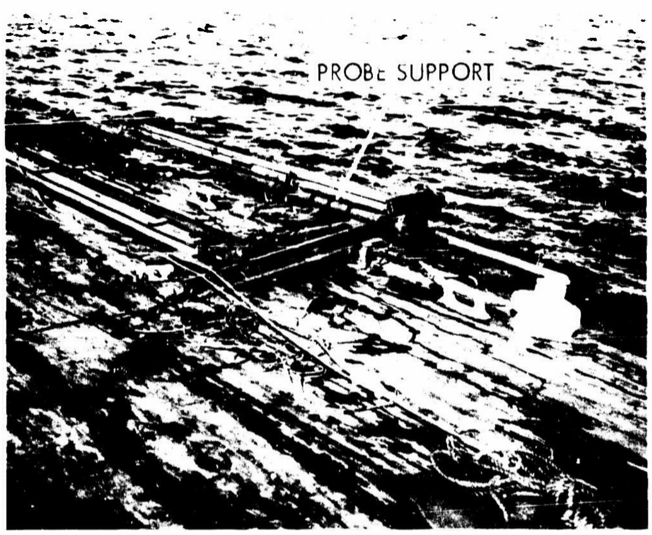

PROBE SUPPORT - 1965 PROGRAM

FIG. 2.7 PROBE SUPPORT METHODS

3. LITHANOL RESULTS

The underwater data obtained from the Lithanol charges are reported in two parts--one for the shock wave effects and one for the bubble effects. Both sets of data are compared with the values for pentolite, where available. The same organization of results from the H_2O_2/Al charges is used in Chapter 4. The photographic analysis of all of the above surface phenomena will be reported in Chapter 5.

3.1 UNDERWATER SHOCK WAVE

While the 50-lb and 300-lb Lithanol charges were fired in two separate programs, recording and subsequent analysis of the pressure-time records was essentially the same. The tape records were played out for measuring purposes on a Minneapolis-Honeywell Visicorder. Generally, six or seven channels were played out simultaneously for convenience in time comparisons used for bubble ranging. Playback speed of the FR-600 was 15 in/sec, Visicorder speed was 160 in/sec. The Visicorder records were converted to digital form by use of a Telereadex, which provided a series of X and Y co-ordinates of the pressure-time curve on punched cards. Calculations of pressure and time, and integration of these digitized data were performed on the IBM 7090 digital computer.

Peak pressures were obtained by plotting the initial portion of the pressure-time curve on semi-logarithmic paper and drawing a straight line through the data, the pressure indicated by this line at zero time being taken as the peak pressure. This method is commonly used by those engaged in shock wave analysis work to eliminate effects such as difficulty in reading the true peak, gage "overshoot", and inadequate frequency response of the recording system (Slifko and Farley, 1959).

For the pentolite charges, energy and impulse were determined out to 5θ*. At this time, the pressure had essentially returned to the baseline. In the case of the Lithanol charges, a "hump" on the shock wave trace (See Fig. 3.1) precluded determining realistic values of θ. This hump probably resulted from the reflection of the detonation wave by the charge case. Therefore, these records were integrated to a point where the pressure had essentially returned to the baseline.

Gage distances had been chosen primarily on the geometric criteria for ranging the bubble migration. For the 300-lb charges, this resulted in obtaining shock wave data over a relatively small scaled distance. It also resulted in obtaining a large number of data points at positions close to the charge and few data points at more distant positions, since these further out gages (corresponding to the upper gages on the array) were not used on the shallower shots. Therefore, it was not possible to obtain a meaningful least squares fit to these data as a function of distance. Instead, the 300-lb data were fitted by assigning a value to the exponent based on previous results, and varying the coefficient to

* θ is defined as the time constant of the shock wave. (Cole, 1948)

obtain a value where the plus and minus scatter was a minimum. The coefficient obtained at this point and the assigned exponent were then taken as representing the best fit to the data. This method was also applied to the 50-lb data to make a more meaningful comparison between the various weights.

3.1.1 <u>50-lb Charges</u>. Pressure-time records were obtained on all four of the 50-lb Lithanol charges. For comparison purposes, shock wave information was also obtained from three 50-lb pentolite standards. Analysis of the pressure-time records yielded the values given below for the coefficients. For Lithanol, the exponents used were obtained with the 8- and 16-lb charges and are given in Table 1.1; the pentolite exponents are from the report by Thiel (1961), which for the sake of completeness have also been included in Table 1.1.

Pentolite:

$$C_P = 2.31 \times 10^4 \tag{3.1}$$

$$C_E = 2.49 \times 10^3 \tag{3.2}$$

$$C_I = 1.34 \tag{3.3}$$

Lithanol:

$$C_P = 1.17 \times 10^4 \tag{3.4}$$

$$C_E = 1.32 \times 10^3 \tag{3.5}$$

$$C_I = 1.63 \tag{3.6}$$

(The subscripts, P, E, and I refer to pressure, energy, and impulse, respectively.)

The pentolite results are in excellent agreement with the results reported by Thiel, the peak pressure coefficient being only about 1.5 percent low. The Lithanol results also agree quite well with the 8- and 16-lb results, in this case the peak pressure coefficient is the same.

The standard deviations for the 50-lb Lithanol shock wave parameters are about the same as those found with the 8- and 16-lb charges. In the case of peak pressure, the standard deviation was 10 percent; and about the same value was obtained for the 50-lb pentolite standards. For the 8- and 16-lb charges, the standard deviations in peak pressure were 6 percent for pentolite and 9 percent for Lithanol. This increase in scatter is to be expected for larger weights as it is increasingly difficult to know precisely the location of the gages.

3.1.2 300-lb Charges. Examples of the pressure-time records for the 300-lb Lithanol and pentolite charges are shown in Figure 3.1. Data were obtained on five Lithanol and six pentolite charges. The following coefficients for pressure, impulse, and energy were obtained:

Pentolite:

$$C_P = 2.24 \times 10^4 \tag{3.7}$$

$$C_E = 2.56 \times 10^3 \tag{3.8}$$

$$C_I = 1.35 \tag{3.9}$$

Lithanol:

$$C_P = 1.17 \times 10^4 \tag{3.10}$$

$$C_E = 1.37 \times 10^3 \tag{3.11}$$

$$C_I = 1.62 \tag{3.12}$$

As with the 50-lb charges, the pentolite results agree acceptably with those reported by Thiel. The peak pressure coefficient is about 5 percent low. The Lithanol results agree with the 8- and 16-lb data and with the 50-lb data. Standard deviations for both pentolite and Lithanol were higher than previously noted, the deviation in peak pressure being about 15 percent for both. This increased scatter probably results from the lack of precise knowledge of the standoff distance of the gage string, as the nominal value was used in the calculations. Because there is no significant variation in shock wave parameters over the range of weights fired, it is concluded that there were no detonation problems with Lithanol.

3.2 BUBBLE

Instrumentation was provided to obtain information on periods, migration, and maximum bubble radius. While the two charge sizes were fired at times separated by a year, this instrumentation was essentially the same. The instrumentation was discussed in detail in Chapter 2 and consisted essentially of a vertical string of PE gages and the NOL bubble probe. Tape speed for the playouts was the same as used for the shock wave records (15 ips). Visicorder speed was slower, however, with playback speeds of 10 and 40 ips being used.

3.2.1 50-lb Charges. Typical bubble pulse records for pentolite are shown in Figure 3.2 and for Lithanol in Figure 3.3. The shape of the first bubble pulse is essentially the same for both explosives. The second and third pulses are considerably different, the Lithanol showing many large spikes as opposed to the generally rounded appearance of the pentolite pulses. In actuality, even more spikes were visible on the original playouts than could be shown on these tracings. The time after detonation of the first and successive periods were measured on pressure-time records from at least six gages and an average value obtained for each period. Periods were read to the highest smoothed values of pressure, rather than to any single spike. The average values are given for Lithanol and the pentolite standards in Table 3.1. The value of K for both compositions was computed using the average value for the first period and applying the bottom and surface corrections given in the report by Niffenegger (1953). It will be noted that the value of K for Lithanol is somewhat higher than that measured previously.

Bubble probe measurements were also obtained; however, because the support system for the probe and charge was designed for the 300-lb charges, the resulting measurements are not believed to be sufficiently accurate to permit computation of J. It is probably more accurate to use the ratio J/K and the value of K obtained from the period measurements to obtain a value of J for this charge weight. J/K for the 8- and 16-lb Lithanol charges was 2.84, thus for the 50-lb charges the following values are obtained:

$$J = 15.9 \tag{3.13}$$

$$K = 5.65 \tag{3.14}$$

The measured maximum radii for the Lithanol and pentolite charges are given in Table 3.2 and are compared with radii calculated using J = 12.6 for the pentolite and the above value for Lithanol. It can be seen that the agreement for both compositions is within about one foot which, while not sufficiently accurate for computation of J, does indicate consistency in the method of computing J for Lithanol.

A fourth bubble pulse was observed for the Lithanol composition. While this pulse was quite weak and considerably smaller than that shown for the third pulse in Figure 3.3, it was definitely observed. This pulse was not predicted, since no fourth pulse was observed on Operation Wigwam; and it is generally believed (c.f. Snay, 1960) that a nuclear bubble will have no more than three significant pulses. The appearance of a fourth pulse on these records does not in itself mean that Lithanol does not simulate a nuclear bubble. It is possible that this fourth pulse is not a true bubble pulse resulting from re-expansion but is a series of small pulses from condensation of the remaining steam. It may also result from the small amount of permanent gases left. In the case of the normal chemical explosive, pentolite, at least six pulses were observed, although only four are reported here.

It will be noted in Table 3.2 that there is a more rapid decrease in the second and third period ratios for Lithanol than for those observed with the pentolite charges. This decrease results from the condensation of steam. A comparison of condensation effects on the bubble parameters with those predicted for a nuclear explosion will be made in Chapter 6.

Two different booster weights were used in the Lithanol charges. Shots PW-46 and 48 used 1-lb pentolite boosters; shots PW-47 and 49 used 2-lb boosters. The two different sizes were used to see if reliable detonation would take place with the smaller booster. A small booster is desirable for these charges since the booster produces permanent gases which will affect the bubble pulsations. In addition, the booster reaction products may also combine with products from the main charge and thus alter the desired chemical reaction. No significant difference was detected in either the shock wave or bubble parameters, which is a good indication that Lithanol detonated properly for both booster sizes. Also of importance is the fact that no significant change in successive periods was noted, which indicates that the amount of permanent gases produced over this range of booster weights (approximately 1/50 and 1/25 of the total charge weight) has little effect on the bubble parameters. However, these gases may have affected the observed surface effects (see Chapter 5).

3.2.2 300-lb Charges. Chronologically, the 300-lb Lithanol charges were the first fired of those discussed in this report, being fired in the fall of 1964. Successive periods were measured on these records, similarly to the measurements made later on the 50-lb charges. The average values of periods are reported in Table 3.3, together with ratios of successive periods and the coefficient K computed from the first bubble period. It will be noted that the value of K for these charges is higher than that obtained with the 8- and 16-lb charges, and also higher than that of the 50-lb charges. The value of K for the pentolite standards is also slightly higher, being about 3 percent higher than the generally accepted value for this composition.

Typical bubble pulse records for pentolite and Lithanol charges are shown in Figures 3.4 and 3.5. As with the 50-lb charges, the pulse shapes for Lithanol differ considerably from those observed with the pentolite charges. The first pulse for both is essentially the same, the second and third considerably different. It is believed that the spikes on the Lithanol records result from the condensation processes. Condensation is believed to take place at the minimum due to instability of the bubble at this time. At and near the minimum, considerable mixing takes place and jets of the surrounding water move into the bubble and thus cool and condense the steam. It is believed that it is the impingement of these jets on one another which produces the spikes on the pressure-time records. Strong upward jetting of the bubble from these charges was also noted from measurements of the above surface effects, as discussed in Chapter 5, and this probably accounts for many of the spikes.

The records shown are typical. The same gage position and charge depth were chosen for illustration purposes as the traces varied considerably with gage position and charge depth. This is particularly true for second and third pulses with Lithanol, where the traces appeared to be quite weak when the gage was located below the depth of the bubble pulse. This can also be attributed to the upward jetting of the bubble, as the signals from such impingement would be quite directional.

Values of bubble migration were obtained by finding the depths of successive bubble pulses by directional ranging. The method of ranging used is discussed in detail in Appendix A; essentially it consists of determining the relative arrival time of the pulse at three positions in a vertical array. The ranging method assumes a point source (in actuality the bubble at its minimum size is considerably larger than a point). Spikes on the records (shown in Figures 3.4 and 3.5) were used for ranging, and it was attempted to pick the same spike on each. This selection requires considerable judgment and generally utilizes shapes, amplitudes, and the positions of one spike relative to others in determining a common spike on all records. In some cases, it was possible to follow a single spike with considerable confidence through the entire array; in other cases it was difficult to find with certainty any common spike on the required three records. Several sets of three gages were used to obtain values of the bubble pulse depth; once this was done, it was again necessary to apply judgment as to the best value. This generally was done by comparing the ranged and known horizontal distance of the string (the closer they compared, the higher the confidence) and the vertical position of the pulse relative to the center of the three gages. Ranging of the shock wave had shown that the most accurate depths were determined when the pulse occurred near the depth of the center gage. The best depths were also found where the ranged and known horizontal distances compared most favorably.

The ranged depths of the shock wave and bubble pulses are given in Table 3.4. It is believed that the accuracy of the ranged depth of the shock wave is about 0.5 feet; for the first bubble pulse, it is about 3 feet; for the second bubble pulse, about 5 to 10 feet; and for the third bubble pulse, about 5 to 15 feet. The accuracy of the Lithanol values is near the lower value because of the precision with which the narrow spikes could be read; the pentolite results tended toward the higher values because of the weak and generally rounded shape of the later pulses.

It is thus possible to find the depth with an accuracy which is adequate for most purposes. However, it is not clear that we know exactly what is being ranged, particularly when the bubble is migrating violently. Thus, it has been assumed (Snay et al, 1952) that for the first pulse, the impingement of the bottom of the bubble against the top as the bubble collapses produces a "water-hammer" effect which results in the observed spikes. Ranging of these would give a depth shallower than the center of the bubble. A comparison of ranged and predicted migration is given in Chapter 6.

The 300-lb Lithanol charges represented the first attempt to use the NOL bubble probe on tests of this size. The radii measured are presented in Table 3.5. Because of the difficulties experienced with the probe on this series, as discussed in Chapter 2, the results were not used to calculate J. It is believed a more accurate value of J can be obtained by using the method used for the 50-lb charges; i.e., by use of the J/K ratio. Since the pentolite K for the 300-lb charges was about

3 percent high (possibly because of incorrect surface and bottom corrections), it is probable the value of K for Lithanol was also high by about the same percentage. Reducing the Lithanol K by this amount, and calculating J from this corrected value, the following bubble coefficients are obtained:

$$J = 16.3 \tag{3.15}$$

$$K = 5.75 \tag{3.16}$$

The calculate value of the maximum radius, A_{max}, using the value of J given in Equation 3.15, is shown on Table 3.2. The difference between the calculated and measured A_{max} for Lithanol is about the same as that of the pentolite charges, which tends to substantiate the method of calculation of J for Lithanol.

No attempt was made to thoroughly analyze the velocity meter and accelerometer records because of the lack of sensitivity of the probe. A brief analysis, however, indicated that the probe experienced little motion.

TABLE 3.1 BUBBLE PERIODS AND COMPUTED K FOR 50-lb CHARGES

Shot No.	Weight (lb)	Depth (ft)	T_1 (sec)	T_2 (sec)	T_3 (sec)	T_4 (sec)	$\frac{T_2}{T_1}$	$\frac{T_3}{T_1}$	$\frac{T_4}{T_1}$	K 1/
Pentolite										
PW-34	50 2/	99.0	0.273	0.230	0.205	0.176	0.842	0.751	0.645	4.38
PW-35	50 2/	100	No timing	--	--	--	--	--	--	--
PW-45	53.8	98.1	0.281	0.235	0.210	0.186	0.836	0.747	0.662	4.38
PW-50	53.8	97.0	0.283	0.240	0.210	0.188	0.848	0.742	0.664	4.38
									MEAN	4.38
H_2O_2/Al										
PW-36	41.1	100	No timing	--	--	--	--	--	--	--
PW-37	41.9	99.0	0.376	0.236	0.171	0.142	0.628	0.455	0.378	6.46
PW-38	44.7	99.3	0.362	0.235	0.157	0.116	0.649	0.434	0.320	6.08
									MEAN	6.27
Lithanol										
PW-46	52.0	98.0	0.354	0.217	0.146	0.110	0.613	0.412	0.311	5.61
PW-47	53.3	99.0	0.360	0.225	0.148	0.116	0.625	0.411	0.322	5.70
PW-48	52.2	97.5	0.358	0.224	0.149	0.108	0.626	0.416	0.302	5.65
PW-49	52.2	97.3	0.358	0.226	0.149	0.096	0.631	0.416	0.268	5.66
									MEAN	5.65

1/ K computed from T_1 using surface and bottom corrections from Niffenegger (1953).

2/ Nominal weight.

TABLE 3.2 MEASURED MAXIMUM BUBBLE RADIUS FOR 50-lb CHARGES

Shot No.	Weight (lb)	Depth (ft)	Probe Standoff (ft)	Bubble Over Probe (ft)	A_{max} (ft)	Predicted A_{max} 2/ (ft)	Remarks
Pentolite							
PW-34	50	99.0	7.30	2.44	9.74	9.1	
PW-35	50	100	--	--	--	9.1	No timing; scope did not trip
PW-45	53.8	98.1	4.65	3.40	8.30 1/	9.3	
PW-50	53.8	97.0	6.15	1.44	8.18 1/	9.3	
H_2O_2/Al							
PW-36	41.1	100	--	1.95	--	--	No timing
PW-37	41.9	99.0	5.85	>4.00	>9.85	11.8	Bubble went over probe entirely.
PW-38	44.7	99.3	9.80	1.37	11.17	12.0	
Lithanol							
PW-46	52.0	98.0	8.25	2.28	10.73 1/	11.6	
PW-47	53.3	99.0	9.00	1.89	10.89	11.6	
PW-48	52.2	97.5	9.55	1.08	10.92 1/	11.6	
PW-49	52.2	97.3	7.80	2.38	10.53 1/	11.6	

1/ Radius corrected for vertical displacement of charge relative to the probe.

2/ A_{max} calculated using J = 12.6 for pentolite, 17.3 for H_2O_2, and 15.9 for Lithanol.

TABLE 3.3 BUBBLE PERIODS AND COMPUTED K FOR 300-lb CHARGES (1964)

Shot No.	Wt. (lb)	Depth (ft)	T_1 (sec)	T_2 (sec)	T_3 (sec)	$\frac{T_2}{T_1}$	$\frac{T_3}{T_1}$	K 1/
Pentolite								
PW-22	316	100	0.514	0.472	0.477	0.918	0.928	4.52
PW-23	310	80	0.578	0.594	--	1.028	--	4.56
PW-24	315	80	0.578	0.594	--	1.028	--	4.54
PW-25	314	100	0.504	0.447	0.449	0.887	0.891	4.44
PW-28	316	100	0.501	0.453	0.449	0.904	0.896	4.41
PW-29	312	60	0.654	0.727	--	1.112	--	4.49
							MEAN	4.49
Lithanol								
PW-26	284	100	0.628	0.476	0.445	0.758	0.709	5.79
PW-27	285	100	0.635	0.487	0.462	0.767	0.728	5.85
PW-30	286	60	0.822	0.832	--	1.012	0.582	5.96
PW-31	300	60	0.846	0.817	--	0.966	--	6.05
PW-32	296	80	0.732	0.637	0.752	0.870	1.027	5.97
							MEAN	5.92

1/ K computed from T_1 using surface and bottom corrections from Niffenegger (1953).

TABLE 3.4 SUMMARY OF RANGING RESULTS
FOR 300-lb CHARGES (1964)

Shot No.	Depth (ft)	Ranged Depths: Shock Wave (ft)	m_1 1/ (ft)	m_2 (ft)	m_3 (ft)
Pentolite					
PW-22	100	98.5	86	69	32
PW-23	80	80.0	50	45	--
PW-24	80	80.0	62	40	--
PW-25	100	100.0	85	--	--
PW-28	100	99.5	86	--	30
PW-29	60	61.5	44	-4	--
Lithanol					
PW-26	100	101.0	82	62	22
PW-27	100	100.0	80	64	48
PW-30	60	60.3	35	23	--
PW-31	60	59.0	34	23	--
PW-32	80	80.4	60	40	--

1/ m_1 is first minimum, m_2 is second minimum, etc.

TABLE 3.5 BUBBLE PROBE RESULTS FOR 300-lb CHARGES (1964)

Shot No.	Weight (lb)	Depth (ft)	Probe Standoff (ft)	Bubble Over Probe (ft)	A_{max} (ft)	Predicted A_{max} (ft)	Remarks
Pentolite							
PW-22	316	100	--	>4.0	--	16.8	Rig tangled; Bubble completely over probe
PW-23	310	80	15.3	1.3	16.6	17.7	
PW-24	315	80	15.0	1.5	16.5	17.7	
PW-25	314	100	12.0	>4.0	>16.0	16.8	Bubble completely over probe
PW-28	316	100	14.0	2.1	16.1	16.8	
PW-29	312	60	14.0	2.1	16.1	18.9	
Lithanol							
PW-26	284	100	18.0	2.0	20.0	21.0	
PW-27	285	100	17.0	1.8	18.8	21.0	
PW-30	286	60	19.0	--	--	23.6	
PW-31	300	60	19.0	2.1	21.1	23.6	
PW-32	296	80	18.0	2.0	20.0	22.2	

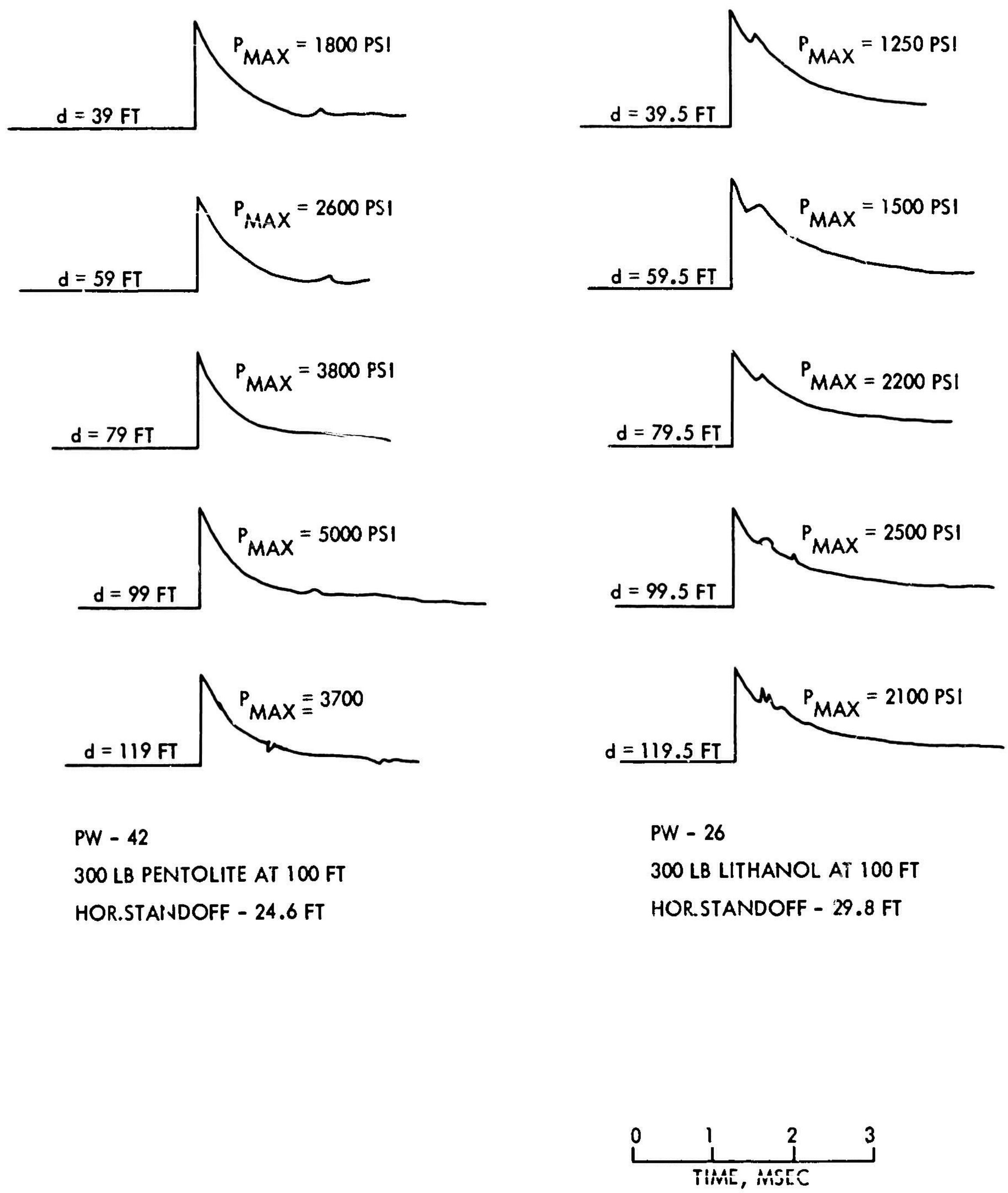

FIG.3.1 TYPICAL SHOCK WAVE RECORDS

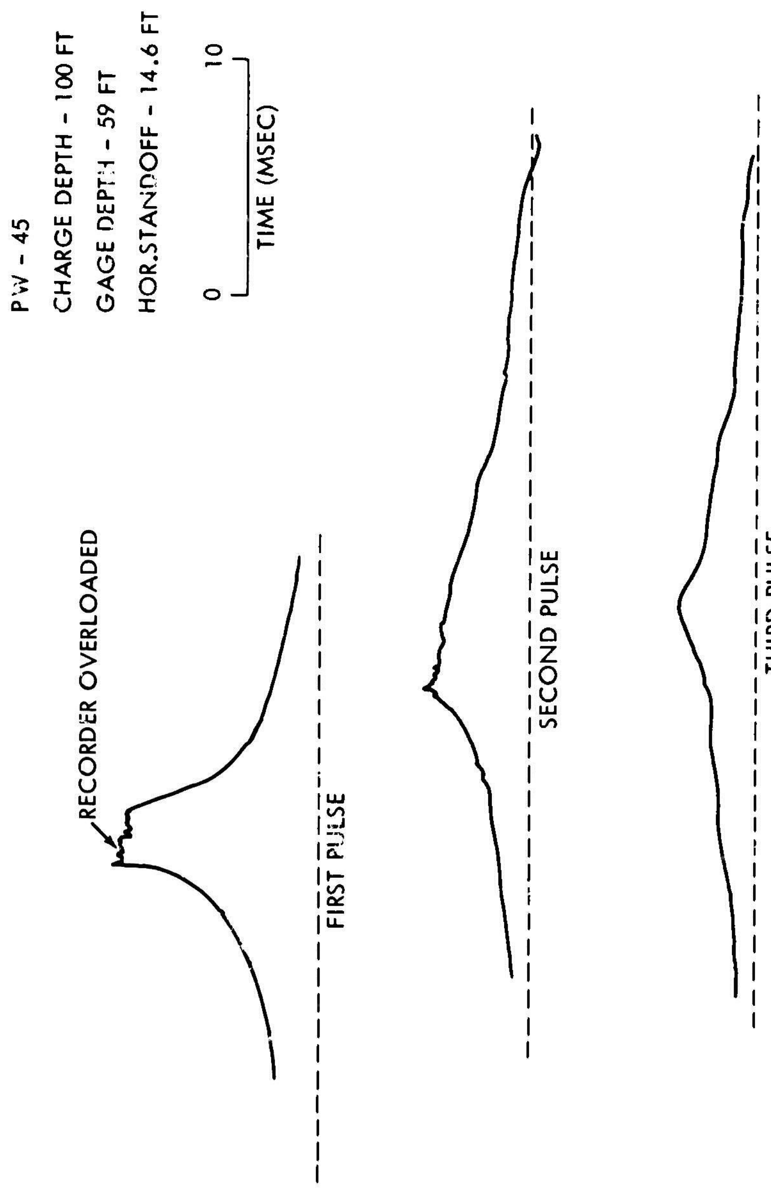

FIG.3.2 TYPICAL BUBBLE PULSE RECORDS, 50 LB PENTOLITE

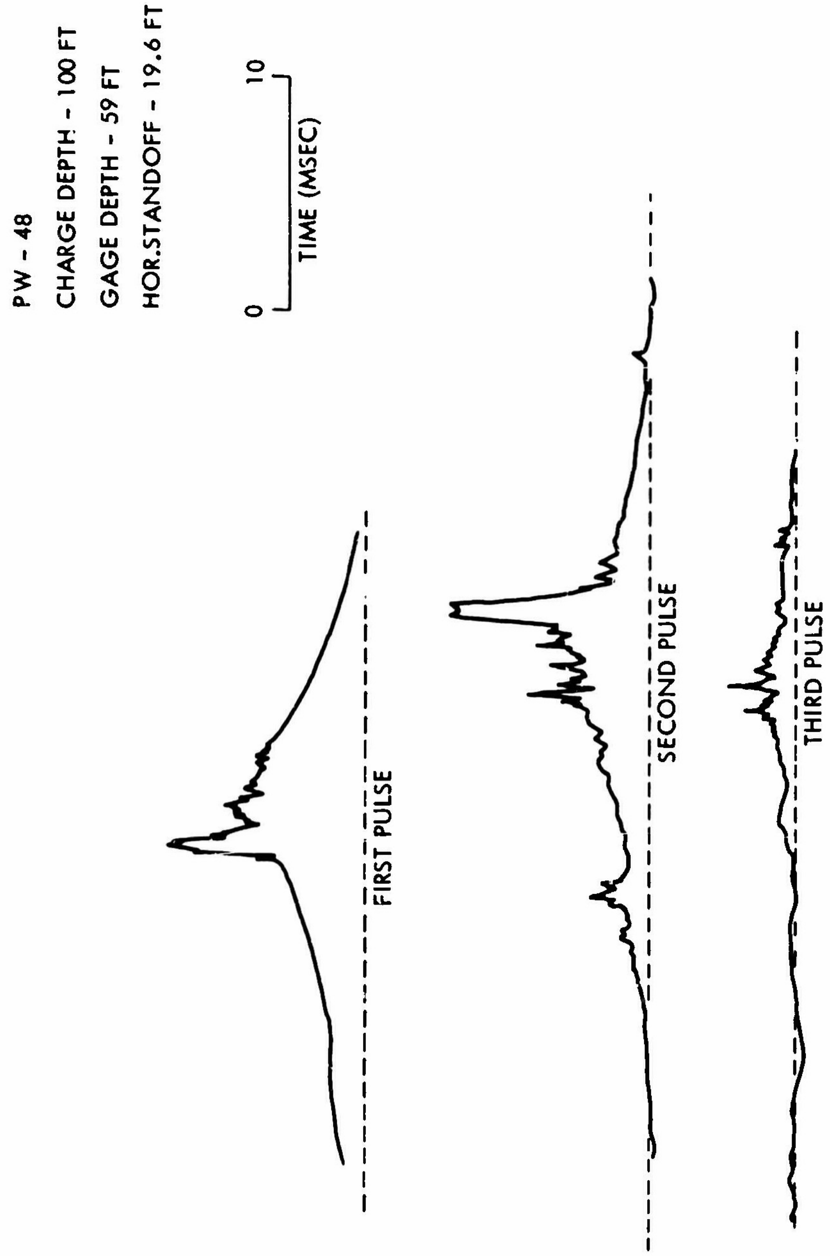

FIG.3.3 TYPICAL BUBBLE PULSE RECORDS, 50 LB LITHANOL

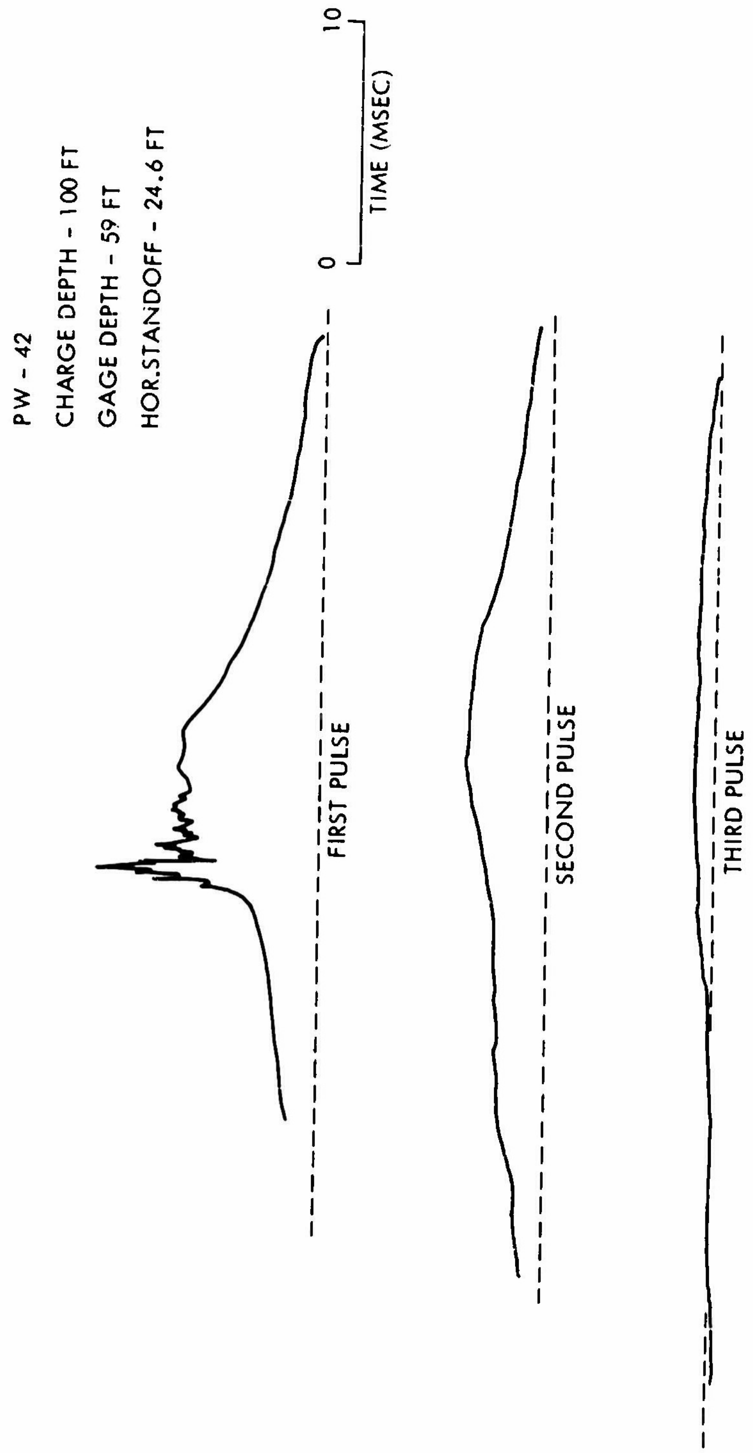

FIG. 3.4 TYPICAL BUBBLE PULSE RECORDS, 300 LB PENTOLITE

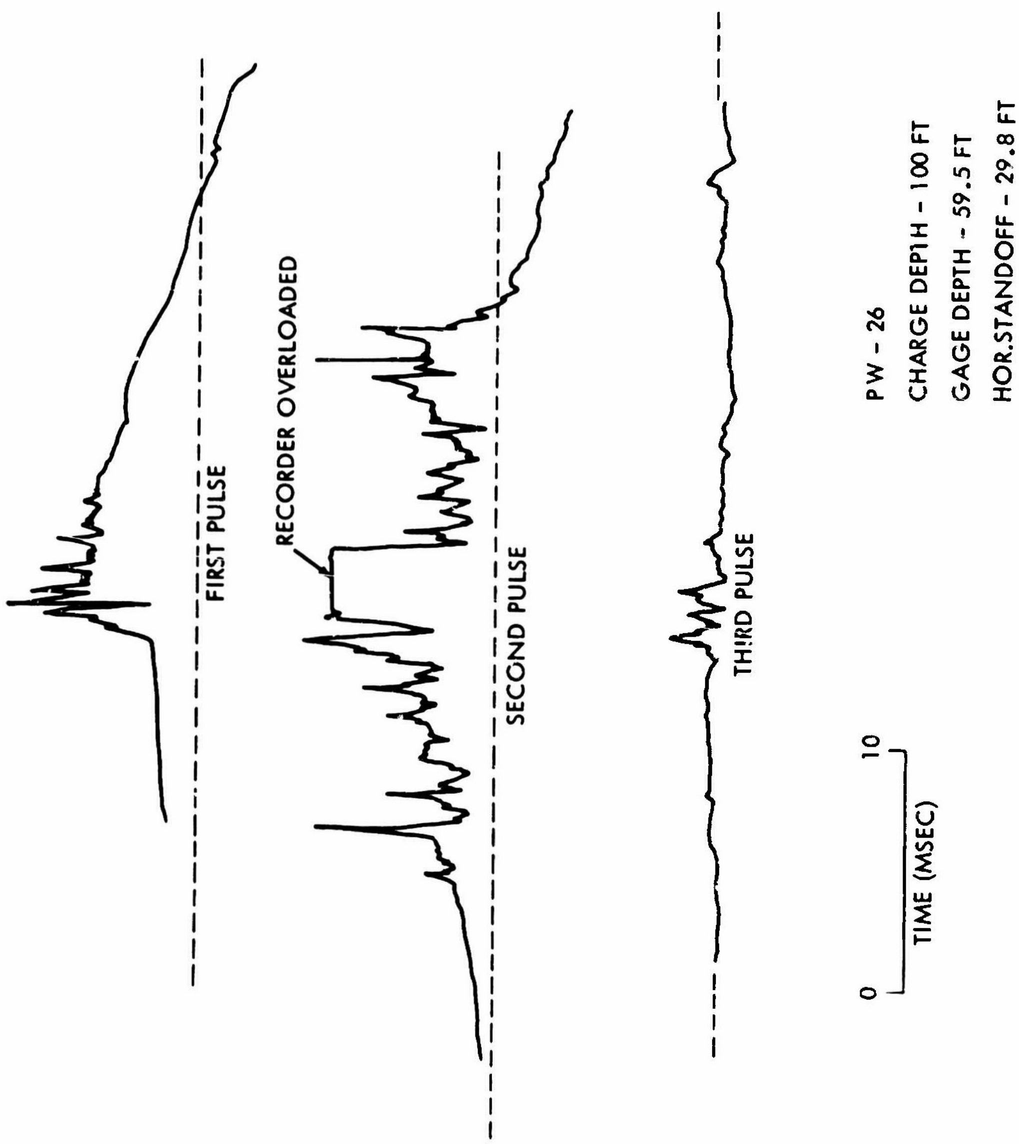

FIG.3.5 TYPICAL BUBBLE PULSE RECORDS, 300 LB LITHANOL

4. H_2O_2/Al RESULTS

4.1 UNDERWATER SHOCK WAVE

Analysis of the shock wave pressure-time records for the two charge weights of the H_2O_2/Al composition was similar to that done for Lithanol. The Visicorder records were manually converted to digital form on the Telereadex and computations and integrations performed on the IBM 7090 digital computer. Peak pressures were determined by plotting the initial portion of the shock wave pressure-time curve on semi-logarithmic paper and drawing a straight line through the data, the pressure at zero time being taken as the peak pressure. As with Lithanol, integrations for the H_2O_2/Al charges were carried out to a point where the trace had essentially returned to the baseline.

4.1.1 50-lb Charges. Of the three 50-lb H_2O_2/Al charges fired, data were obtained on only two, as the timing failed on PW-36. Analysis of the data for the other two shots produced the coefficients given below for the shock wave parameters. The values for the 50-lb pentolite charges used as standards here were reported in Section 3.1.1. As had been done with the Lithanol results, the exponents used to determine the coefficients were obtained from the 8- and 16-lb results, which are given in Table 1.1.

H_2O_2/Al:

$$C_P = 1.60 \times 10^4 \tag{4.1}$$

$$C_E = 3.49 \times 10^3 \tag{4.2}$$

$$C_I = 2.66 \tag{4.3}$$

It will be noted that these values are considerably higher than those obtained with the smaller charges, as given in Table 1.1. The peak pressure is about 84 percent greater, the energy 117 percent greater, and the impulse 23 percent greater. The standard deviation in the data, however, was about the same as that obtained with the 8- and 16-lb H_2O_2/Al charges. For peak pressure, this deviation was about 26 percent; it was 24 percent with the smaller charges of this composition. The increase in the shock wave parameters, together with the improved shape of the pressure pulse, indicates that a more complete detonation took place for these charges than had taken place for the 8- and 16-lb charges. The large scatter in the data, however, still indicates problems in detonation.

The pressure vs distance data from the two 50-lb H_2O_2/Al charges actually differed considerably and the curve given by Equation 4.1 lies between the two sets of data. The peak pressures for Shot PW-37 are perhaps 20 percent higher than the mean, pressures from PW-38 are about 20 percent lower. As noted in Section 4.2.1, a similar difference was observed for the bubble period coefficient, K. Therefore, while the output of these charges is greater than that of the 8- and 16-lb charges, there is considerable doubt that complete high order detonation is taking place.

4.1.2 300-lb Charges. Pressure-time records for the 300-lb H_2O_2/Al charges are shown in Figure 4.1. Data were obtained from three pentolite charges and six H_2O_2/Al charges. The following coefficients for peak pressure, energy, and impulse were obtained:

H_2O_2/Al:

$$C_P = 1.98 \times 10^4 \tag{4.4}$$

$$C_E = 4.48 \times 10^3 \tag{4.5}$$

$$C_I = 2.89 \tag{4.6}$$

Pentolite:

$$C_P = 2.28 \times 10^4 \tag{4.7}$$

$$C_E = 2.59 \times 10^3 \tag{4.8}$$

$$C_I = 1.39 \tag{4.9}$$

The pentolite results again agree favorably with previous results. The H_2O_2/Al results are, as with the 50-lb charges, considerably higher than the 8- and 16-lb results. Peak pressure is 128 percent higher, energy is 178 percent higher, and impulse 34 percent higher. The 300-lb H_2O_2/Al results are also somewhat higher than the mean values of the 50-lb results, peak pressure being about 25 percent higher. The 50-lb shot FW-37 agrees very well with the 300-lb results. Scatter has been reduced considerably for the 300-lb charges. For peak pressure, the standard deviation was 16 percent for the H_2O_2/Al composition, compared to 10 percent obtained with the pentolite standards.

4.2 BUBBLE

4.2.1 50-lb Charges. Typical bubble pulse records for H_2O_2/Al are shown in Figure 4.2. The shape of these curves is the same as that observed with Lithanol. First and successive periods were measured for these charges in the same way as done previously for Lithanol. Because these charges were fired as part of the same series as the 50-lb Lithanol charges, these data have been included in Table 3.1. A similar number of gages were read and average values determined for the periods. As was observed with the lithium perchlorate composition, the value of K is somewhat higher than that measured for the 8- and 16-lb charges.

As with Lithanol, a fourth bubble pulse was observed with the H_2O_2/Al charges. This pulse was very weak but definitely visible on the playouts.

A value of J can be calculated from K using the ratio J/K from the 8- and 16-lb charges. For the hydrogen peroxide charges, this ratio was 2.76. Thus the bubble parameters for the 50-lb hydrogen peroxide composition are:

$$J = 17.3 \tag{4.10}$$

$$K = 6.27 \tag{4.11}$$

As indicated in Table 3.2, a bubble radius was measured on only one of the three H_2O_2/Al shots, Shot PW-38. Calculation of A_{max} from the value of J given in Equation 4.10 shows agreement of less than a foot with this measured radius and, as with Lithanol, is about as good as can be expected from this size charge with the support system used.

It will be noted that there is considerable difference in the values of K obtained for the two H_2O_2/Al charges. Similar to the difference observed with the shock wave parameters, Shot PW-37 is about 30 percent higher than the mean, PW-38 is about 30 percent lower. However, even the lower value of K is higher than the value of K obtained for the 8- and 16-lb charges.

4.2.2 300-lb Charges. Typical bubble pulse records are shown in Figure 4.3. These are similar to the bubble pulses observed with the 300-lb Lithanol charges. As with Lithanol, the pulses varied greatly for gages located above or below the one illustrated. This was particularly true for the second and third pulses, where the amplitude was quite low for gages below the depth of origin of the pulse. Only the general shapes of the pulses are shown; the actual traces contained considerably more spikes than could be shown here.

Period information for the 300-lb hydrogen peroxide charges is given in Table 4.1. The method for obtaining this information is the same as that reported previously for Lithanol. It will be noted that the value of K for the 300-lb H_2O_2/Al charges is higher than either the 8- and 16-lb results or the 50-lb results. The increase in K with increasing charge weight was also noted for Lithanol; this increase will be discussed in greater detail in Chapter 6. The decrease in successive periods due to condensation is also apparent.

Migration information was also obtained by ranging the successive bubble pulses. This information is reported in Table 4.2. As with the Lithanol results, the accuracy of the reported migration decreases with succeeding pulses and, for the later pulses, was more precise for the H_2O_2/Al charges than for pentolite because of the pulse shape. The precision of the migration data for successive pulses is about the same as that reported in Chapter 3.

Successful measurements of the maximum bubble radius were obtained on this program. Using the value of standoff (obtained from the arrival time of the shock wave) and the distance the bubble traversed the probe, the measured value of A_{max} and the computed value of J are given in Table 4.3. If the measured values for J and K for the H_2O_2/Al charges are corrected by the same percentage as the error in the values of J and K for pentolite (2 percent for J, 4 percent for K), agreement of better than one percent is obtained between the experimentally determined K and the one calculated using the ratio J/K from the 8- and 16-lb charges. The experimentally determined bubble parameters for the 300-lb H_2O_2/Al charges thus are:

$$J = 17.3 \tag{4.12}$$

$$K = 6.35 \tag{4.13}$$

As had been noted previously, these values are higher than those previously observed. This will be discussed in greater detail in Chapter 6.

The probe was instrumented with two accelerometers to detect any motion due to water flow from the expanding bubble. The accelerometer records were integrated to obtain a velocity-time curve, which was then integrated to obtain displacement as a function of time. Only records from the 25 g accelerometer were integrated, as the 10 g accelerometer consistently read negative after the shot.

Integration of the accelerometer records indicated that the probe acquired a velocity away from the charge of about 5 - 6 ft/sec. This velocity was imparted to the probe beginning about 30 msec after detonation. By 160 msec after detonation, the accelerometer record had returned to the baseline. This indicated a constant velocity of the probe at this time. Up to 160 msec, the accelerometer measured a displacement of less than 0.5 feet. Continuing the probe at this constant velocity up to the time of the maximum radius would give a total displacement of 1.0 - 1.5 feet. It seems unlikely that the probe continued to move in this manner, however. Rather, it should decelerate and eventually stop moving entirely.

Why no deceleration was indicated on the accelerometer is not known. It may have been a peculiarity of the accelerometer (similar to that observed with the 10 g), or it could have been that the deceleration was too slight to be measured on the records. It thus appears that movement of the probe was about 1.0 (± 0.5) feet, the upper limit assuming a constant velocity, the lower limit the actual measured displacement. Since the range of 0.5 to 1.0 feet is the more likely, the 0.4-foot average difference between the predicted and measured radii appears reasonable as resulting from displacement of the probe.

TABLE 4.1 BUBBLE PERIODS AND COMPUTED K FOR 300-lb CHARGES (1965)

Shot No.	Weight (lb)	Charge Depth (ft)	T_1 (sec)	T_2 (sec)	T_3 (sec)	$\frac{T_2}{T_1}$	$\frac{T_3}{T_1}$	K
Pentolite								
PW-39	304	80	0.574	0.593	--	1.033	--	4.56
PW-42	306	100	0.512	0.470	0.467	0.918	0.912	4.55
PW-52	303	60	0.659	0.740	--	1.123	--	4.57
							MEAN	4.56
H_2O_2/Al								
PW-40	257	80	0.790	0.780	0.708	0.987	0.896	6.79
PW-41	261	80	0.779	0.769	0.717	0.987	0.920	6.66
PW-43	262	100	0.689	0.559	0.546	0.811	0.792	6.55
PW-44	265	100	0.694	0.568	0.540	0.818	0.778	6.57
PW-53	267	60	0.883	8.893	--	1.010	--	6.60
PW-54	265	60	0.887	0.885	--	0.998	--	6.65
							MEAN	6.64

TABLE 4.2 SUMMARY OF RANGING RESULTS FOR 300-lb CHARGES (1965)

Shot No.	Depth	Ranged Depths			
		Shock Wave	m_1 1/	m_2	m_3
	(ft)	(ft)	(ft)	(ft)	(ft)
Pentolite					
PW-39	80	78.6	64	--	--
PW-42	100	98.4	87	69	--
PW-52	60	59.8	41	19	--
H_2O_2/Al					
PW-40	80	78.5	58	25	12
PW-41	80	81.1	60	34	20
PW-43	100	99.1	78	45	25
PW-44	100	99.5	80	53	27
PW-53	60	60.5	34	20	--
PW-54	60	59.8	32	28	--

1/ m_1 is first minimum, m_2 is second minimum, etc.

TABLE 4.3 MEASURED MAXIMUM BUBBLE RADIUS AND COMPUTED J FOR 300-lb CHARGES (1965)

Shot No.	Weight (lb)	Depth (ft)	Probe Standoff (ft)	Bubble Over Probe (ft)	A_{max} (ft)	J
Pentolite						
PW-39	304	78.6	16.1	1.29	17.39	12.48
PW-42	306	98.4	14.6	1.58	16.18	12.29
PW-52	303	59.8	16.3	1.90	18.20	12.27
				MEAN		12.35
H_2O_2/Al						
PW-40	257	78.5	21.2	1.22	22.42	16.99
PW-41	261	81.1	18.4	4.00	22.40	17.00
PW-43	262	99.1	18.8	2.46	21.26	16.88
PW-44	265	99.5	20.1	1.03	21.13	16.79
PW-53	267	60.5	23.0	1.18	24.18	17.01
PW-54	265	59.8	22.6	1.84	24.44	17.24
				MEAN		16.98

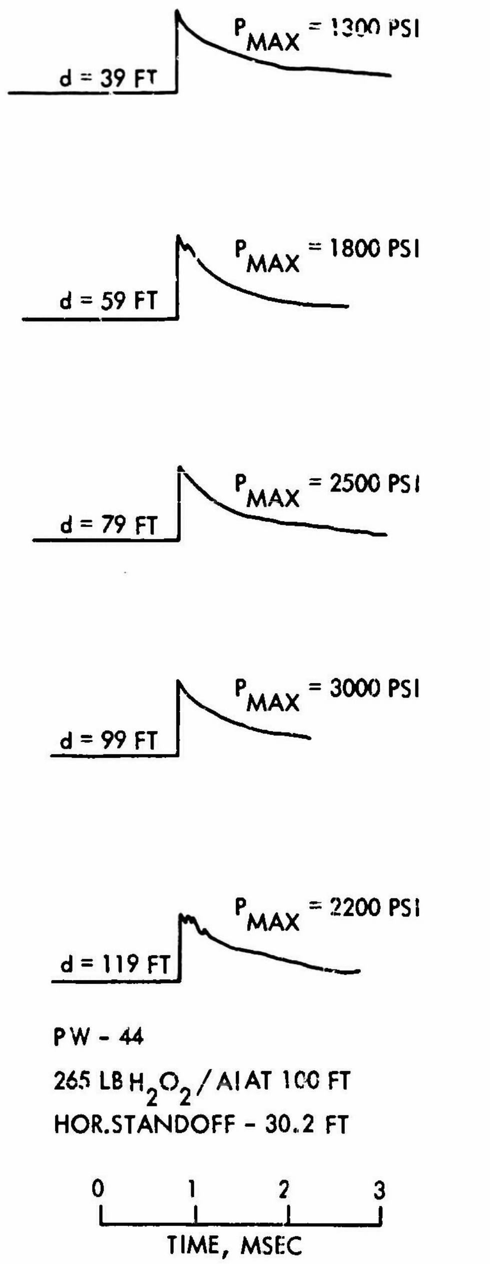

FIG.4.1 TYPICAL SHOCK WAVE RECORDS

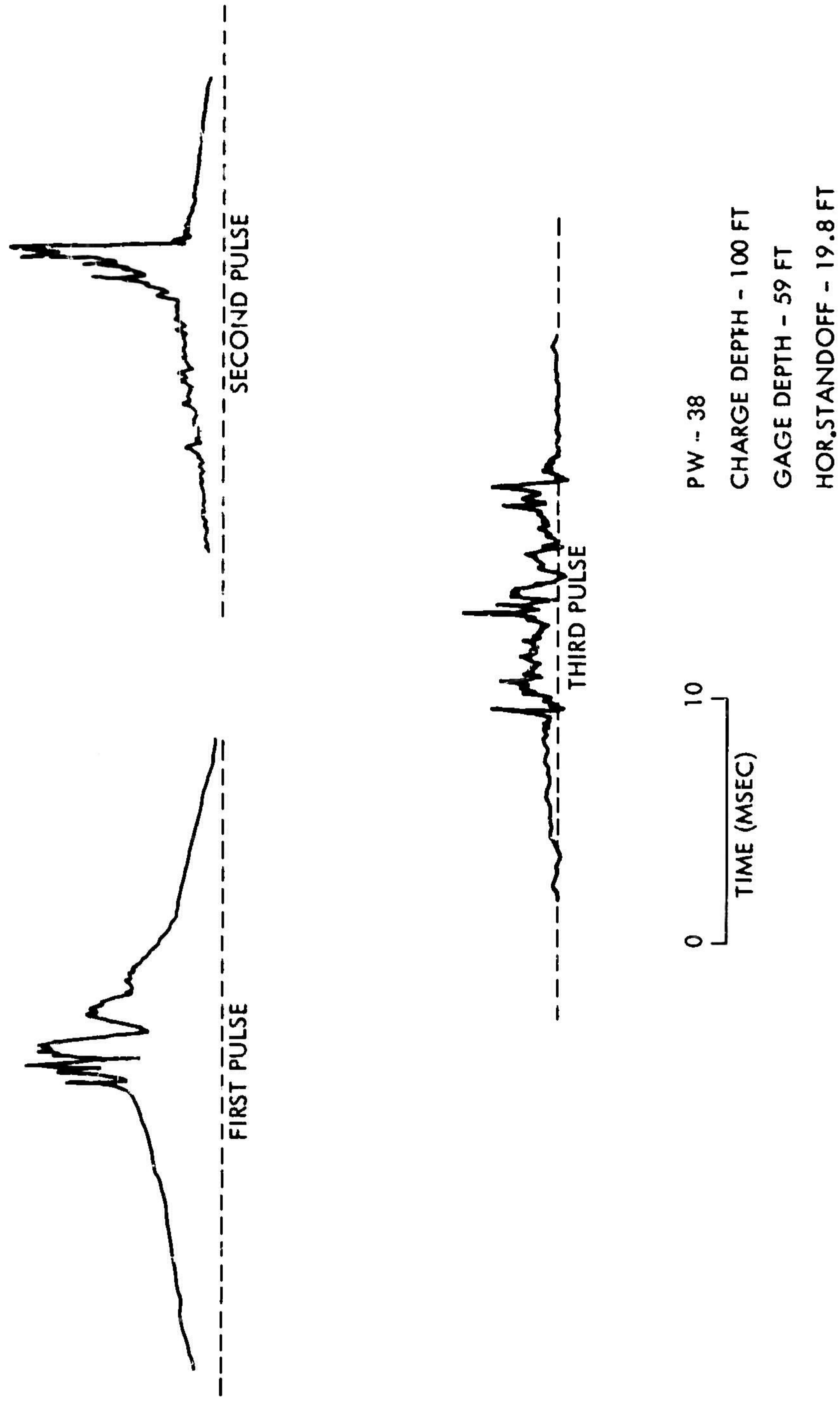

FIG. 4.2 TYPICAL BUBBLE PULSE RECORDS, 50 LB H_2O_2/Al

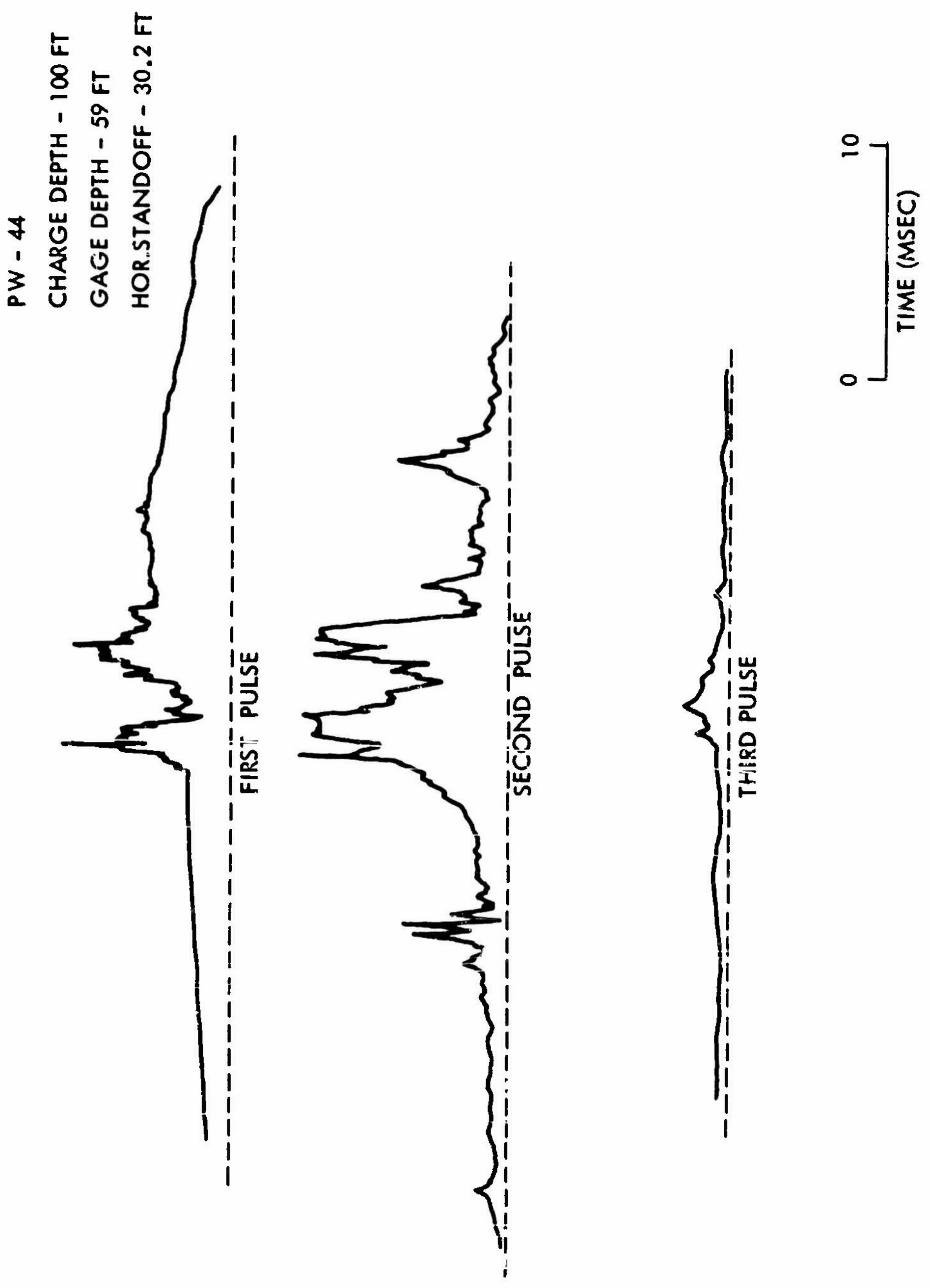

FIG.4.3 TYPICAL BUBBLE PULSE RECORDS, 265 LB H_2O_2/Al

5. PHOTOGRAPHIC RESULTS

5.1 50-lb CHARGES

The surface phenomena observed with the 50-lb charges were very limited, since these charges were fired at comparatively great depths. The first visible surface effect was spray produced by the reflection of the underwater shock wave at the water surface (Cole, 1948). This spray was fairly dense but reached a height of only a few inches. The spray then settled to the water surface and, by perhaps one second after the burst, was entirely gone. However, the water surface retained a ruffled appearance until the arrival of the bubble.

The appearance of the surface effects produced by the arrival of the bubble products for the 50-lb pentolite charges is illustrated in Figure 5.1. It appeared to result from the arrival of a single bubble of explosion gases at the surface. The initial rise of this mound (not illustrated) retained the original surface roughness, its surface then gradually became smooth and glossy in appearance. The mound reached a height of about 7 feet and attained a maximum diameter of 26 feet; it then broke up and collapsed, spreading out along the water surface. The maximum measured height was about 9 feet.

The arrival times of the bubble products at the water surface for the pentolite charges are given in Table 5.1. These arrival times are somewhat later than would be expected if the velocity attained by the bubble during migration remained constant throughout its rise to the surface. The average velocity through four pulsations is 26.2 ft/sec, which would give an arrival time at the surface of 3.9 seconds. However, the observed arrival times varied between 5.1 and 5.8 seconds.

Because of the lower shock wave pressures of the two steam compositions, much less spray was produced from the charges. The arrival of the bubble at the surface for these compositions was not nearly as spectacular as that observed with the pentolite charges. As can be seen in Figure 5.1, this arrival produced practically no vertical displacement, but instead generally produced only a lateral spread of a patch of smoothed water outward from surface zero. The first appearance of the bubble was always a smoothing of the water surface, subsequent appearances then varied from shot to shot. For the hydrogen peroxide charges and one of the Lithanol charges (PW-48), the only observed effect was a continued lateral spread of this patch of smoothed water. Two of the Lithanol charges (PW-46 and 47) showed a continued arrival of material at the surface for several seconds after the initial arrival. This material produced a series of jets, probably the result of the arrival and breakup of a series of small bubbles at the surface. On the final 50-lb Lithanol shot (PW-49), there appeared to be a single, larger bubble arriving at the surface. However, the maximum vertical displacement was still small, being less than a foot.

The arrival times of the bubble products at the surface for the steam charges are also given in table 5.1. It was much more difficult to determine these times than it had been for pentolite because of the small surface disturbance initially observed with both compositions. Because of the larger bubble produced by these charge, the velocity imparted during migration was higher than for pentolite. For the hydrogen peroxide charges, a value of 36.0 ft/sec was computed; for Lithanol, a value 37.7 ft/sec was computed. These values of velocity would give arrival times at the surface of 3.0 sec and 2.87 sec, respectively. The much longer time required for the bubble to reach the surface is in accordance with the other evidence indicating nearly complete condensation of the bubble after three pulsations. In actuality, there probably are some gases left from the booster and from any incomplete chemical reaction of the charge. This small gas bubble probably broke up into smaller bubbles as it rose toward the surface. The motion of these smaller bubbles is more apt to be influenced by density gradients in the water caused by temperature and salinity, which would account for the large variation in arrival times observed for these compositions.

The anomaly mentioned above was Shot PW-49, where the remaining bubble products apparently did not break up but rose to the surface as a single larger bubble, resulting in a considerably earlier arrival time and more vertical displacement than observed with the other steam charges. Whether this is due to the booster gases (a 2-lb booster was used, all except PW-47 used 1-lb boosters), incomplete chemical reaction, or the result of environmental conditions, is not definitely known. Both shock wave and bubble measurements indicate no significant difference in the detonation characteristics of this charge from the other 50-lb Lithanol charges.

Initial studies of containment (Young, In Preparation) have also shown such apparent anomalies. These studies have indicated that the depth at which these charges were fired is close to the critical depth below which no surface effects will be observed from steam charges of this weight. Thus, the surface arrival would be strongly affected by environmental effects such as temperature and salinity gradients. It is possible that PW-49 was fired at a time when these gradients were such as to allow a rapid rise of the remaining products to the surface, while the other shots were fired when the gradients tended to retard the upward motion. Unfortunately, no information on temperature and salinity is available to substantiate this hypothesis.

5.2 300-lb CHARGES

The purpose of obtaining above-surface photography of the 300-lb explosions was to obtain estimates of the period of bubble pulses which occurred too close to the water surface to be detected by PE gages. Since discontinuities in the motion of the surface phenomena are caused by the bubble pulses, estimates of the periods can be made by correlating the discontinuities in the height-vs-time curves of the surface phenomena with such pulses. Much of the period information on which the migration equations used here are based were obtained in this manner (Snay, 1962).

As with the 50-lb charges, the first visible surface phenomena from explosions fired at these depths result from the reflection of the underwater shock wave at the water surface, which produces a dome of spray. The bubble pulses also produce domes similar to those of the shock wave. Finally, the arrival of the bubble products at the surface produces plumes which may be either vertical or lateral in their initial motion, depending on the phase of the bubble when it reaches the surface. It is generally believed that if the bubble reaches a minimum just under the surface, the resulting plumes will be vertical; if it is near a maximum as it emerges, lateral plumes will be formed.

5.2.1 Pentolite. The appearance of the plumes from 300-lb pentolite charges are shown in Figure 5.2. Comparisons of measured height-vs-time curves with bubble migration for pentolite charges are shown in Figures 5.3, 5.4, and 5.5 for the three depths fired. Representative curves were chosen as all shots for a given depth gave essentially the same results. The migration shown is based on the actual measured periods from the pressure-time recordings, using the depths at the time of bubble minima as calculated by Dr. Snay's equations. The size of the bubble at its maxima was also calculated from Dr. Snay's equations; the depth of the center of the bubble was taken as midway between the depths of the minima. In cases where no period was measured, the period shown was also calculated from Dr. Snay's equations.

At a depth of 60 feet, the bubble pulsated twice before reaching the water surface. Both pulses were measured on the PE records. The initial displacement of the water surface indicated on Figure 5.3 is the spray dome. The first bubble pulse produced no visible discontinuity in the height-vs-time curve and the major development of plumes appears to have resulted from the second pulsation of the bubble. This plume development apparently resulted from the strong upward movement of the bubble near the minimum and from jetting action of the bubble. This jet is produced by the rapid upward motion of the bottom of the bubble near the minima. The jet penetrates the top of the bubble and rises above it. The possible path of such a jet (from the bottom of the bubble at its maximum through the position of the measured pulse) is shown on Figure 5.3. The plumes illustrated in Figure 5.2 show both a central jet resulting from this jetting action and lateral plumes formed by the arrival of the bubble itself.

Four bubble pulses, of which three were measured on the PE records, are predicted for the 80-foot depth. As shown in Figure 5.4, discontinuities in the height-vs-time curve can be attributed to the second and third bubble pulses. At this depth, it appears that the average motion of the bubble imparted through migration produced the final plumes observed. The curve shown for the average motion was drawn through the first three pulses as the time and position of the fourth pulse is somewhat in doubt. It seems probable that by the time the bubble had pulsated four times, the pulsation was weak and jetting or any marked increase in velocity near the minimum was quite small. It is possible that no fourth pulse actually occurred, since its predicted depth is only four feet beneath the surface and the prediction of the time and position of the later pulses is admittedly crude.

Three bubble pulses were also measured on the PE records for the 100-foot depth, although five were predicted. As can be seen in Figure 5.5, discontinuities in the height-vs-time curve can be attributed to two of the last three bubble pulses. On some of the other pentolite shots at this depth, it was possible to attribute discontinuities to all three of these pulses. It is apparent that, at this depth, motion imparted to the bubble through the migration process probably accounts for the final discontinuity in the surface effects. In this case, the average curve is based on the first four pulses. It is also possible that the bubble pulsated more than five times since as many as seven pulses have been observed for underwater explosions. However, if it did pulse again, this pulse was probably very weak and had little effect on the motion of the bubble products.

5.2.2 Lithanol. The appearance of the surface phenomena for the 300-lb Lithanol charges is shown in Figure 5.6. Correlations of the height-vs-time curves with bubble migration for the 300-lb Lithanol charges are shown in Figures 5.7, 5.8, and 5.9. At the 60-foot depth, shown in Figure 5.7, the bubble pulsed twice before reaching the water surface. Both of these pulses were measured on the PE records. The first discontinuity on the height-vs-time curve can be attributed to the first bubble pulse. The major surface upheaval was produced by the second pulse, probably both by jetting and the strong upward migration of the bubble near the minimum. As can be seen in Figure 5.6, both a central jet resulting from the bubble jet and plumes more lateral in direction which resulted from the re-expansion of the bubble, were observed. The above surface effects in general were quite similar to those observed for the 60-foot pentolite shots, although the separate plumes were more distinct for this composition because the second pulse occurred at a depth somewhat shallower than for pentolite.

Three pulses were measured on the PE records for the 80-foot depth and three are also predicted. Figure 5.8 shows that the first pulse produced no discontinuity; discontinuities can be attributed to the second and third pulses. The time of occurrence of the third pulse measured on the PE records disagreed somewhat with that predicted (see Chapter 6). The position of the bubble at this time therefore is not known with confidence and the agreement in terms of arrival time between jetting and observed surface effects is not as good as had been previously noted. However, the rate of rise of the surface eruption correlates well with that of the jet, which tends to indicate that this eruption also originated from jetting of the bubble. The primarily vertical nature of the plumes, as shown in Figure 5.6, also indicates such an origin.

The correlation between bubble migration and observed surface effects for the 100-foot Lithanol shot is shown in Figure 5.9. At this depth, discontinuities on the height-vs-time curve can be attributed to the second and third bubble pulses. The final discontinuity, which produced the largest surface upheaval, apparently resulted from the arrival of the water jet produced by the final collapse of the bubble. In this case, the final pulse took place at a depth of about 42 feet. The velocity and arrival time at the surface of a jet formed at the time of the third pulse are in excellent agreement with the observed final surface phenomena. In addition, the plumes observed here were vertical, which also tends to substantiate the concept of jetting. There was no evidence of a fourth bubble pulse.

5.2.3 H_2O_2/Al. Because the size and period of the bubble for the 300-lb charges of the H_2O_2/Al composition were quite similar to those of Lithanol, the correlation between migration and surface effects were essentially the same for the two compositions. A comparison of these two phenomena therefore will not be made for this composition. The conclusions reached from such correlation are the same as those given for Lithanol in the previous section.

5.2.4 Summary. For both HE and the steam charges, it was possible to correlate discontinuities in the above surface effects with the shock wave, bubble pulses, and arrival of the bubble products at the water surface. The time of these discontinuities extrapolated back to the water surface and their probable origins are given in Table 5.2 for all shots. As can be seen in the previous figures, these times often represent considerable extrapolation of the height-vs-time curve or result from very slight changes in velocity. In some cases, no discontinuity was observed for a pulse although it was observed on other shots of the same composition fired at the same depth. In spite of these large extrapolations, good correlation with the bubble phenomena was obtained. No evidence of a fourth bubble pulse was observed for the 300-lb charges of either steam composition, in agreement with the current description of the behavior of a steam bubble. However, such a pulse was observed with the 50-lb steam charges.

It appears that the final bubble collapse is such that an upward jet of water is formed which contains the residual momentum of the system. This is evident from the agreement of such a jet with the origin and velocity of the surface effects, and from the generally vertical nature of the plumes which are formed. On the other hand, the average motion of the entire bubble appears to be the mechanism of rise for the HE charges, unless the minimum occurs close to the surface. Further work, especially in a tank where photography of the bubble is possible, is needed to verify this jetting action, since the conclusions reached are based on a limited amount of data.

5.3 OTHER SURFACE PHENOMENA RESULTS

While the times of the discontinuities showed good reproducibility for the same explosive fired at the same depth, the dimensions of the above surface effects varied considerably. The maximum height of the phenomena for each shot is included in Table 5.2. As expected, a trend of decreasing height with depth is evident for each composition. The greater height attained by the steam charges result from the larger initial bubble formed by the compositions (which essentially resulted in a shallower depth in terms of the migration process) and from the jetting action of the bubble, which produced a plume which was primarily vertical rather than lateral.

The reproducibility of surface phenomena dimensions is generally considered to be of the order of 30 percent; and with the exception of one depth for the H_2O_2/Al composition, the scatter of heights was well within this range. The 60-foot depth for this composition produced a marked difference in heights for the two shots fired, although the general appearance of the plumes was the same. The predicted position of the second bubble pulse was only four feet below the water surface. It seems likely that the actual depth of origin of this pulse was slightly different for these two shots and at such a shallow depth, a small difference is probably quite critical, which accounts for the wide difference in observed heights.

TABLE 5.1 ARRIVAL TIME OF BUBBLE CONTENTS AT SURFACE FOR 50-lb CHARGES

Shot No.	Camera No.	Arrival Time (sec)	Remarks
Pentolite			
PW-34	653	5.6	
	657	5.2	
PW-35	653	--	No timing
	657	5.8	
PW-45	653	5.1	
	657	--	
PW-50	653	5.1	
	657	5.4	
Lithanol			
PW-46	653	10.8	
	657	--	SZ out of field
PW-47	653	--	No timing
	657	--	SZ out of field
PW-48	653	12.2	
	657	12.5	
PW-49	653	5.8	
	657	6.3	
H_2O_2/Al			
PW-36	653	--	No zero frame
	657	--	No zero frame
PW-37	653	11.4	
	657	11.2	
PW-38	653	9.5	
	657	9.9	

NOTE: Camera 653 equipped with 100mm lens, camera 657 with a 150mm lens.

TABLE 5.2 TIMES OF DISCONTINUITIES IN HEIGHT-VS-TIME CURVES FOR 300-lb CHARGES

Shot No.	Depth (ft)	Composition	Time of Discontinuity - seconds 1	2	3	4	Max. Height (ft)
PW-22	100	Pentolite	1.25(T_3)	1.89(T_4)	2.39(T_5)	2.97(M)	53
PW-23	80	Pentolite		No Timing			--
PW-24	80	Pentolite	1.17(T_2)	1.75(T_3)	2.40(T_4)	--	72
PW-25	100	Pentolite	1.38(T_3)	1.85(T_4)	2.35(T_5)	3.05(M)	46
PW-26	100	Lithanol	0.98(T_2)	1.60(T_3)	2.04(J)	--	73
PW-27	100	Lithanol	1.05(T_2)	1.57(T_3)	1.98(J)	--	117
PW-28	100	Pentolite	1.35(T_3)	2.33(M)	--	--	35
PW-29	60	Pentolite	1.30(J)	--	--	--	134
PW-30	60	Lithanol	0.94(T_1)	1.60(J)	--	--	235
PW-31	60	Lithanol	0.94(T_1)	1.66(J)	--	--	>212
PW-32	80	Lithanol	1.36(T_2)	2.12(J)	--	--	139
PW-39	80	Pentolite	1.92(T_3)	2.40(T_4)	--	--	78
PW-40	80	H_2O_2/Al	1.57(T_2)	--	--	--	104
PW-41	80	H_2O_2/Al	1.44(T_2)	2.30(J)	--	--	109
PW-42	100	Pentolite	1.45(T_3)	1.91(T_4)	2.40(T_5)	3.10(M)	42
PW-43	100	H_2O_2/Al	1.20(T_2)	1.80(T_3)	2.07(J)	--	114
PW-44	100	H_2O_2/Al	1.25(T_2)	1.75(T_3)	2.00(J)	--	115
PW-52	60	Pentolite	1.34(J)	--	--	--	132
PW-53	60	H_2O_2/Al	0.98(T_1)	1.82(J)	--	--	200
PW-54	60	H_2O_2/Al	0.98(T_1)	1.77(J)	--	--	>315

( ) indicates probable source of discontinuity: J-jetting of bubble; M-mass motion imparted from migration; T-bubble pulses.

5.9 SECONDS

16.0 SECONDS

6.4 SECONDS

17.6 SECONDS

7.2 SECONDS

PENTOLITE

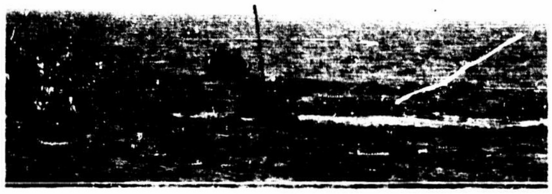

19.7 SECONDS

LITHANOL

FIG. 5.1 BUBBLE ARRIVAL FOR 50-LB PENTOLITE AND LITHANOL CHARGES FIRED AT A DEPTH OF 100 FEET

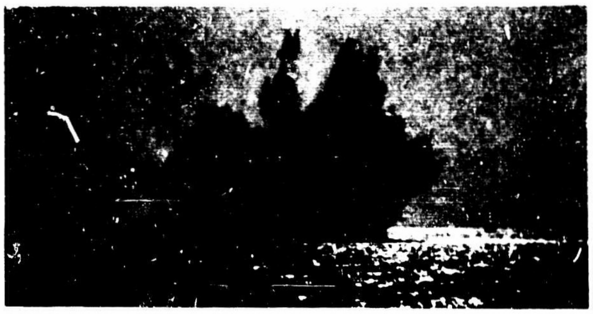

60 FT DEPTH 3.77 SEC

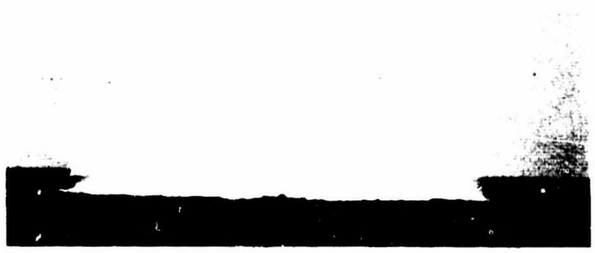

80 FT DEPTH 4.11 SEC

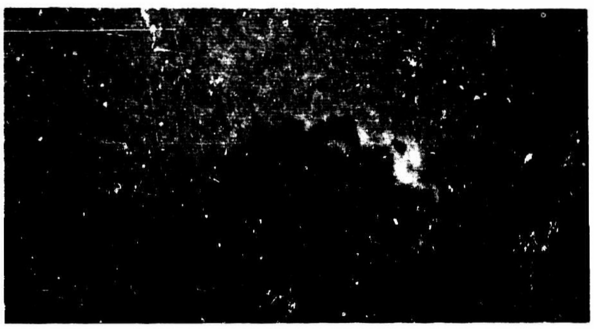

100 FT DEPTH 3.76 SEC

FIG. 5.2 PLUME PHENOMENA FROM 300-LB PENTOLITE CHARGES

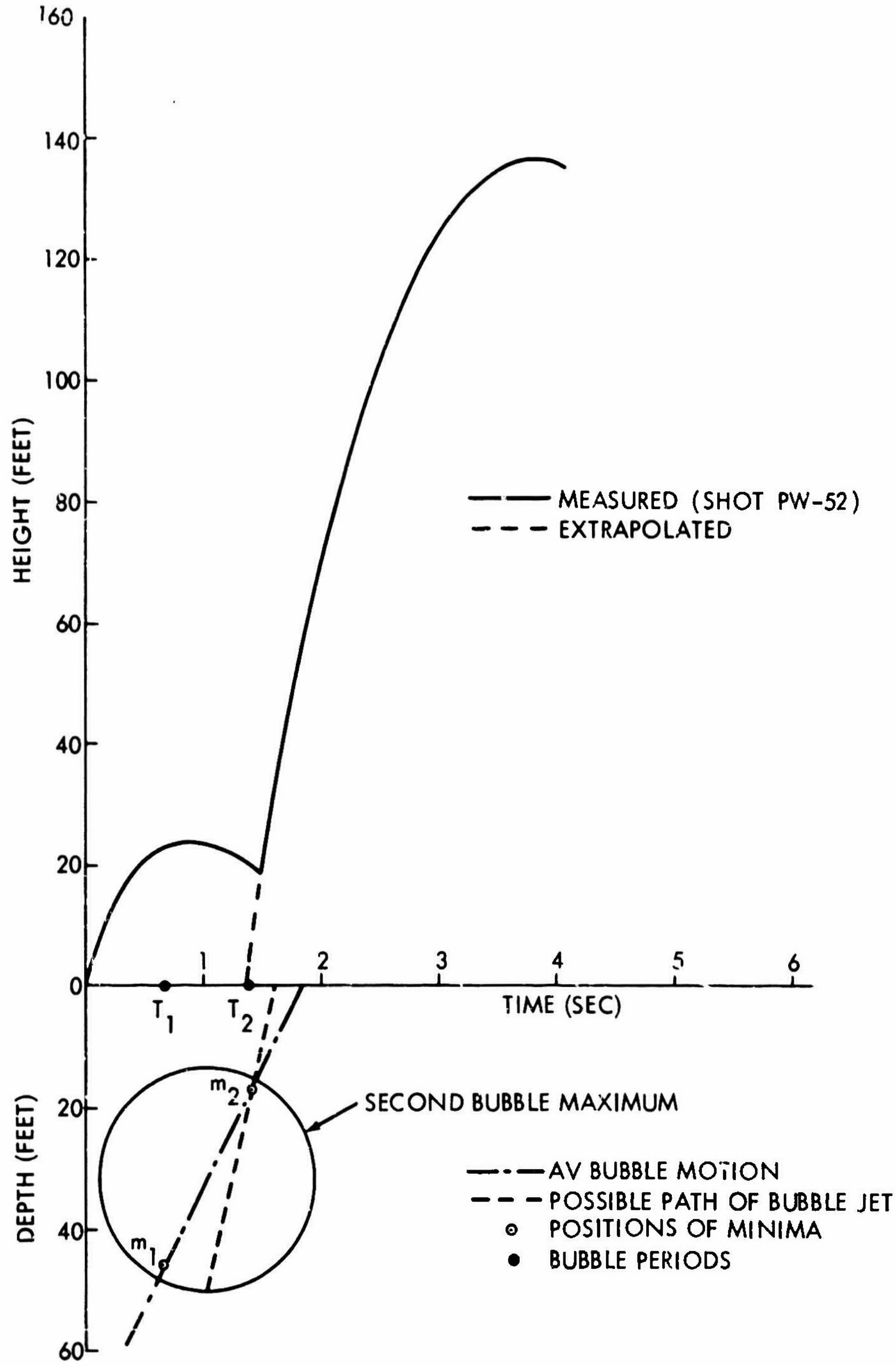

FIG.5.3 COMPARISON OF ABOVE SURFACE EFFECTS WITH BUBBLE MIGRATION, 300-LB PENTOLITE AT 60 FEET

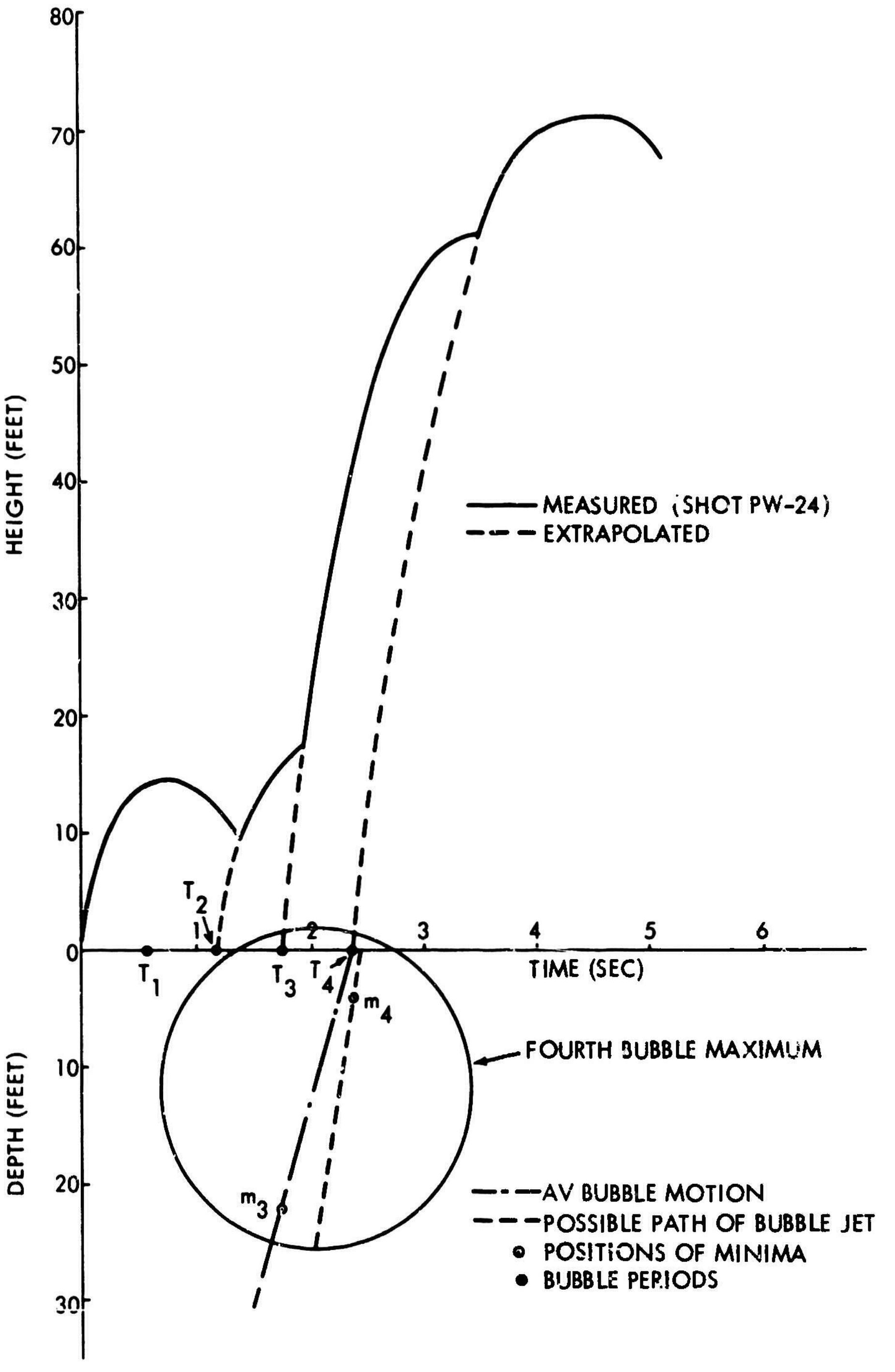

FIG. 5.4 COMPARISON OF ABOVE SURFACE EFFECTS WITH BUBBLE MIGRATION, 300-LB PENTOLITE AT 80 FEET

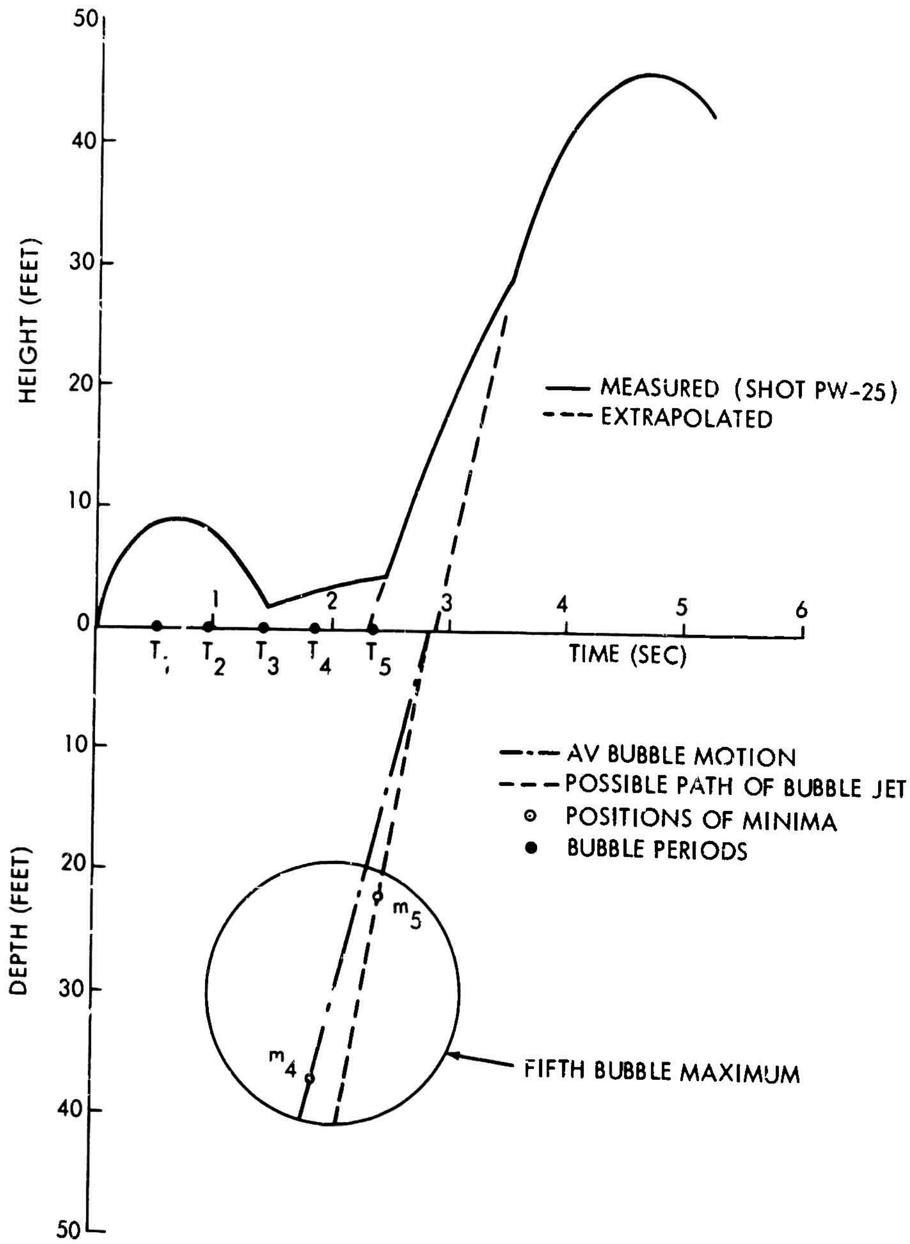

FIG. 5.5 COMPARISON OF ABOVE SURFACE EFFECTS WITH BUBBLE MIGRATION, 300-LB PENTOLITE AT 100 FEET

60 FT DEPTH 1.90 SEC

80 FT DEPTH 3.22 SEC

100 FT DEPTH 3.47 SEC

FIG.5 6 PLUME PHENOMENA FROM 300-LB LITHANOL CHARGES

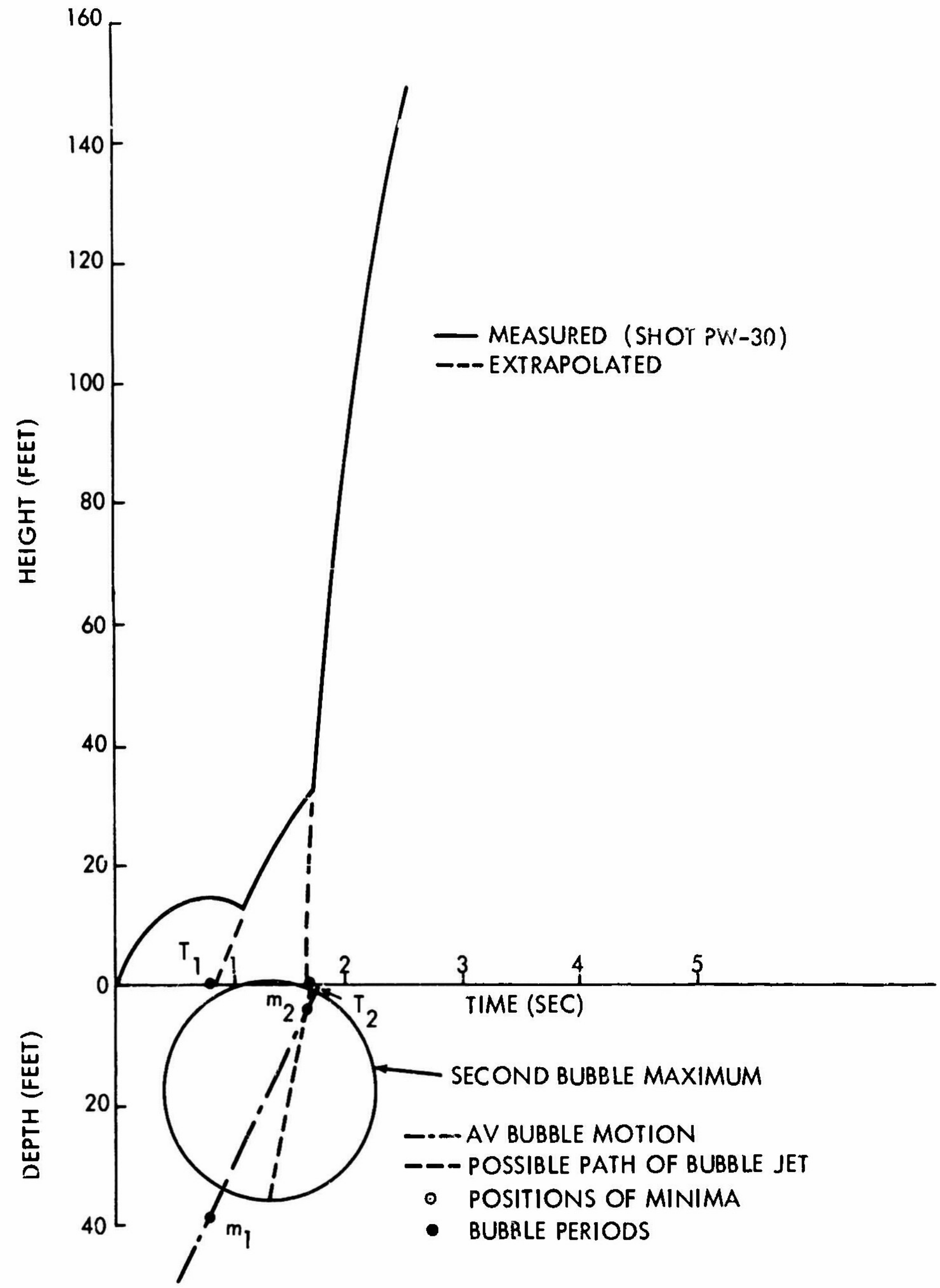

FIG.5.7 COMPARISON OF ABOVE SURFACE EFFECTS WITH BUBBLE MIGRATION, 300-LB LITHANOL AT 60 FEET

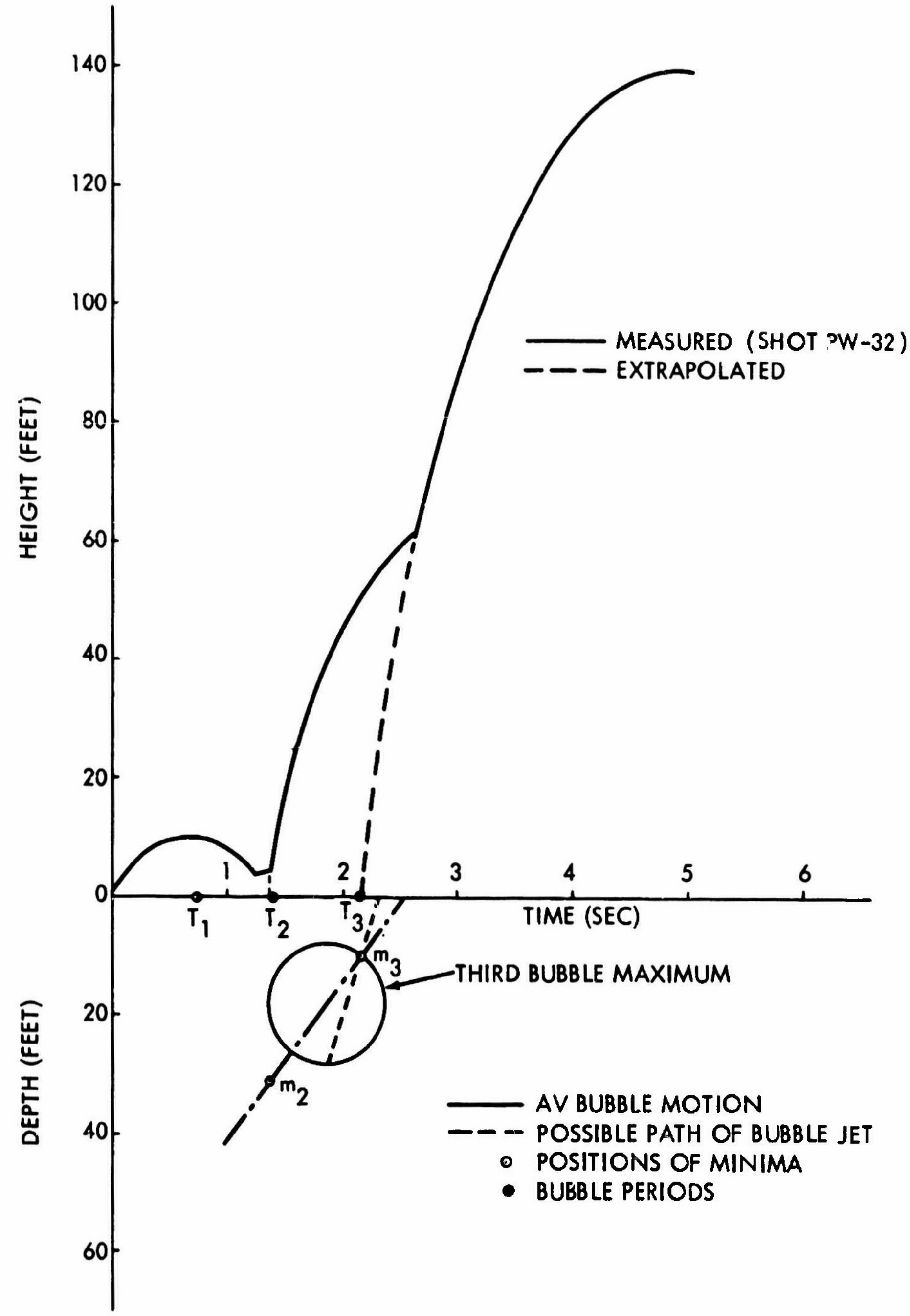

FIG.5.8 COMPARISON OF ABOVE SURFACE EFFECTS WITH BUBBLE MIGRATION, 300-LB LITHANOL AT 80 FEET

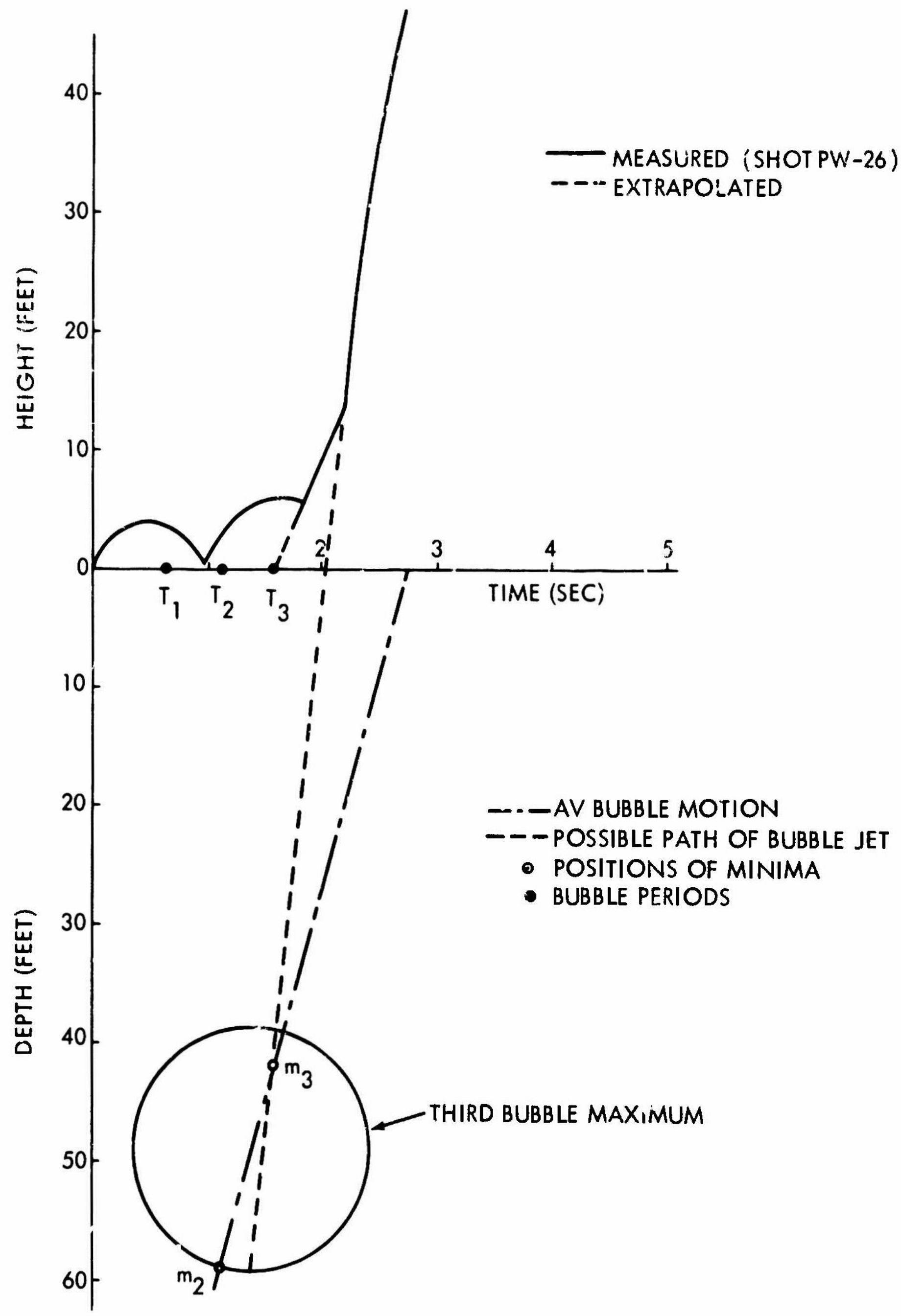

FIG.5.9 COMPARISON OF ABOVE SURFACE EFFECTS WITH BUBBLE MIGRATION, 300-LB LITHANOL AT 100 FEET

6. COMPARISON WITH PREVIOUS WORK

6.1 PREVIOUS LITHANOL AND H_2O_2/Al DATA

As has been indicated above, data have been obtained for these two compositions in 8- and 16-lb charge sizes (Phillips and Heathcote, 1966). In addition, some bubble data from 1-lb charges of the Lithanol composition are also available (Phillips and Scott, 1965). Combined with the data given in this report, information for a range of weights from 1 to 300 lb is now available.

6.1.1 Shock Wave. The shock wave parameters for both compositions are given in tabular form in Table 6.1. The agreement for Lithanol over the range of weights fired is excellent; the closeness of the values is possibly somewhat fortuitous as the slopes of the 50- and 300-lb data were adjusted to the slope of the 8- and 16-lb results. However, the results show no evidence of problems of initiation for Lithanol.

As can be seen in Table 6.1, this is not true for the hydrogen peroxide composition. It had been felt that the smaller charges of this composition did not detonate properly, and this is substantiated by the increase in shock wave parameters for the larger charges. The increase in peak pressure is shown graphically in Figure 6.1. It generally has been possible to improve the detonation characteristics of smaller charges by using a very large booster. This, however, has certain disadvantages for this composition since the booster introduces permanent gases into the bubble; in addition, the booster gases may modify the postulated chemical reaction. Thus, while it might solve the detonation problem, the introduction of additional permanent gases may render the composition useless for its intended purpose.

6.1.2 Bubble. As has been indicated in Chapters 3 and 4, a definite increase in bubble parameters J and K with increasing charge weight was noted. The values for J and K for the various weights is given in tabular form in Table 6.2 and shown graphically in Figure 6.2. For both J and K, the values for the steam compositions have been adjusted by the percentage that the pentolite standards differed from the accepted value. For K, this correction was less than one percent for all but the 300-lb charges, where it was as high as 4 percent; for J it was as large as 6 percent for some of the smaller charges, due possibly to the nonspherical shape of the bubble for these charges. In cases where no meaningful values of bubble radius were obtained, J was calculated using the ratio of J/K obtained from the 8- and 16-lb charge programs. As was noted in Chapter 4 for the 300-lb hydrogen peroxide charges (where good radius measurements were obtained) this method appears to be sufficiently accurate.

This increase in J and K with increasing charge weight is not usually observed with conventional high explosives; rather, thay have a constant value over a wide range of charge weights. In the case of the hydrogen peroxide composition, this increase possibly is the result of the detonation problems observed, although this probably does not account fully for it. The shock wave results indicate that proper detonation took place for Lithanol; thus, the increase in the bubble parameters for this composition undoubtedly is real. It probably results from the longer time available to burn the aluminum in the composition. If the increase is the result of the increased burning of aluminum, it would be expected that J and K would level off at a weight where sufficient time was available to completely oxidize the aluminum. This increase is of immediate concern in that one of the planned uses of these compositions is in scaling studies which are dependent on the bubble parameters (see Chapter 7). Larger charge weights than those fired to date will be used and the values of J and K must be known in order to properly scale the conditions.

6.2 COMPARISON WITH NUCLEAR EXPLOSIONS

It has already been reported (Phillips and Heathcote, 1966) that the shock waves from both of the compositions do not simulate to any degree the shock wave of a nuclear explosion, having a much lower pressure and a longer duration. While the increased shock wave pressures of the larger hydrogen peroxide charges improved the shock wave simulation for this composition over that from the small charges previously reported, even the 300-lb charge does not bring it close to nuclear. As the prime objective was to simulate the bubble effects, this lack of shock wave similarity is of little consequence and will not be discussed further in this report.

Of primary interest insofar as simulation of the bubble is concerned is the condensation effect. In determining how well the condensation effects of these compositions compare to those of a nuclear bubble, comparison of successive periods is used. This is the only available means to make these comparisons for field size charges. Snay (1960) has given the following relationship for the ratios for successive periods relative to the first:

$$\frac{T_n}{T_1} = \left(\frac{Z_1}{Z_n}\right)^{5/6} \left(\frac{r_n}{r_1}\right)^{1/3} \left(\frac{1 - 0.1\, A_n/d_n}{1 - 0.1\, A_1/d_1}\right) \qquad (6.1)$$

The subscript 1 refers to the first cycle of oscillation of the bubble. The subscript n refers to successive cycles (n = 2, 3, etc.). The ratio r_n/r_1 is the fraction of energy remaining in the bubble after the n-th pulsation. It is this ratio which is markedly different between the HE and nuclear cases because of the reduction in bubble energy due to condensation. Dr. Snay has made estimates of this ratio for nuclear bubbles based on the general slope of the HE energy curves (Snay, 1960). He used the limited steam bubble data available at the time from electric sparks fired under water and from the periods measured on Operation Wigwam.

The period ratios T_2/T_1 and T_3/T_1 for both steam compositions measured on these programs are compared in Figures 6.3 and 6.4 to those predicted on the basis of Equation 6.1 and ratios r_n/r_1 given in the reports by Snay (1960, 1962). For T_2/T_1, this ratio is somewhat lower than predicted but considerably lower than that predicted for HE. The pentolite values are also lower than predicted; thus, for the steam charges, the agreement still is good, the difference being about the same as that observed for this ratio and for the 50-lb pentolite charges. In the case of the 300-lb charges, the third pulse occurred close to the surface and not as good agreement was obtained. This possibly is due to improper correction for the proximity of the surface. It is also due, at least in part, to the lack of precise knowledge of the nuclear bubble parameters in this region. The values for r_n/r_1 currently available do not permit a realistic prediction of the third pulse for depths only slightly shallower than the Wigwam condition ($Z_1/A_1 = 5.42$). This is equivalent to a firing depth of about 90 feet for a 300-lb charge. A third pulse was detected at a depth of 80 feet ($Z_1/A_1 = 4.91$), however. It thus appears that the steam charge results can be used to improve our prediction capability, particularly for the later bubble pulses at scaled firing depths shallower than Wigwam.

Another comparison which can be made with nuclear results is the ranged migration of the bubble. Ranging results which were given previously in Chapters 3 and 4 are compared graphically in reduced form in Figures 6.5 and 6.6.

Bubble migration to the first minimum (which occurs at T_1) is shown in Figure 6.5. The migration ΔZ represents the difference between the ranged depth of burst and the ranged depth of the first bubble pulse. Previous experimental work with HBX-1 charges in free water yielded the following empirical equation describing this migration (Snay et al, 1952):

$$\Delta Z = 100 \frac{W^{1/2}}{Z} \qquad (6.2)$$

Goertner (1956), in tank studies of bubble migration, has shown that Equation 6.2 corresponds to the observed top of the bubble at its minimum radius and thus tends to confirm the concept that ranging is accomplished using signals generated by the water hammer effect as the bottom of the bubble impinges on the top. Applying Equation 6.2 to a 300-lb charge of Lithanol, using the factor $W_{HBX-1} = 1.58\ W_{Lithanol}$ (Snay et al, 1952), this equation reduces to:

$$\frac{\Delta Z}{Z} = \frac{2110}{Z^2} \qquad (6.3)$$

and is represented by the line in the figure.

The first migration measured on these tests is consistently higher than previous results shown by the line. For instance, at a depth of 100 feet, the reduced migration $\Delta Z/Z$ is about 0.027 greater than predicted; ΔZ is thus about 3.6 feet greater. The uncertainty in ranging is of this order, thus these results are in acceptable agreement with other previous experimental values.

Figure 6.6 shows the bubble migration between the first and second minima for both pentolite and the steam compositions. This has been compared with the migration predicted by Snay (1960). No indication of the expected decrease in migration of the steam bubble is evident from the experimental data. This is probably because the possible errors in ranging are greater than the expected differences. For instance, the difference in migration for a 300-lb Lithanol charge fired at a depth of 100 feet is only five feet using Dr. Snay's HE and nuclear bubble energies. As noted in Chapter 3, uncertainty in ranging the pulses was greater than this. In addition, ranging of the second pulse for the pentolite charges was extremely difficult and there is considerable uncertainty in the accuracy of the values obtained. Thus, the values shown for pentolite cannot be used as a standard as has been done previously in comparing HE and steam charge results. It thus appears that comparison of the observed and predicted migration for steam and conventional charges is too insensitive a parameter to indicate the condensation effect.

Based on the bubble period data, it appears that both of the steam compositions reproduce to an acceptable degree the condensation effects of a nuclear bubble. Conversely, the results also tend to increase the confidence in the current prediction methods for free water nuclear bubble behavior which, as has been pointed out, are based on the extrapolation of HE results using only a very limited amount of nuclear and spark bubble data.

TABLE 6.1 SUMMARY OF SHOCK WAVE PARAMETERS FOR ALL WEIGHTS OF THE STEAM COMPOSITIONS

Composition	Variable	Nominal Weight (lb)	Parameters	
			C	α
Lithanol	P_m	8-16	$1.17x10^4$	1.03
		50	$1.17x10^4$	1.03
		300	$1.17x10^4$	1.03
	$E/W^{1/3}$	8-16	$1.54x10^3$	1.86
		50	$1.32x10^3$	1.86
		300	$1.37x10^3$	1.86
	$I/W^{1/3}$	8-16	1.98	0.88
		50	1.63	0.88
		300	1.62	0.88
H_2O_2/Al	P_m	8-16	$0.87x10^4$	1.09
		50	$1.60x10^4$	1.09
		300	$1.98x10^4$	1.09
	$E/W^{1/3}$	8-16	$1.61x10^3$	2.15
		50	$3.49x10^3$	2.15
		300	$4.48x10^3$	2.15
	$I/W^{1/3}$	8-16	2.16	1.05
		50	2.66	1.05
		300	2.89	1.05

NOTES: Variable = $C\left(\frac{W^{1/3}}{R}\right)^{\alpha}$

Data for 50- and 300-lb charges was fitted to slope obtained on 8-16 lb programs.

TABLE 6.2 SUMMARY OF BUBBLE PARAMETERS FOR ALL WEIGHTS OF THE STEAM COMPOSITIONS

Weight	J	K	No. Shots	Source of Data
Lithanol				
1.0	15.0	5.26	5	NOLTR 65-176
7.7	15.4	5.45	3	Unpublished
8.0	15.2	5.37	6	NOLTR 66-79
16.3	14.7	5.29	5	NOLTR 66-79
52.5	15.9 1/	5.62	4	Section 3.2.1
290	16.3 1/	5.75	5	Section 3.2.2
H_2O_2/Al				
7.4	16.1	5.77	4	NOLTR 66-79
14.6	16.0	5.83	4	NOLTR 66-79
43.3	17.4 1/	6.25	2	Section 4.2.1
263	17.3	6.35	6	Section 4.2.2

1/ Calculated from the experimentally determined K and the J/K ratio from the 8- and 16-lb programs.

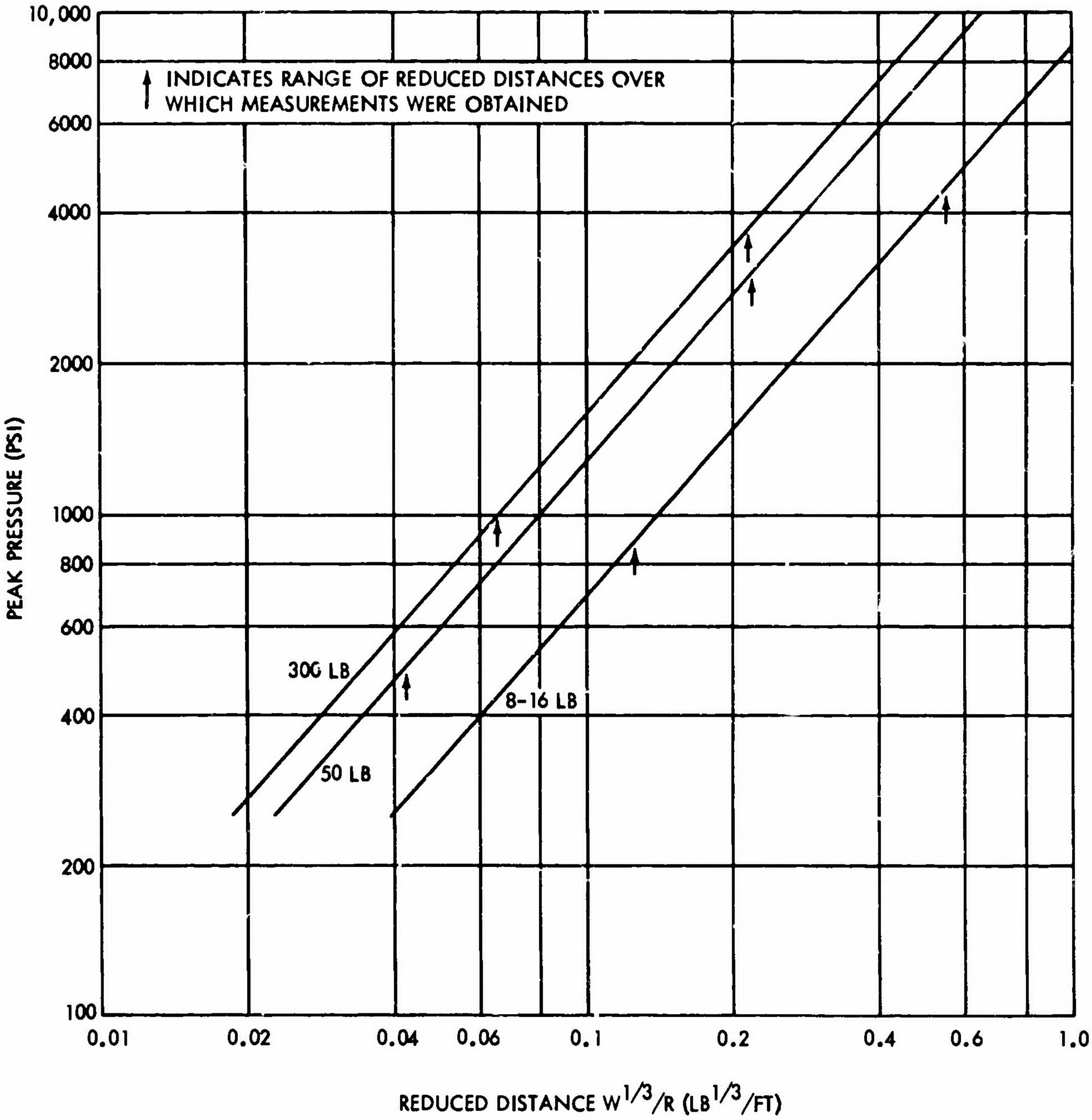

FIG. 6.1 COMPARISON OF PEAK PRESSURES OBTAINED WITH VARIOUS WEIGHTS OF H_2O_2/Al

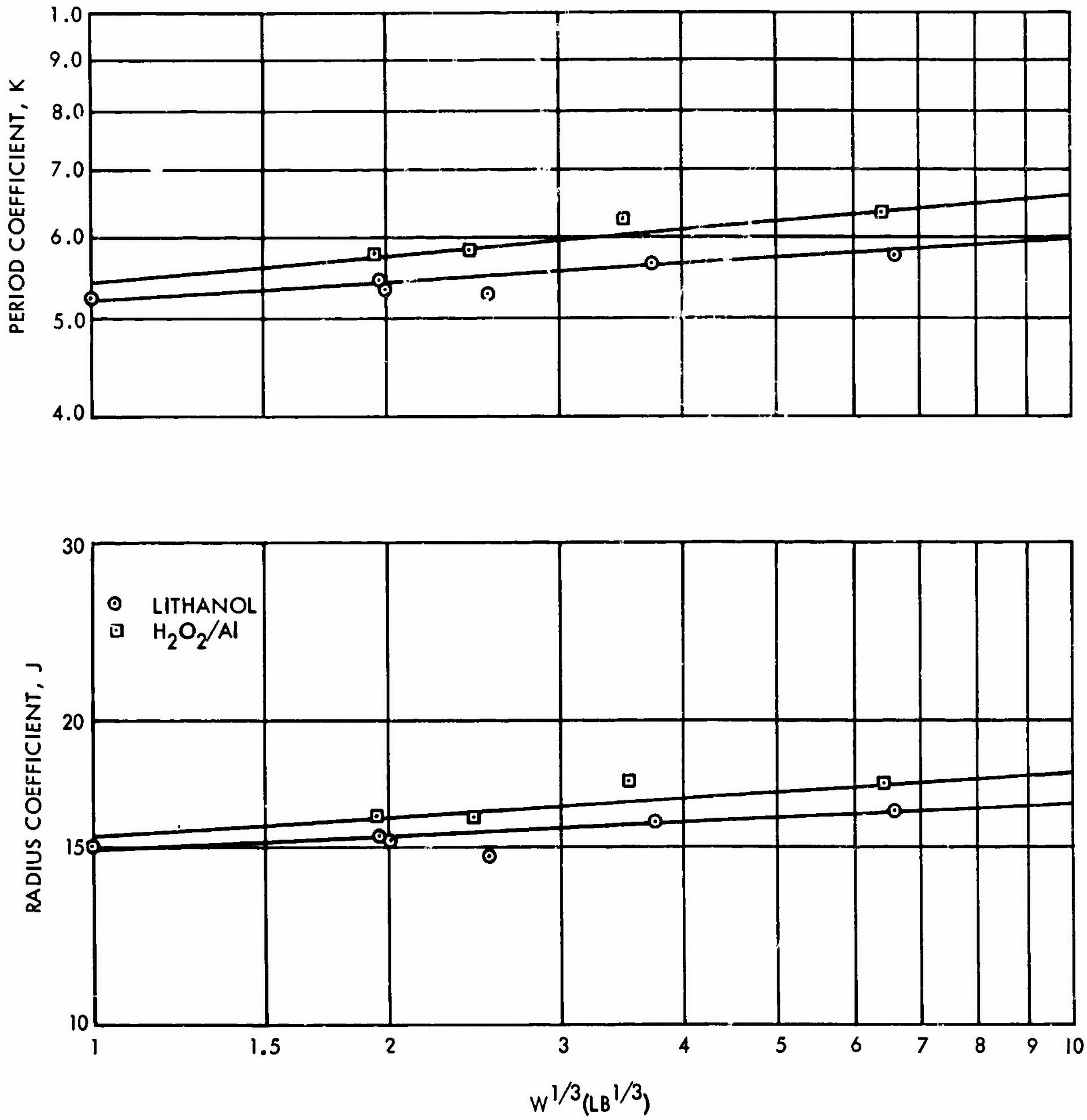

FIG. 6.2 INCREASE OF BUBBLE COEFFICIENTS J AND K WITH INCREASING CHARGE WEIGHT

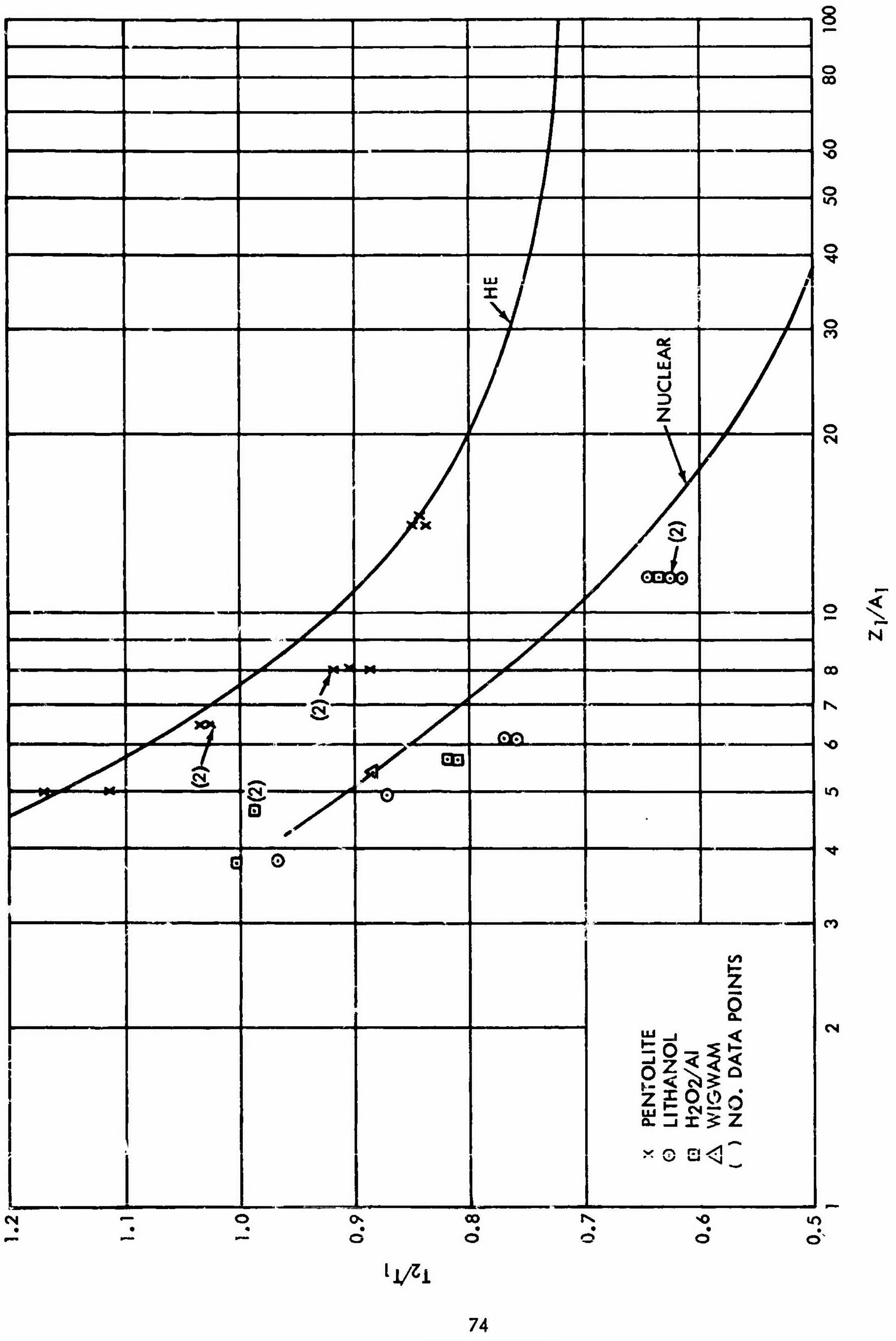

FIG. 6.3 COMPARISON OF PREDICTED AND MEASURED SECOND PERIOD RATIO

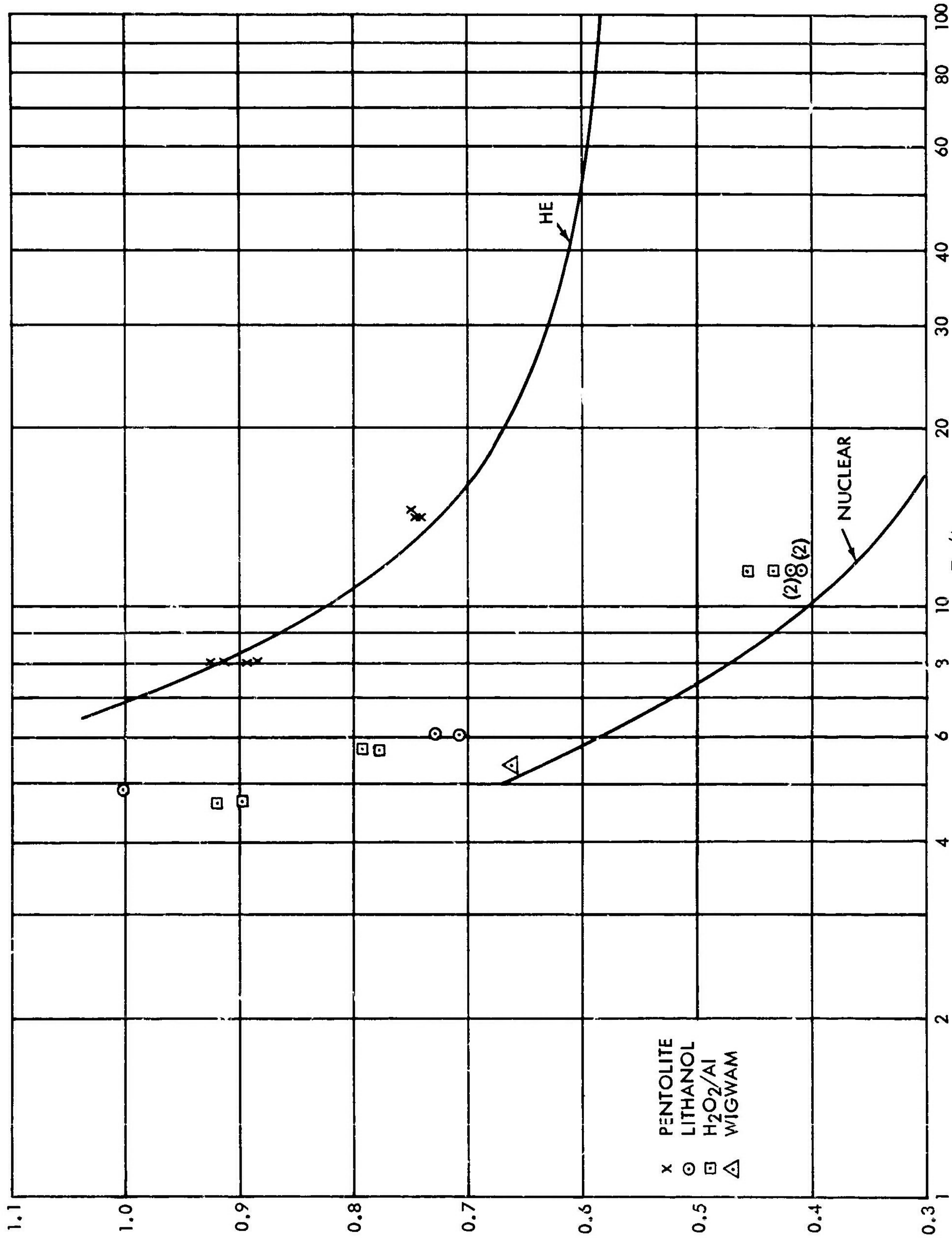

FIG. 6.4 COMPARISON OF PREDICTED AND MEASURED THIRD PERIOD RATIO

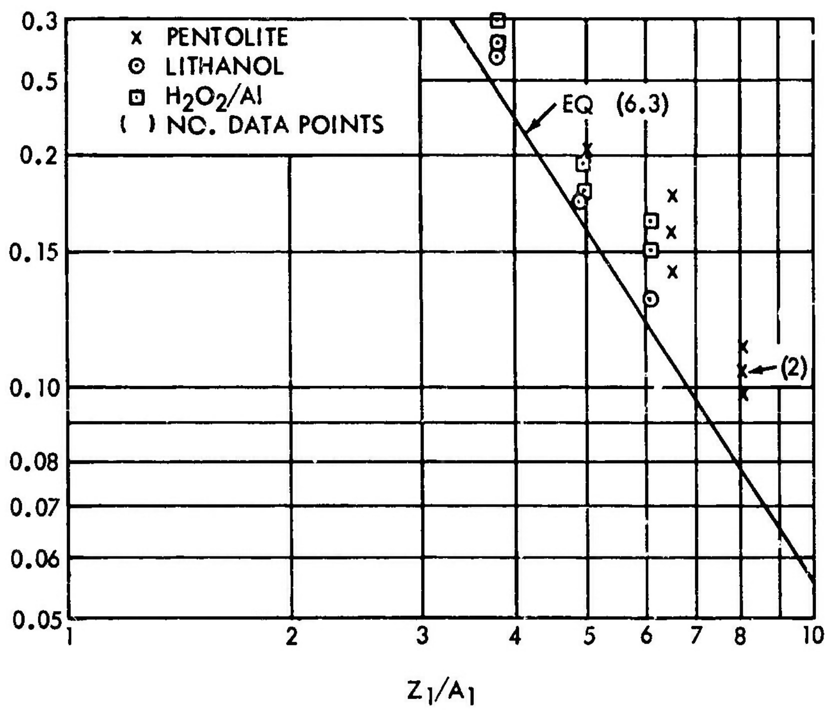

FIG. 6.5 BUBBLE MIGRATION TO FIRST MINIMUM

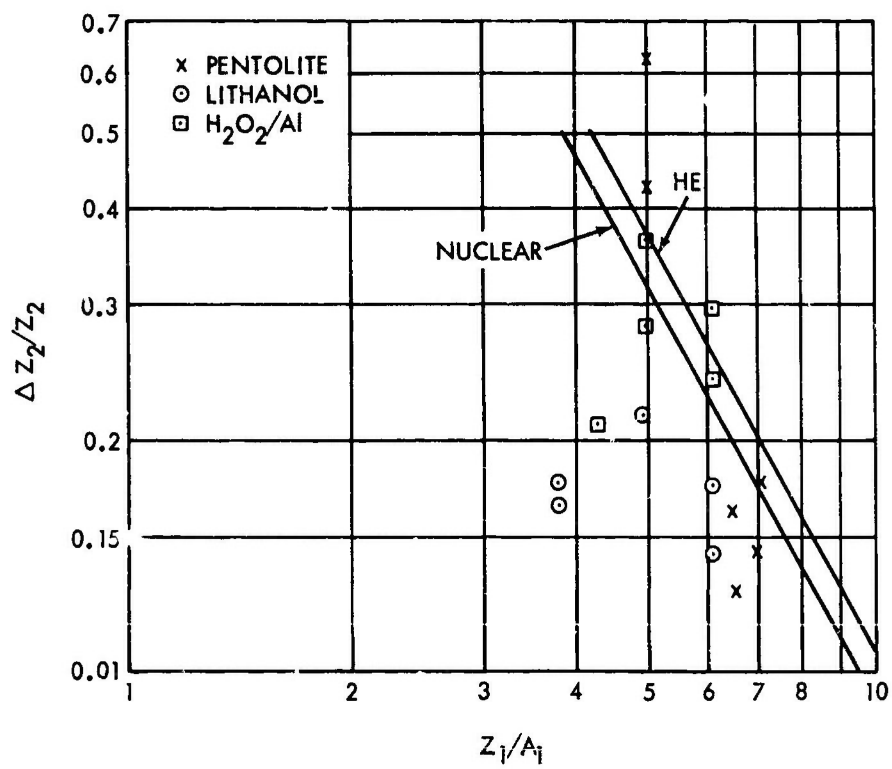

FIG. 6.6 BUBBLE MIGRATION BETWEEN FIRST AND SECOND MINIMA

7. SCALING OF STEAM CHARGE RESULTS

In scaling shallow underwater explosions, cube root scaling is used. The reduced depth of such an explosion is defined as (Snay, 1964):

$$\lambda_d = \frac{d}{W^{1/3}} \qquad (7.1)$$

where: λ_d = reduced depth, $ft/lb^{1/3}$

d = charge depth, feet

W = charge weight, lb

Two nuclear tests have been fired in the shallow region. These were Crossroads Baker (23 kt at 90 feet) and Shot Umbrella of Operation Hardtack (8 kt at 150 feet). Converting the yield to lb (1 kt = 2 x 10^6 lb), the reduced depths for these two shots are 0.251 $ft/lb^{1/3}$ and 0.595 $ft/lb^{1/3}$, respectively.

In scaled explosion studies in this region, the prime contributor to the above surface effects is the action of the bubble. Therefore, it has been attempted to simulate the action of the bubble. This was done by placing the conventional charge at a different reduced depth than the nuclear device to account for different bubble energies. Specifically, this scaled depth was determined by use of the following equation:

$$\lambda_{d(HE)} = \frac{J_{HE}}{J_{NUC}} \lambda_{d(NUC)} \qquad (7.2)$$

where: subscripts HE and NUC refer to conventional high explosives and nuclear, respectively.

Extensive use has been made of HBX-1 in previous scaling studies as this explosive has nearly the same energy partition between shock wave and bubble as does a nuclear explosion. For HBX-1, J is equal to 14.4; thus the reduced depths for scaling Baker and Umbrella with this explosive (using Equation 7.2) are 0.304 $ft/lb^{1/3}$ and 0.720 $ft/lb^{1/3}$, respectively.

While this same procedure can be used for the steam charges, it becomes more complicated because J is a function of charge weight. Therefore, in order to properly place the charge, it is necessary that the value of J be determined for the charge weight fired. This value can then be used in Equation 7.2 to determine the proper reduced depth. For example, suppose it is desired to fire a 50-lb Lithanol charge at the same reduced depth as Umbrella. From Figure 6.2, it can be found that J is equal to 15.8. Using this value, Equation 7.2 becomes:

$$\lambda_{d(HE)} = \frac{15.8}{11.9}(0.595) \tag{7.3}$$

$$\lambda_{d(HE)} = 0.790 \tag{7.4}$$

From Equation 7.1:

$$d = 2.91 \text{ ft} \tag{7.5}$$

For a different weight, the value of λ_d will be different for scaling the same nuclear condition. Table 7.1 lists the values of J and resulting scaled depths for Baker and Umbrella for several weights of Lithanol.

For reproducing exactly the bubble parameters of a nuclear burst, the bubble size for both the steam composition and nuclear must be the same. In other words:

$$(A_{max})_{HE} = (A_{max})_{NUC} \tag{7.6}$$

or:

$$\left(\frac{JW^{1/3}}{Z^{1/3}}\right)_{HE} = \left(\frac{JW^{1/3}}{Z^{1/3}}\right)_{NUC} \tag{7.7}$$

Since the charge depth and hence the hydrostatic head Z are the same for both HE and nuclear, this equation becomes:

$$W_{HE} = \left(\frac{J_{NUC}}{J_{HE}}\right)^3 W_{NUC} \tag{7.8}$$

Nuclear weapons are being developed in the 20-ton range. Again considering Lithanol, if the relationship shown in Figure 6.2 continues to be valid for larger charge weights, J will have a value of 17.2 for a charge weight of 13,000 lb. Using this value of J in Equation 7.7:

$$W_{HE} = \left(\frac{11.9}{17.2}\right)^3 (40,000) \tag{7.9}$$

$$W_{HE} = 13,300 \text{ lb} \tag{7.10}$$

Thus, 13,300 lb of Lithanol will produce a bubble of the same size as a 20-ton nuclear burst.

It is not expected that J will continue to increase in the manner shown in Figure 6.2 but will level off at some value. Thus the above weight is probably conservative. Until further information on the variation of J and K with charge weight is obtained, it is recommended that only charges weighing less than 1000 lb be fired if these parameters cannot be experimentally determined.

TABLE 7.1 UMBRELLA AND BAKER SCALED DEPTHS FOR VARIOUS WEIGHTS OF LITHANOL

Wt (lb)	J	$\frac{J_{HE}}{J_{NUC}}$	λ_d(Baker) ($ft/lb^{1/3}$)	λ_d(Umbrella) ($ft/lb^{1/3}$)
8	15.4	1.29	0.324	0.768
16	15.6	1.31	0.329	0.780
50	15.8	1.33	0.334	0.791
100	15.9	1.34	0.336	0.798
300	16.3	1.37	0.344	0.816
1,000	16.4	1.38	0.346	0.821

8. CONCLUSIONS AND RECOMMENDATIONS

8.1 CONCLUSIONS

Tests of both compositions were successfully made. Measurement of the shock wave parameters for Lithanol indicated no initiation problem over the range of weights fired. The coefficients for pressure, impulse, and energy were essentially the same and the scatter in the data, when compared to the scatter obtained with the pentolite standards, showed no significant differences. The shock wave parameters for this composition are considerably lower than usually observed with high explosives or with a nuclear burst. For example, peak pressure is only about 56 percent of that of pentolite and about [illegible] percent of that of an equivalent nuclear explosion.

Handling techniques for the H_2O_2/Al charges were successfully developed and the problems in loading and handling these charges were overcome. Measurements of shock wave parameters for this composition, however, indicated a definite initiation problem. The reduced peak pressures from the 300-lb charges were nearly double those from the 8- and 16-lb charges; reduced impulse and energy also showed considerable increase. Shock wave peak pressures for the 300-lb charges were closer to that of pentolite, 91 percent, and were 16 percent higher than those predicted for nuclear charges.

Both compositions showed acceptable agreement in reproducing the condensation effects of a nuclear bubble. This was indicated by comparing the measured ratio of successive periods to the first with that predicted for a nuclear explosion. The values of J and K for both compositions were also higher than observed with either HE or nuclear charges. For 300-lb charges, the Lithanol J was about 29 percent higher than pentolite and 37 percent higher than the nuclear case. H_2O_2/Al was about 37 percent and 45 percent higher, respectively.

Both compositions showed an increase in bubble coefficients J and K with increasing charge weight. For H_2O_2/Al, this increase may be attributed, at least in part, to the initiation problem. For Lithanol, however, where there appears to be no initiation problem, the increase is real and is believed to result from the increased time available to completely oxidize the aluminum. If this is the reason, it would be expected that J and K would level off at some value where time permitted complete oxidation to take place.

A fourth bubble pulse was measured on the PE records for the 50-lb charges of both steam compositions. No more than three bubble pulses were observed for the 300-lb steam charges, either on the PE records or from discontinuities in the above surface effects.

8.2 RECOMMENDATIONS

Both compositions appear to be about equal in reproducing the condensation effects. Because of the initiation problems experienced with the H_2O_2/Al charges, it is recommended that Lithanol be used as the nuclear bubble simulant in future work. This composition also has the advantage of being a much easier explosive with which to work; moreover, control of the percentage composition is more easily accomplished. Sensitivity and stability tests of Lithanol (Appendix B) indicate no safety problems with this explosive.

The increase in J and K with increasing charge weight is of concern since large charges will probably be fired at depths too shallow to permit these parameters to be experimentally determined. Therefore, it is planned to fire charges in deep water to obtain these parameters for weights as great as those to be fired in shallow water. For this purpose, 13,000-lb charges of Lithanol will be fired at sufficiently great depths to obtain period and radius measurements. This charge, as was mentioned in Chapter 7, will produce a bubble approaching that of a 20-ton nuclear burst and is probably close to the best weight to simulate a 20-ton nuclear device in shallow water.

While the overall agreement with the current nuclear free water prediction method was acceptable, it appears that there are areas in this prediction method which could be improved. In particular, the time and depth of the third pulse is uncertain. It is recommended that attempts be made to improve these values, using the steam charge information currently available and to be obtained in the near future.

Finally, a note of caution. Lithanol (or H_2O_2/Al) produces a bubble whose contents are steam and whose condensation processes have been shown to closely simulate those of the nuclear bubble. It does not, however, simulate all the aspects of a nuclear bubble. One important area where it differs is in the internal structure of the bubble. The nuclear bubble has both density and temperature gradients from its center to the outer edge (Snay, 1960). Conventional explosives, including Lithanol, have a constant density throughout. Thus Lithanol will be useful in studying condensation effects; it should, however, be used with caution in studying effects where the actual structure of the bubble is of importance.

ACKNOWLEDGEMENTS

The successful completion of the two experimental programs discussed in this report, and the subsequent analysis of the resulting data, is the result of the efforts of many people. While it is impossible to recognize each of these individually, it is appropriate to mention those who made significant contributions.

The authors wish to acknowledge the guidance given by H. G. Snay of this Laboratory, who originally recognized the need for charges of the type discussed in this report. Discussions with Dr. G. A. Young, also of NOL, on the resulting data were extremely helpful in understanding and correlating the large amount of data which was obtained. Computer programming of Dr. Snay's bubble migration equations by T. E. Farley greatly expedited comparison of the results of these tests with the existing knowledge of the nuclear bubble behavior.

The authors also wish to acknowledge the efforts of L. E. Starr and Rolf Goderstad of the Chemical Engineering Division, who solved the many varied problems which arose in fabricating the experimental charges. The cooperation and assistance given by the NOL Test Facility, Solomons, Maryland, also greatly expedited firing of these programs.

Finally, the authors wish to acknowledge the assistance of Mrs. Marjorie N. Coleman, who performed the long and often tedious task of analyzing most of the data obtained. The quality of her work enhanced, to a great extent, the quality of this report.

BIBLIOGRAPHY

Arons, A. B., et al, 1947, "Measurement of Bubble Pulse Phenomena. IV: Pressure-Time Measurements in Free Water", NAVORD Report 408, Bureau of Ordnance, Unclassified.

Aronson, C. J., et al, 1956, "Underwater Free-Field Pressures to Just Beyond Target Locations", Operation Wigwam, Project 1.2, WT-1005, U. S. Naval Ordnance Laboratory, Secret Restricted Data.

Bulletin No. 104, "Materials of Construction for Equipment in Use with Hydrogen Peroxide", FMC Corp., Inorganic Chemicals Division, Buffalo, New York, Unclassified.

Buntzen, R. R., 1964, "The Underwater Distribution of Explosion Products from a Submerged Exploding Wire", USNRDL-TR-778, U. S. Naval Radiological Defense Laboratory, Unclassified.

Cole, R. H., 1948, "Underwater Explosions", Princeton University Press, Unclassified.

Goertner, J. F., 1956, "Vacuum Tank Studies of Gravity Migration of Underwater Explosion Bubbles", NAVORD Report 3902, U. S. Naval Ordnance Laboratory, Confidential.

Hudson, G. E., 1955. "The Analysis of Data from Some Small Explosives in Shallow Water", Contract NOrd 14663, New York University, Confidential.

Murphy, M. F., 1963, "Two Explosives Generating Condensible Products", NOLTR 63-12, U. S. Naval Ordnance Laboratory, Unclassified.

Niffenegger, C. R., 1953, "Comparisons of the Underwater Power of Explosions in Small Charges: I. Miscellaneous Compositions", NAVORD Report 2922, U. S. Naval Ordnance Laboratory, Confidential.

Phillips, D. E., and Scott, B. W., 1965, "Development of Probes for Measuring the Maximum Radius of Underwater Explosion Bubbles", NOLTR 65-176, U. S. Naval Ordnance Laboratory, Unclassified.

Phillips, D. E. and Heathcote, T. B., 1966, "Underwater Explosion Tests of Two Steam Producing Explosives I. Small Charge Tests", NOLTR 66-79, U. S. Naval Ordnance Laboratory, Unclassified.

Slifko, J. P. and Farley, T. E., 1959, "Underwater Shock Wave Parameters for TNT", NAVORD Report 6634, U. S. Naval Ordnance Laboratory, Unclassified.

Snay, H. G., et al, 1952, "Small Scale Experiments to Determine Migration of Explosion Gas Globes Towards Submarines", NAVORD Report 2280, U. S. Naval Ordnance Laboratory, Confidential.

Snay, H. G., 1960, "The Hydrodynamic Background of the Radiological Effects of Underwater Nuclear Explosions (U)", NavWeps 7323, U. S. Naval Ordnance Laboratory, Confidential.

Snay, H. G., 1962, "Underwater Explosion Phenomena: The Parameters of Migrating Bubbles", NAVORD Report 4185, Unclassified.

Snay, H. G., 1964, "Model Tests and Scaling", NOLTR 63-257, U. S. Naval Ordnance Laboratory, Unclassified.

Thiel, M. A., 1961, "Revised Similitude Equations for the Underwater Shock Wave Performance of Pentolite and HBX-1", NavWeps 7380, U. S. Naval Ordnance Laboratory, Unclassified.

Young, G. A., (In preparation), "A Preliminary Study of the Containment of Underwater Explosions", To be published as an NOLTR, U. S. Naval Ordnance Laboratory, Confidential FRD.

"Explosion Effects Data Sheets", NavOrd Report 2986, U. S. Naval Ordnance Laboratory, 1 Jun 1955, Confidential.

APPENDIX A

RANGING OF BUBBLE PULSES

The migration of an underwater explosion bubble is often determined by ranging the bubble pulses with a vertical string of PE gages. Because the ranging method was developed several years ago, reports describing it are no longer readily available. Therefore, the derivation of the ranging formulae will be given in this appendix. These derivations were taken from the report by Schneider and Cole (1946)*.

Ranging makes use of a vertical string of three equally spaced PE gages. The geometry is shown in Figure A.1. The separation of the gages is defined as α. The coordinate system has its origin at the center gage with the vertical (y) axis positive in the downward direction.

From Figure A.1, it can be seen that:

$$R_1^2 = r^2 + (\alpha + y)^2 \tag{A.1}$$

$$R_2^2 = r^2 + y^2 \tag{A.2}$$

$$R_3^2 = r^2 + (\alpha - y)^2 \tag{A.3}$$

Thus:

$$R_1^2 - R_2^2 = \alpha^2 + 2\alpha y \tag{A.4}$$

$$R_3^2 - R_2^2 = \alpha^2 - 2\alpha y \tag{A.5}$$

If the difference in distances between the source and successive gages is defined as Δ, then:

$$\Delta_{12} = R_1 - R_2 \tag{A.6}$$

$$\Delta_{32} = R_3 - R_2 \tag{A.7}$$

Δ_{12} (or Δ_{32}) is also equal to the difference in arrival times of the source at the two gages multiplied by the sound speed in water ($c\ \Delta t$). It is this time difference which is measured on the PE records. By solving equations (A.6) and (A.7) for R_1 and R_3, respectively, and substituting in Equations (A.4) and (A.5), the following equations are obtained:

* See Bibliography on page A-2.

$$\Delta_{12}\,(2R_2 + \Delta_{12}) = \alpha^2 + 2\alpha y \qquad (A.8)$$

$$\Delta_{32}\,(2R_2 + \Delta_{32}) = \alpha^2 - 2\alpha y \qquad (A.9)$$

Solution of (A.8) and (A.9) yields:

$$y = \frac{\alpha}{2}\left[\frac{\Delta_{12} - \Delta_{32}}{\Delta_{32} + \Delta_{12}}\right]\left[1 + \frac{\Delta_{12}\Delta_{32}}{\alpha^2}\right] \qquad (A.10)$$

$$R_2 = \frac{\alpha^2 - \frac{1}{2}\Delta_{12}^{\;2} - \frac{1}{2}\Delta_{32}^{\;2}}{\Delta_{12} + \Delta_{32}} \qquad (A.11)$$

Again referring to Figure A.1, it can be seen that the depth of the source, D, is given by:

$$D = g_2 + y \qquad (A.12)$$

where: g_2 = depth of center gage, ft.

The horizontal distance, r, of the source from the gage string, as given in Equation (A.2), is:

$$r = \left[R_2^{\;2} - y^2\right]^{1/2} \qquad (A.13)$$

BIBLIOGRAPHY - APPENDIX A

Schneider, W. G., and Cole, R. H., 1946, "Underwater Trajectory of the Squid Projectile. Part I. The Depth vs Sinking-Time Curve", OSRD Report No. 6257 (NDRC A-379), Underwater Explosives Research Laboratory, Woods Hole Oceanographic Institution, Secret.

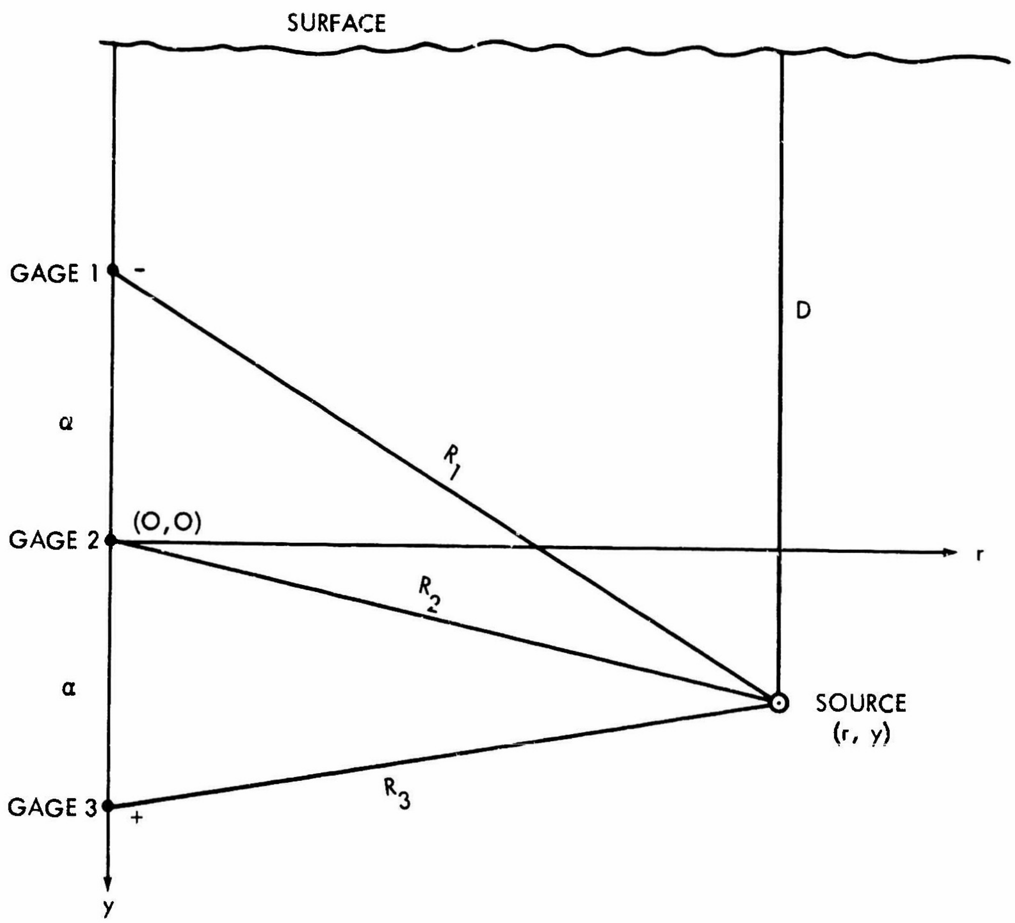

FIG.A.1 GEOMETRY OF BUBBLE RANGING

APPENDIX B

SENSITIVITY AND STABILITY TESTS OF LITHANOL

In order to safely use an explosive in other than laboratory conditions, it is necessary to know its sensitivity to various physical effects to which it may be subjected, or to know if its existence in particular media will affect its sensitivity. Because little information is available on the sensitivity of perchlorates and none on Lithanol, several tests have been conducted to determine its sensitivity. These tests were conducted either by or under the direction of the Chemical Engineering Division at NOL. They are presented here to indicate to other potential users the sensitivity of Lithanol.

Details of the tests have been omitted since they are available elsewhere in the literature for those who desire more information on the significance of these tests. Reference to reports where much detail is available have been given, comparison of results with other common high explosives have been made where possible to indicate, on a relative basis, the sensitivity of Lithanol.

B.1 50 PERCENT IMPACT HEIGHT (Ref: NAVORD Report 3592)

Lithanol	>320cm (highest attainable)
TNT	150 - 215cm
Pentolite (cast)	35cm
HBX-1	90 - 150cm

B.2 SHOCK SENSITIVITY (BOOSTER SENSITIVITY) (Ref: NAVORD Report 2986)

Lithanol	1.76 in
TNT	1.38 in
Pentolite (cast)	2.64 in
HBX-1	1.54 in

B.3 20-FT DROP TEST (Ref: NOLTR 62-150)

Lithanol	610cm (highest attainable)	no action
TNT	610cm	pop and smoke on some drops
Pentolite (cast)	366cm	high order detonation
HBX-1	610cm	pop and smoke on some drops

B.4 FRICTION SENSITIVITY TEST

Twenty samples tested. No response on any samples at the highest attainable Test Initiation Level (940-lb force).

B.5 ELECTROSTATIC SPARK TEST (Ref: NOLTR 65-124)

Twenty samples tested. No response from Lithanol at 7500 volts, 1.0μf capacitor discharge (2.81×10^8 ergs) for metal/metal or metal/rubber electrodes. This is the highest output attainable on the testing machine.

B.6 COOK-OFF TEST

Lithanol did not explode as temperature was raised. Melted at 150°C. No smoke or burning was noted; however, some fuming did take place, possibly the result of dehydration of the trihydrate. Boiling and vaporization of Lithanol occurred with temperature oscillating between 250 and 450°C.

B.7 VACUUM STABILITY TEST

Test conducted at 100°C under a partial vacuum of nitrogen. Water of hydration driven off during first hour of test. For the next 48 hours, gassing was less than 0.1 gm/ml.

B.8 DIFFERENTIAL THERMAL ANALYSIS

Water driven off at 100°C. Slight differential to 260°C. No further change through 400°C.

BIBLIOGRAPHY - APPENDIX B

Montesi, L. J., 1966, "The Electrostatic Spark Sensitivity of Various Organic Explosives and Metal/Oxidant Mixtures", NOLTR 65-124, U. S. Naval Ordnance Laboratory, Confidential.

NAVORD Report 2986, 1955, "Explosion Effects Data Sheets", U. S. Naval Ordnance Laboratory, Confidential.

Starr, L. E., et al, 1962, "NOL Drop Test (U)", NOLTR 62-150, U. S. Naval Ordnance Laboratory, Confidential.

Svadeba, G., 1953, "Factors Affecting the Behavior of Explosives to Mechanical Shock", NAVORD Report 3592, U. S. Naval Ordnance Laboratory.

DISTRIBUTION LIST

	Copies
Chief of Naval Operations Washington, D. C. 20360 Attn: OP-75	1
Chief of Naval Research Washington, D. C. 20360 Attn: Code 418	1
Code 429	1
Code 466	1
Commander, Naval Ordnance Systems Command Washington, D. C. 20360 Attn: ORD-0332	1
ORD-0352	1
ORD-03522	1
ORD-05311	2
ORD-05411	1
ORD-9132	2
Commander, Naval Ships Systems Command Washington, D. C. 20360 Attn: NADSC-6423	2
Code 0352	1
Commander, Naval Facilities Engineering Command Washington, D. C. 20360	1
Commanding Officer & Director U. S. Naval Radiological Defense Laboratory San Francisco, California 94135 Attn: Code 222	1
Code 911	1
Code 934	1
Code 908	1
Commanding Officer U. S. Naval Ordnance Station Indian Head, Maryland 20640 Attn: Library Division	1
Commanding Officer U. S. Naval Explosive Ordnance Disposal Facility Indian Head, Maryland 20640 Attn: Library Division	1

DISTRIBUTION LIST (continued)

	Copies
Commander, Naval Weapons Laboratory Dahlgren, Virginia 22448 Attn: Experimental Officer	1
Commander, Naval Ordnance Test Station China Lake, California 93556 Attn: Technical Library	1
Commander, Naval Ordnance Test Station Pasadena, California 91107	1
Director, Naval Research Laboratory Washington, D. C. 20390	2
Commanding Officer & Director David Taylor Model Basin Washington, D. C. 20007 Attn: Library Dr. W. W. Murray	 1 1
Commanding Officer & Director Underwater Explosions Research Division David Taylor Model Basin Portsmouth, Virginia 23709	1
Superintendent U. S. Naval Postgraduate School Monterey, California 93940	1
Director, U. S. Navy Electronics Laboratory San Diego, California 92152	1
Commanding Officer U. S. Naval Underwater Weapons Research & Engineering Station Newport, Rhode Island 02840	1
Commander, U. S. Naval Weapons Station Yorktown, Virginia 23491 Attn: Research & Development Division	1
Commanding Officer Naval Torpedo Station Keyport, Washington 98345	1
Commanding Officer & Director U. S. Navy Underwater Sound Laboratory Fort Trumbull New London, Connecticut 06321	1

Unclassified
Security Classification

DOCUMENT CONTROL DATA - R & D

(Security classification of title, body of abstract and indexing annotation must be entered when the overall report is classified)

1. ORIGINATING ACTIVITY (Corporate author) U. S. Naval Ordnance Laboratory White Oak, Silver Spring,Md. 20910	2a. REPORT SECURITY CLASSIFICATION Confidential 2b. GROUP 4

3. REPORT TITLE
Underwater Explosion Tests of Two Steam Producing Explosives
II. 50- and 300-lb Charge Tests (U)

4. DESCRIPTIVE NOTES (Type of report and inclusive dates)

5. AUTHOR(S) (First name, middle initial, last name)
Donald E. Phillips
Richard L. Willey

6. REPORT DATE	7a. TOTAL NO. OF PAGES	7b. NO. OF REFS
22 March 1967	v + 90	19

8a. CONTRACT OR GRANT NO.	9a. ORIGINATOR'S REPORT NUMBER(S)
b. PROJECT NO. WEPTASK No. 51001/212-8/F008-21-03(003) (DASA NWER 14.086)	NOLTR 67-7
c. WEPTASK No. 51001/212-8/F008-21-03(005) (DASA NWER 14.108)	9b. OTHER REPORT NO(S) (Any other numbers that may be assigned this report)
d.	

10. DISTRIBUTION STATEMENT
No restrictions other than security.

11. SUPPLEMENTARY NOTES	12. SPONSORING MILITARY ACTIVITY
	Defense Atomic Support Agency

13. ABSTRACT

Charges of Lithanol and H_2O_2/Al weighing 50 and 300 lb were fired under water to obtain shock wave and bubble measurements. An initiation problem with H_2O_2/Al was apparent; no initiation problem was indicated for Lithanol. Both compositions exhibited an increase in bubble parameters with increasing charge weight. (U)

DD FORM 1 NOV 65 1473 (PAGE 1)
S/N 0101-807-6801

Unclassified
Security Classification

14 KEY WORDS	LINK A		LINK B		LINK C	
	ROLE	WT	ROLE	WT	ROLE	WT
Underwater Explosions						
Explosion Bubbles						
Steam Bubbles						
Lithanol						
H_2O_2/Al						

Naval Ordnance Laboratory, White Oak, Md.
(NOL technical report 67-7)
UNDERWATER EXPLOSION TESTS OF TWO STEAM PRODUCING EXPLOSIVES. II. 50- AND 300 LB CHARGE TESTS (U), by D. E. Phillips and R. L. Willey. 22 March 1967. v.p. illus., charts, tables. BuWeps tasks 51001/212-8/F008-21-03 (003) and 51001/212-8/F008-21-03 (005).

CONFIDENTIAL

Charges of lithanol and H_2O_2/Al weighing 50 and 300 lb were fired under water to obtain shock wave and bubble measurements. An initiation problem with H_2O_2/Al was apparent; no initiation problem was indicated for lithanol. Both compositions exhibited an increase in bubble parameters with increasing charge weight. (U)

1. Explosions, Underwater
2. Bubbles, Explosion
I. Title
II. Phillips, Donald E.
III. Willey, Richard L., jt. author
IV. Project
V. Project

Abstract card is unclassified.

Naval Ordnance Laboratory, White Oak, Md.
(NOL technical report 67-7)
UNDERWATER EXPLOSION TESTS OF TWO STEAM PRODUCING EXPLOSIVES. II. 50- AND 300 LB CHARGE TESTS (U), by D. E. Phillips and R. L. Willey. 22 March 1967. v.p. illus., charts, tables. BuWeps tasks 51001/212-8/F008-21-03 (003) and 51001/212-8/F008-21-03 (005).

CONFIDENTIAL

Charges of lithanol and H_2O_2/Al weighing 50 and 300 lb were fired under water to obtain shock wave and bubble measurements. An initiation problem with H_2O_2/Al was apparent; no initiation problem was indicated for lithanol. Both compositions exhibited an increase in bubble parameters with increasing charge weight. (U)

1. Explosions, Underwater
2. Bubbles, Explosion
I. Title
II. Phillips, Donald E.
III. Willey, Richard L., jt. author
IV. Project
V. Project

Abstract card is unclassified.

Naval Ordnance Laboratory, White Oak, Md.
(NOL technical report 67-7)
UNDERWATER EXPLOSION TESTS OF TWO STEAM PRODUCING EXPLOSIVES. II. 50- AND 300 LB CHARGE TESTS (U), by D. E. Phillips and R. L. Willey. 22 March 1967. v.p. illus., charts, tables. BuWeps tasks 51001/212-8/F008-21-03 (003) and 51001/212-8/F008-21-03 (005).

CONFIDENTIAL

Charges of lithanol and H_2O_2/Al weighing 50 and 300 lb were fired under water to obtain shock wave and bubble measurements. An initiation problem with H_2O_2/Al was apparent; no initiation problem was indicated for lithanol. Both compositions exhibited an increase in bubble parameters with increasing charge weight. (U)

1. Explosions, Underwater
2. Bubbles, Explosion
I. Title
II. Phillips, Donald E.
III. Willey, Richard L., jt. author
IV. Project
V. Project

Abstract card is unclassified.

Naval Ordnance Laboratory, White Oak, Md.
(NOL technical report 67-7)
UNDERWATER EXPLOSION TESTS OF TWO STEAM PRODUCING EXPLOSIVES. II. 50- AND 300 LB CHARGE TESTS (U), by D. E. Phillips and R. L. Willey. 22 March 1967. v.p. illus., charts, tables. BuWeps tasks 51001/212-8/F008-21-03 (003) and 51001/212-8/F008-21-03 (005).

CONFIDENTIAL

Charges of lithanol and H_2O_2/Al weighing 50 and 300 lb were fired under water to obtain shock wave and bubble measurements. An initiation problem with H_2O_2/Al was apparent; no initiation problem was indicated for lithanol. Both compositions exhibited an increase in bubble parameters with increasing charge weight. (U)

1. Explosions, Underwater
2. Bubbles, Explosion
I. Title
II. Phillips, Donald E.
III. Willey, Richard L., jt. author
IV. Project
V. Project

Abstract card is unclassified.

Naval Ordnance Laboratory, White Oak, Md.
(NOL technical report 67-7)
UNDERWATER EXPLOSION TESTS OF TWO STEAM PRODUCING EXPLOSIVES. II. 50- AND 300 LB CHARGE TESTS (U), by D. E. Phillips and R. L. Willey. 22 March 1967. v.p. illus., charts, tables. BuWeps tasks 51001/212-8/F008-21-03 (003) and 51001/212-8/F008-21-03 (005).

CONFIDENTIAL

Charges of lithanol and H_2O_2/Al weighing 50 and 300 lb were fired under water to obtain shock wave and bubble measurements. An initiation problem with H_2O_2/Al was apparent; no initiation problem was indicated for lithanol. Both compositions exhibited an increase in bubble parameters with increasing charge weight. (U)

1. Explosions, Underwater
2. Bubbles, Explosion
I. Title
II. Phillips, Donald E.
III. Willey, Richard L., jt. author
IV. Project
V. Project

Abstract card is unclassified.

Naval Ordnance Laboratory, White Oak, Md.
(NOL technical report 67-7)
UNDERWATER EXPLOSION TESTS OF TWO STEAM PRODUCING EXPLOSIVES. II. 50- AND 300 LB CHARGE TESTS (U), by D. E. Phillips and R. L. Willey. 22 March 1967. v.p. illus., charts, tables. BuWeps tasks 51001/212-8/F008-21-03 (003) and 51001/212-8/F008-21-03 (005).

CONFIDENTIAL

Charges of lithanol and H_2O_2/Al weighing 50 and 300 lb were fired under water to obtain shock wave and bubble measurements. An initiation problem with H_2O_2/Al was apparent; no initiation problem was indicated for lithanol. Both compositions exhibited an increase in bubble parameters with increasing charge weight. (U)

1. Explosions, Underwater
2. Bubbles, Explosion
I. Title
II. Phillips, Donald E.
III. Willey, Richard L., jt. author
IV. Project
V. Project

Abstract card is unclassified.

Naval Ordnance Laboratory, White Oak, Md.
(NOL technical report 67-7)
UNDERWATER EXPLOSION TESTS OF TWO STEAM PRODUCING EXPLOSIVES. II. 50- AND 300 LB CHARGE TESTS (U), by D. E. Phillips and R. L. Willey. 22 March 1967. v.p. illus., charts, tables. BuWeps tasks 51001/212-8/F008-21-03 (003) and 51001/212-8/F003-21-03 (005).

CONFIDENTIAL

Charges of lithanol and H_2O_2/Al weighing 50 and 300 lb were fired under water to obtain shock wave and bubble measurements. An initiation problem with H_2C_2/Al was apparent; no initiation problem was indicated for lithanol. Both compositions exhibited an increase in bubble parameters with increasing charge weight. (U)

1. Explosions, Underwater
2. Bubbles, Explosion
I. Title
II. Phillips, Donald E.
III. Willey, Richard L., jt. author
IV. Project
V. Project

Abstract card is unclassified.

Naval Ordnance Laboratory, White Oak, Md.
(NOL technical report 67-7)
UNDERWATER EXPLOSION TESTS OF TWO STEAM PRODUCING EXPLOSIVES. II. 50- AND 300 LB CHARGE TESTS (U), by D. E. Phillips and R. L. Willey. 22 March 1967. v.p. illus., charts, tables. BuWeps tasks 51001/212-8/F008-21-03 (003) and 51001/212-8/F008-21-03 (005).

CONFIDENTIAL

Charges of lithanol and H_2O_2/Al weighing 50 and 300 lb were fired under water to obtain shock wave and bubble measurements. An initiation problem with H_2O_2/Al was apparent; no initiation problem was indicated for lithanol. Both compositions exhibited an increase in bubble parameters with increasing charge weight. (U)

1. Explosions, Underwater
2. Bubbles, Explosion
I. Title
II. Phillips, Donald E.
III. Willey, Richard L., jt. author
IV. Project
V. Project

Abstract card is unclassified.